Review Article

Pablo D. Tagle-Salazar, Krishna D.P. Nigam, and Carlos I. Rivera-Solorio*

Parabolic trough solar collectors: A general overview of technology, industrial applications, energy market, modeling, and standards

https://doi.org/10.1515/gps-2020-0059
received May 28, 2020; accepted September 28, 2020

Abstract: Many innovative technologies have been developed around the world to meet its energy demands using renewable and nonrenewable resources. Solar energy is one of the most important emerging renewable energy resources in recent times. This study aims to present the state-of-the-art of parabolic trough solar collector technology with a focus on different thermal performance analysis methods and components used in the fabrication of collector together with different construction materials and their properties. Further, its industrial applications (such as heating, cooling, or concentrating photovoltaics), solar energy conversion processes, and technological advancements in these areas are discussed. Guidelines on commercial software tools used for performance analysis of parabolic trough collectors, and international standards related to performance analysis, quality of materials, and durability of parabolic trough collectors are compiled. Finally, a market overview is presented to show the importance and feasibility of this technology. We believe the compilation of reviews related to the above aspects will further provide impetus for the development of this technology in the near future.

Keywords: Solar energy, parabolic trough collector, industrial application, energy market, performance modeling

*** Corresponding author: Carlos I. Rivera-Solorio,** Tecnologico de Monterrey, School of Engineering and Sciences, Ave. Eugenio Garza Sada 2501, Monterrey, N. L., México, 64849,
e-mail: rivera.carlos@tec.mx
Pablo D. Tagle-Salazar: Tecnologico de Monterrey, School of Engineering and Sciences, Ave. Eugenio Garza Sada 2501, Monterrey, N. L., México, 64849
Krishna D.P. Nigam: Tecnologico de Monterrey, School of Engineering and Sciences, Ave. Eugenio Garza Sada 2501, Monterrey, N. L., México, 64849; Department of Chemical Engineering, Indian Institute of Technology, Delhi, New Delhi, 110016, India

Nomenclature

Acronyms

AOP	advanced oxidation process
ARC	antireflective coating
CAPEX	capital expenditure
CFD	computational fluid dynamics
COP	coefficient of performance
CPC	compound parabolic collector
CPV	concentrating photovoltaics
CSP	concentrating solar power
DNI	direct normal irradiation
FDA	finite-difference analysis
FEA	finite-element analysis
FO	forward osmosis
FVA	finite volume analysis
GHG	greenhouse gasses
GNI	global normal irradiation
HPC	heterogenous photocatalysis
HTF	heat transfer fluid
IEA	International Energy Agency
LCOE	levelized cost of energy
LFC	linear Fresnel collector
MED	multieffect distillation
MSF	multistage flash
NCC	nonconcentrating collectors
O&M	operational and maintenance
PD	parabolic dish
PFP	photo-Fenton process
PTC	parabolic trough collector
PVC	photovoltaic concentrator
RO	reverse osmosis
SC	selective coating
s-CO_2	supercritical carbon dioxide
SHIP	solar heating industrial process
SG	steam generation
ST	solar tower

TES thermal energy storage
T-PVC thermal-photovoltaic concentrator

Symbols

a_1, a_2, a_3 coefficients of thermal losses
A aperture area (m^2)
C_r concentration factor
F_c soiling factor (dimensionless)
I_b beam direct solar radiation (W/m^2)
I_d diffuse solar radiation (W/m^2)
$K(\theta)$ incident angle modifier K as function of incidence angle θ
Q heat received (W)
$\dot{q}_{ab,type}$ type heat transfer flow per length from boundary a to boundary b (W/m)
$\dot{q}_a$ incident heat transfer flow per length at boundary a (W/m)
$\dot{q}_l$ heat losses of receiver (W/m)
T_a temperature at boundary a (°C)
T_r reduced temperature $(\Delta T_f/(I_b \cos(\theta)))$, m^2 K/W)
v_w wind velocity (m/s)

Greek letters

α_{sc} absorptivity of the selective coating
γ interception factor
ΔT_{ab} temperature difference between average absorber temperature and ambient temperature (°C)
ΔT_f temperature difference between average fluid temperature and ambient temperature (°C)
η overall efficiency
η_{op} optical efficiency
$\eta_{op,0}$ peak optical efficiency(at normal incidence)
η_{peak} peak thermal efficiency
ρ_m reflectance of the mirrors
τ_{cg} transmittance of the cover glass

Boundaries

1_{ave} fluid mean bulk
2 inner surface of pipe
3 outer surface of pipe
4 inner surface of cover glass
5 outer surface of cover glass
A atmosphere
C sky
S outside of the brackets (extended surface)

1 Introduction

In the last few decades, the energy demand of industries and commercial sectors has substantially increased. Most of the energy has been generated by using fuel fossil technologies that have increased the emission of pollutants to the atmosphere, contributing to global warming and deterioration in the health of humankind. Solar energy is one of the green energy resources that can be used to reduce the consumption of fuel fossils to meet the demands of the industrial and the commercial sectors. Further, the cost of energy of solar photovoltaic (PV) and solar thermal power has tended to fall as their performance efficiency increased in late years [1–3]. Many technologies are used in industry to convert solar energy into thermal and electrical energies. These technologies are classified and represented in Figure 1. Solar technologies can be classified as either passive or active, depending on the type of system, with active technologies requiring external components, such as pumps or electronic control, to convert energy. The type of energy supplied to the process is the energy produced directly from the solar collection system used in the industrial process, which can be either thermal or nonthermal (e.g., PV). Solar collector type is determined based on the total radiation transmitted to the reception area compared to the radiation received in the collection area. Solar concentration is achieved by reflecting or refracting solar radiation from a large area (collection) to a smaller one (receiver) using mirrors or lenses. The concentration factor is the

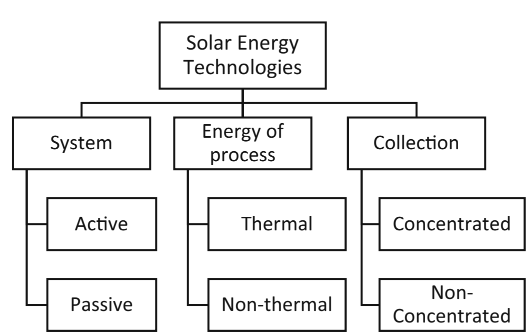

Figure 1: Classification of solar energy technologies.

ratio between the collection area and the receiver area, so it is a dimensionless geometric factor having a value greater than 1 for concentrating technologies. Parabolic trough collectors (PTCs) have a common concentration ratio above 10 and lesser than 100, which is considered as "medium concentration" [4]. To realize energy conversion, concentrating technologies require external components, which are generally related to fluid transport or solar tracking, and so they are considered active.

In industrial applications, solar concentration (collectors) technologies are divided into four technologies: PTCs, linear Fresnel collectors (LFCs), solar towers (STs), and parabolic dishes. Table 1 represents the principal differences between these technologies based on their functionality. The receiver can be mobile or stationary depending on the concentration process, and the shape of the focus (where the sunlight is concentrated) can be either a line or a point. Concentration factor is one of the most important parameters which differs among these technologies. This factor is usually smaller than 100 for PTCs and LFCs, whereas for the others it can be greater than 1,000. Table 2 displays the main technical and operational characteristics of these four technologies. PTC and ST have some advantages, such as maturity and typical capacity, making them the most important technologies used for solar energy conversion. Nowadays, PTC is the most deployed technology and has major share in the worldwide energy market compared to other solar concentrating technologies [1].

A PTC is basically a mirror with a cylindrical–parabolic shape and a receiver duct located along the focal line of the parabola, as represented in Figure 2. This configuration increases the energy intensity of sunlight along the receiver, where sunlight is getting converted into heat and transferred to fluid circulating through the receiver. PTCs operate at low to medium temperatures, with the working fluid reaching temperature between 50°C and 400°C [4], a temperature range where many industrial processes are carried out.

A PTC uses direct solar radiation as a heat source. As the sun's relative position changes every second, a solar tracking system is needed to improve its efficiency. Two types of solar tracking are used in PTCs namely, north-south and east-west, as represented in Figure 3. Tracking methods are so named based on the direction of rotation of collector's aperture plane. In north-south tracking, the receiver (parallel to tracking axis) is aligned to east-west direction, so the collector's aperture plane rotates from north to south and *vice versa*. The opposite case is the east-west tracking type in which the receiver is aligned to north-south direction and the aperture plane rotates from east to west. The north-south tracking method has the advantage of lower tracking energy consumption, but with a higher end- effect. For east-west tracking systems, the opposite is the case (lower end effect and higher energy consumption).

These collector systems have the following advantages:

- Low emissions to the environment during the system's life cycle: Right from the manufacture of components (structure, electronic components, anodized mirrors, etc.), to their use in final deposition, the environmental impact from the life cycle of these collectors is lower than that from energy technologies using fossil fuels. Burkhardt et al. [5] realized a life cycle assessment of about a 103-MW concentrating solar power (CSP) plant based on PTC when comparing some plant designs. Klein and Rubin [6] realized a similar life cycle study with a 110-MW CSP plant. Both studies reported an estimation of between 30 and 70 kg CO_2eq/MW h for a CSP plant with storage system, which is much lower than 400 kg CO_2eq/MW h reported for a natural gas power plant with combined cycle [6].
- Lower maintenance and operating costs: This is a major advantage of renewable energy technologies over conventional fossil fuel systems. The contribution of the fuel to the operation and maintenance (O&M) cost is important, which includes its price, availability, type, purity, and other aspects [7]. Since renewable systems do not need the kind of fossil fuels and equipment, O&M costs are much less compared to the conventional power technologies. Nevertheless, renewable energy systems require some maintenance. For example, the estimated O&M cost for solar energy generating system plants in California is USD 0.04/kW h, which is

Table 1: Characteristics of solar concentrating technologies [2]

	Focus type	
Receiver type	**Line (one-axis tracking)**	**Point (two-axis tracking)**
Stationary (only the mirror moves, receiver is fixed)	Linear Fresnel collectors	Solar tower
Mobile (receiver and mirror track the sun)	Parabolic trough collectors	Parabolic dish

Table 2: Comparison of solar concentrating technologies [1,3]

	 Parabolic Trough	 Solar Tower	 Linear Fresnel	 Parabolic Dish
Typical capacity (MW)	10–300	10–200	10–200	0.01–0,025
Maturity	Commercially proven	Commercially proven	Recent commercial project	Demonstration projects
Technology development risk	Low	Medium	Medium	Medium
Operating temperature (°C)	350–400	250–565	250–350	550–750
Plant peak efficiency (%)	14–20	23–35[a]	18	30
Annual solar to electricity efficiency (%)	11–16	7–20	13	12–25
Annual capacity factor (%)	25–28 (no TES) 29-43 (7 h TES)	55 (10 h TES)	22–24	25–28
Concentration factor	10–80	>1,000	>60	Up to 10,000
Receiver/absorber	Absorber attached to collector, moves with collector, complex design	External surface or cavity receiver, fixed	Fixed absorber, no evacuation secondary reflector	Absorber attached to collector, moves with collector
Storage system	Indirect two-tank molten salt at 380°C ($dT = 100$ K)	Direct two-tank molten salt at 550°C ($dT = 300$ K)	Short-term pressurized steam storage (<10 min)	No storage for Stirling dish, chemical storage under development
Hybridization	Yes and direct	Yes	Yes, direct (steam boiler)	Not planned
Grid stability	Medium to high (TES or hybridization)	High (large TES)	Medium (back-up firing possible)	Low
Cycle	Superheated Rankine steam cycle	Superheated Rankine steam cycle	Saturated Rankine steam cycle	Stirling
Steam conditions (°C/bar)	380–540/100	540/100–160	260/50	n.a.
Maximum slope of solar field (%)	<1–2	<2–4	<4	10 or more
Water requirement (m^3/MW h)	3 (wet cooling) 0.3 (dry cooling)	2–3 (wet cooling) 0.25 (dry cooling)	3 (wet cooling) 0.2 (dry cooling)	0.05–0.1 (mirror washing)
Application type	On-grid	On-grid	On-grid	On-grid/off-grid
Suitability for air cooling	Low to good	Good	Low	Best
Storage with molten salt	Commercially available	Commercially available	Possible, but not proven	Possible but not proven

TES: thermal energy storage.
[a] Upper limit if the solar tower powers a combined cycle turbine.

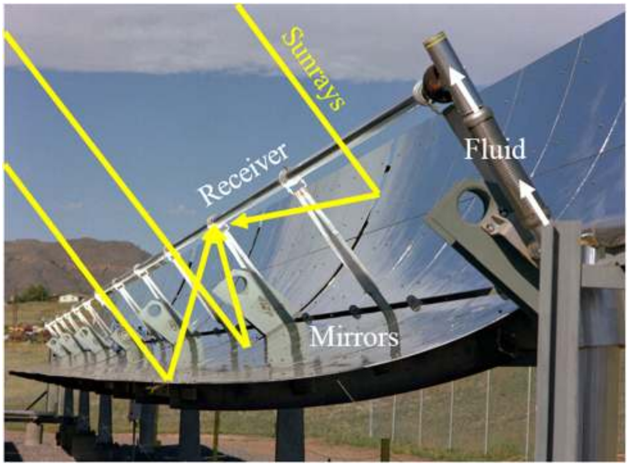

Figure 2: Parabolic trough collector system. (Retrieved from the NREL website: https://images.nrel.gov.)

considered the highest cost in terms of solar concentration with parabolic troughs [1].
- Long life span: As they operate at moderate temperatures, PTCs have longer life span.

The main disadvantages are the following:
- Large area required for installation due to the diffuse nature of solar radiation (a flux of around 1 kW/m^2 on earth's surface); so large areas or land are required to collect enough heat to meet the energy load of the process.
- High initial investment and medium- and long-term recovery: The total cost of manufacturing materials affects the total capital cost, recovery, and levelized cost of energy. But note that O&M costs are low as stated before.
- Intermittence of the resource: PTCs use direct solar radiation and so intermittence is a rule as energy cannot be collected at night. Further, PTCs can operate efficiently only on clear-sky days as clouds affect the energy production.

The main purpose of this review is to present the state-of-the-art of PTC technology and its role in industry. This study presents a general overview of the technology that includes both technical and economic aspects. Industrial applications are discussed in a practical approach, explaining the principal aspects and each purpose. Another objective is to compile reviews and technical and economic reports so that readers can use them as a "starting point" to focus research on a specific topic about PTC technology. Moreover, the intention of the study is to present information about modeling as a tool for designing and the status of technical standardization for practical analysis of a collector (i.e., for certification) and thermal systems.

This review consists of five sections. Section 1 presents the collector components and describes construction materials, desired properties, design data (for frameworks and receivers), and advancements in technology for each component. Section 2 describes and analyzes the status of PTC technology applications in industry, methods and processes used, and potential applications for implementation. A market overview and a brief description of the status of relevant economic parameters and future trends related to PTCs are given in Section 3. Section 4 is a summary of the mathematical methods and software tools used for performance analysis. Finally, international standards for performance analysis and materials quality are reported in Section 5. Several reviews and reports about the materials used, economic analysis, and industrial processes in solar energy conversion are discussed. To the best of our

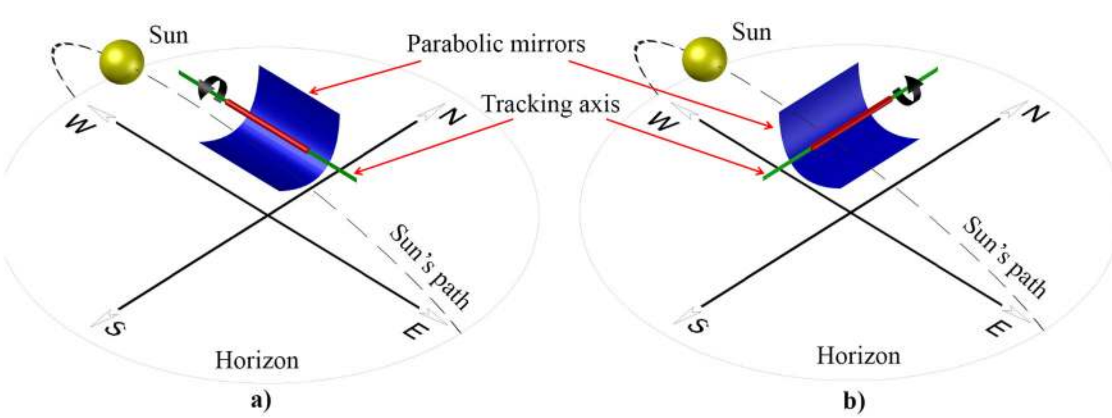

Figure 3: Common tracking methods: (a) north-south, (b) east-west.

knowledge, a review using a holistic approach considering a brief description and detailed information of components (with common properties of materials used), economics, and standards, related to PTC technology has not been reported so far.

2 Components of PTC

A PTC mainly consists of five major components: mirrors, a supporting structure, a receiver, working fluid, and a tracking system. Each component is designed to perform a specific purpose and is fabricated using materials based upon its functions and desired properties. These components are explained in detail as follows.

2.1 Mirrors

The principal function of mirrors is to reflect solar radiation and concentrate it onto the receiver. Mirrors are made of high-reflective material layers (aluminum or silver) with substrates and superstrates that protect the reflective layer against corrosion or abrasion so that longer life is achieved. Table 3 represents the principal types of mirrors used in applications. Silvered glass mirror, anodized sheet aluminum (sometimes coated with a polymer film), aluminized polymers, and silvered polymer films are the most commonly used materials for production. Granqvist [8] analyzed the main methods for applying reflective coatings (for mirrors) and selective coatings (SCs; for receivers), and described the general properties of some materials.

It is known that dirt, abrasion, and corrosion affect the optical performance of the mirrors, resulting in a decrease in the efficiency of thermal performance for the collector. Selection of the appropriate coating based on the desired properties of the reflective surface is a prerequisite for high thermal performance. Atkinson et al. [16] analyzed the literatures on reflective and SCs applied on concentrating solar systems as well as their main properties. Further, the deflection of the supporting structure may have a potential effect and it can decrease optical performance. Arancibia-Bulnes et al. [17] studied the main methods for evaluating the optical efficiency of solar concentrating collectors. Fernández-García et al. [18] presented the innovations made by R&D centers in recent years, under current investigation, or expectations about improvements in materials to increase optical performance of mirrors. They also considered the aspects of

Table 3: Types of mirrors with coatings [8–14]

Type	Description	Typical hemispherical reflectance	Cost ($\$/m^2$) [15,24]	Properties
Silvered glass mirrors	A copper substrate (replaced by a water-insoluble precipitate layer in recent years) protected by paint coatings in the back, with a silvered-based coating and a high-transmittance low-reflective glass as cover (superstrate, usually a low-iron glass)	Up to 0.96	20–30	- High resistance to corrosion - Commercially deployed - Heavy and fragile
Aluminized reflectors	Polished aluminum sheet with an aluminum-based reflective layer and oxide-enhancing layer	Up to 0.9	<20	- Lightweight and flexible - Low cost - High variability of durability - More applicable for low-enthalpy concentrators - Low durability in polluted locations
Silvered polymer reflectors	Silvered-reflective layer coated with flexible polymer and a very thin UV-screening film superstrate	0.9–0.95	20–30	- Under development - Less expensive - High reflectance and lightweight - Higher flexibility - Long term performance needs to be proven

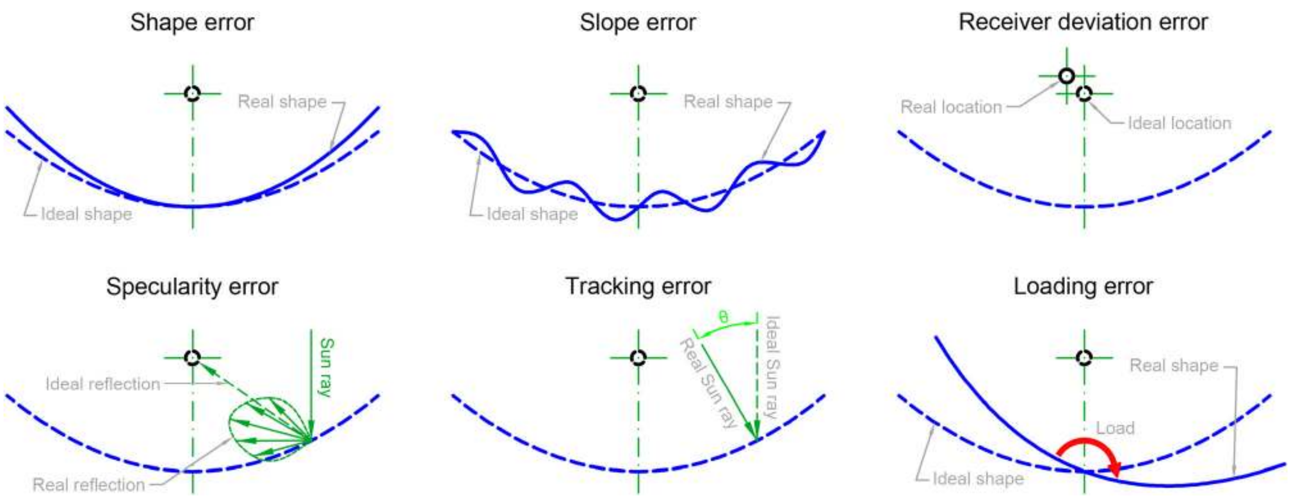

Figure 4: Geometrical errors in PTCs.

antisoiling coatings, high-reflective materials, high-temperature mirrors for secondary reflectors, and mirrors based on stainless steel and presented challenges, benefits, and research requirements of these concepts.

SolarPACES Task III group has published a guideline about characterization of reflectance properties and methods to determine the reflectance of mirrors used in solar concentrating technologies [19]. This guideline presents a method to characterize reflectance properties of solar reflective materials with reliable results, including recommended instrumentation requirements for field measurements. Zhu et al. [20] present a method for characterization of the reflectance of mirrors in PTCs combining total specular reflectance and specularity profile of the mirror; they also presented a case of study using the proposed method. Sutter et al. [21] proposed a prototype for field measurement of reflectance based on the recommendation given in the SolarPACES Guideline. The commercial instruments used in both outdoor and indoor field measurements (with a description of prototypes under development) were analyzed by Fernández-García et al. [22].

Further, they reviewed the methods and models based on the theoretical statements or experiment parameters for estimating the reflectance of solar reflective materials.

The results of the two most used reflectometers to measure the reflectance of back-silvered glass mirrors used in CSP applications are compared by Sansom et al. [23].

Deviations or errors may occur in the collector during manufacturing and normal operation which affect the concentration and, consequently, the optical efficiency. The most important errors are shape error, slope error, receiver deviation error, specularity error, tracking deviation, and frame deformation. Shape error estimates the eccentricity of the focal line (where the receiver is) due to deviations and misalignments of the mirrors. Slope error is the deviation of the rays due to slight ripples presented in the mirror shape. The receiver is not completely aligned to the focal line, so this misalignment is measured by the receiver deviation error. Specularity error refers to the error due to the imperfect reflection of mirrors (no-ideal reflective materials). As the collector is not always perfectly pointed to the sun, tracking error occurs during operation (see Section 2.5). The other factor that affects the geometry of the collector during operation is normal loading (principally by self-weight, wind, and torsional loads), which acts on the frame of the collector and may deform it. Figure 4 represents these errors (the deviations are exaggerated to illustrate the origin of error).

Generally, manufacturing process consists of deposition of the reflective layers and protective coating over a solid (or polymer, in the case of silvered polymer reflectors) substrate. For silvered glass mirrors: the glass is heated to mold it into the parabolic shape, then tempered so it does not lose the parabolic shape, and finally coated with the reflective and protective layers in the back [24]. For aluminized reflectors, the reflective layer is deposited over a metal substrate (usually aluminum) and then coated with protective layers. Finally, the reflective silvered layer is deposited on a polymer substrate and coated in the front in silvered polymer reflectors.

2.2 Supporting structure

The main purpose of the supporting structure is to fix the components of the collector, which provides rigidity and stability to the whole system. The structure is generally made of structural materials such as steel or aluminum. PTC supporting structure consists of three parts from a structural perspective: the main support (columns, piles, and box), the frame, and the receiver brackets (Figure 5).

– The main support serves as the structural anchor of a collector and holds it. Structurally, the main support will have the capacity to withstand wind loads as the aperture of the collector is exposed to the wind [25].
– The frame gives rigidity to the mirrors, allowing them to retain its parabolic shape at all times. It also transmits the torque of the tracking system.
– The brackets are attached to the support of the mirrors and the receiver is fixed at the focal line of the parabola. An insulating material is usually placed between both components to reduce heat losses from the receiver to the bracket.

The parabolic shape of the mirrors and the location of the receiver at the focal line of the parabola should be maintained always to prevent misalignments, which will result in performance losses. So a proper design of the structural framework is very important. The most important mechanical properties that are considered during manufacturing are bending and torsion of the framework, which are principally produced by self-weight and wind forces. These two parameters will affect the performance if the frame is not properly designed. Giannuzzi et al. [25] proposed structural design criteria for parabolic trough solar collectors and presented a methodology to calculate loads for structural designs based on European codes. Other studies on wind loads are based on experiments and computational fluid dynamics (CFD). Hosoya et al. [26] estimated experimentally wind loads of a 7.9-m section, 5 m aperture scaled PTC facing the wind as isolated single module and array configuration in a wind tunnel with a turntable platform (to determine wind loads with different wind directions). Like Hosoya et al., Randall et al. [27] conducted a similar experimental study, but the collector was tested under different geometric parameters. The effect of wind loads using windbreaks in PTCs was estimated according to Torres-García et al. [28]. Mier-Torrecilla et al. [29] conducted a CFD analysis to obtain the wind loads in a single model PTC under different yaw and pitch angles, and the results were compared with wind-tunnel experiments. Like Mier-Torrecilla, Paetzold et al. [30] made a similar CFD analysis but used three different focal length of the parabola. Naeeni and Yaghoubi [31] performed a two-dimensional CFD analysis of a PTC under different wind velocities and pitch angles to observe the flow behavior around the collector. Naeeni and Yaghoubi [31], similar two-dimensional CFD analysis was conducted by Zemler et al. [32] and Hachicha et al. [33] but focused on wind loads and both aerodynamics and heat transfer, respectively. Many patents of frameworks are found in the literature but the most important are those used in CSP plants around the world. The principal characteristics of the most commonly used parabolic trough frameworks are presented in Table 4.

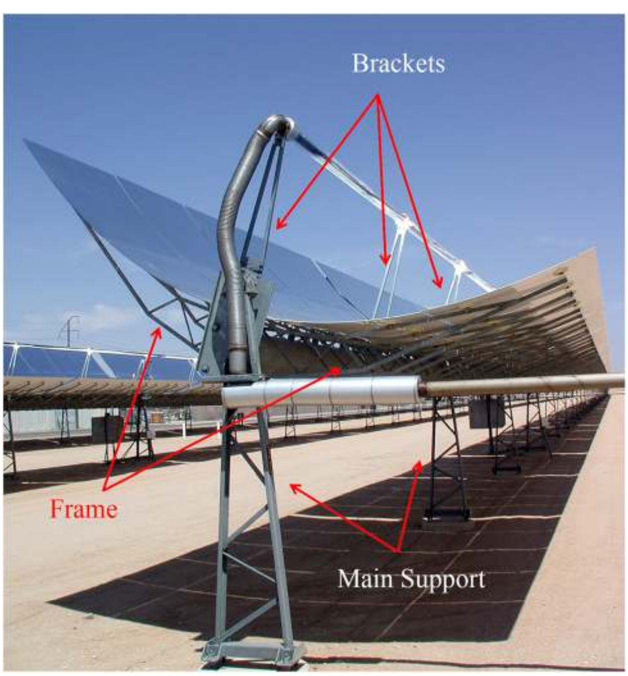

Figure 5: Structural division of a PTC. (Retrieved from the NREL website: https://images.nrel.gov.)

2.3 Receiver

The principal function of the receiver is to absorb as much radiation as possible and to transfer this energy to the heat transfer fluid (HTF) efficiently. The receiver can be fabricated from metal (heating) or glass (solar disinfection) depending on its application. For heating applications, the receiver has three principal components: the pipe receiver, the cover glass, and the SC. The cover glass minimizes the heat losses on the pipe and protects it from degradation. The SC is applied to the external surface of the pipe to increase the solar heat flux absorption. A vacuum is applied in the annular region between the glass and the tube to minimize the heat losses and the receiver is sealed to prevent vacuum losses. These kinds of receivers are called evacuated receivers. The bellows are the airtight part of the receiver, and they also allow thermal expansion of the pipe and

Table 4: Parabolic trough models used in CSP plants [34–50]

Developer	Model	Year	Structural design	Aperture Length (m)	Length (m)	Concentration ratio	Optical efficiency	Mirror reflectance
Luz International	LS-2	1985	Torque tube	5	47	71	0.737	0.94
	LS-3	1989	V-truss	5.76	99	82	0.8	0.94
Eurotrough Consortium	ET100	2002	Torque box	5.76	100	82	0.8	0.94
	ET150	2002	Torque box	5.76	150	82	0.8	0.94
ENEA	ENEA	2004	Torque tube	5.76	100	75–80	0.78	NA
Acciona	SGX-2	2005	Aluminum struts	5.76	100–150	82	0.77	NA
SENER	Sener Trough	2005	Torque tube	5.76	150	80	NA	NA
Abengoa Solar	Astr0	2007	Torque box	5.76	150	NA	NA	NA
	Phoenix	2009	Aluminum struts	5.76	150	NA	NA	NA
	E2	2011	Steel struts	5.76	125	82	NA	NA
TSK Flagsol	Skal-ET	NA	Torque box	5.77	148.5	82	0.8	NA
	Helio trough	2009	Torque tube	6.77	191	76	NA	NA
	Ultimate Trough	NA	Torque box	7.51	246	NA	0.89	0.94
IST Solucar	PT-2	2010	NA	4.4	148.5	63	0.75	NA
SkyFuel Inc.	Sky Trough	2010	Aluminum struts	5.7	115	72	0.76	0.94
Urssa Energy Co.	Urssa Trough	2011	Torque tube	5.76	150	82	0.768	0.93
Albiasa	AT 150	NA	NA	5.77	150	NA	NA	NA
Solarlite	SL 4600	NA	NA	4.6	12	66	0.75	NA
Gossamer Space Frames/3 M	LAT 73	2012	Struts	7.3	192	103	NA	≈0.95

NA: no data available.

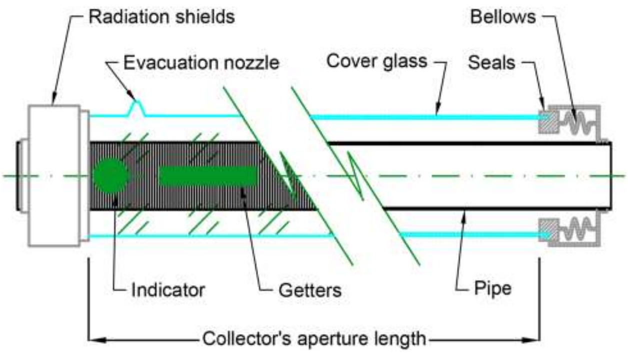

Figure 6: Receiver for heating applications.

glass cover. It is a known fact that the pipe and the glass cover do not expand at the same rate in the entire operation. Bellows allow thermal expansion without losing vacuum in the annulus because of high temperature difference with the atmosphere. The principal function of the hydrogen getters is to adsorb residual hydrogen that can be formed due to thermal degradation of the HTF. The glass-to-metal seal is the joint between pipe and glass cover, and its main function is to reduce mechanical stresses that occur due to differences in thermal expansion. Figure 6 represents the components of an evacuated receiver. Some prefabricated receivers and their characteristics are shown in Table 5. Small-aperture collectors and prototypes usually have nonevacuated receivers. Table 6 displays the characteristics of the most representative small-aperture collectors available in market.

The ideal material selected for a pipe receiver should have high resistance to corrosion, low thermal expansion, and high thermal conductivity, and stainless steel is the most commonly used material. Stainless steels have low thermal conductivity and a high resistance to corrosion, and they are malleable (so fabrication of tubes is easy).

The cover glass is made of a material with high transmittance, low reflectance, and low refractive index. It is very important that it should transmit the highest possible amount of the incident radiation reflected from the mirrors. Deubener et al. [62] analyzed the most important properties of glasses used in solar thermal, solar PV, and solar chemical applications and reported techniques to improve the optical performance of those materials. Antireflective coatings (ARCs) are

Table 5: Characteristics of some prefabricated receivers [51–57]

Manufacturer	Archimede solar energy			Siemens[a]	Rioglass			Sunda		
Country	Italy			Germany	Spain			China		
Model	HCEMS11	HCEOI12	HCESHS12	UVAC 2010	UVAC 70-7 G	UVAC 90-7 G	PTR 70-4 G	SEIDO 6-1	SEIDO 6-2	SEIDO 6-3
Metal receiver										
Length (m)	4.06	4.06	4.06	4.06	4.06	4.06	4.06	2	2	4.06
Diam. (mm)	70	70	70	70	70	88.9	70	38	63.5	70
Material	Stainless steel									
Cover glass										
Length (m)	3.9	3.9	3.9	NS	NS	NS	NS	NS	NS	NS
Diam. (mm)	125	125	125	115	115	135	125	102	102	115
Thickness (mm)	3	3	3	NS	3	3	2.5	NS	NS	NS
Material	Borosilicate (AR coated)									
Transmittance	0.966	0.966	0.966	0.964	0.967	0.964	0.97	0.95	0.95	0.95
Selective coating										
Absorptance	0.95	0.96	0.95	0.96	0.962	0.962	0.94	0.94	0.94	0.94
Emittance (@400°C)	0.073	0.085	0.073	0.09	0.095	0.095	0.095	0.12	0.12	0.12
Other characteristics										
Max. operating conditions	30 barg, 580°C	37 barg, 400°C	104 barg, 550°C	NS	40 barg, 350°C	40 barg, 350°C	41 barg, 350°C	15 barg, 300°C	30 barg, 390°C	40 barg, 450°C
Lifetime (year)	25	25	25	25	25	25	25	NS	NS	NS
Annulus pressure (mbar)	$<10^{-4}$	$<10^{-4}$	$<10^{-4}$	$<10^{-4}$	$<10^{-4}$	$<10^{-4}$	$<10^{-4}$	NS	NS	NS

NS = not specified.
[a] Rioglass bought Siemens CSP assets [52].

applied to the external surface of the cover glass for enhancing its transmittance. Further, they create a transition on the refractive index from air to the cover [16]. Silica and low-iron glasses are the most common types of glasses used in solar applications (for example, borosilicate is extensively employed in solar applications) [62]. The measurement of transmittance is performed by standard spectrophotometry at near-normal incidence (e.g., ASTM-G173-03 direct) [24].

The SCs should absorb as much solar radiation as possible and transmit it to the pipe receiver. They are applied to the external surface of the pipe to increase heat flux absorption. The SC should have the properties such as high short-wave absorptance, low long-wave emittance, good surface adhesion, and chemical stability in the working temperature range of collectors. Atkinson et al. [16] and Wijewardane and Goswami [63] reported state-of-the-art reviews of SC and focused on the capabilities, designs, and fabrication methods of coatings used for solar applications. The measurement of reflectance of the SC is performed using standard spectrophotometry at near-normal incidence (e.g., ASTM-G173-03 direct), and absorptance is obtained assuming opaque conditions ($\alpha = 1 - \rho$) [24]. Receivers used are entirely different in solar disinfection. Here, heat losses are not important, but the low transmission of UV radiation is important. In this case, the receiver is a tube made of a chemically inert material with a high-UV-radiation (short-wave) transmittance and low reflectance, like the cover glasses mentioned earlier.

The manufacturing process consists of coating the pipe (by methods shown in Ref. [8]) with an SC and the glass cover with an ARC. Prior to coating the glass, it is welded to the seals and treated in the surface for stress releasing and with other surface treatments. The pipe usually is treated on the external surface for a better application of the SC. Pipe, glass, getters, and vacuum

Table 6: Characteristics of some small-aperture collectors [58–61]

Manufacturer	**IST Solucar**[a]		**Solitem**		**NEP solar**		**Sopogy inc.**			
Country	**USA**		**Germany**		**Australia**		**USA**			
Model	**PT-1**	**RMT**	**PTC-1,800**	**PTC-1,000**	**Polytrough 1,200**	**Polytrhough 1,800**	**Sopoflare**	**Soponova**	**Sopohelios**	**Sopotitan**
Collector characteristics										
Length (m)	6.1	3.68	5.09	2.5	24	20.9	2.44	3.66	3.67	3.76
Aperture (m)	2.3	1.15	1.8	1.1	1.2	1.845	0.76	1.65	2.09	3.05
Concentration ratio	14.36	14.39	15.08	14	15.04	17.2	10.52	21	20.79	20.23
Focal length (m)	0.8	NA	0.78	NA	0.65	0.65	0.208	0.305	0.406	0.914
Optical eff. (%)	0.763		NA	NA	0.68	NA				
Mirror	Aluminized						NA			
Reflectance	0.89			NA	0.93	0.89	0.94	0.89		0.95
HTF	Pressurized water		Pressurized water/thermal oil				NA			
Metal receiver										
Diam. (mm)	51	25.4	38	NA	28	34	23	25	32	48
Material	Stainless steel						NA			
Cover glass										
Diam (mm)	75	51	65	NA	45	56	NA			
Material	Pyrex			NA		Borosilicate	NA			
Transmittance	0.95–0.96		0.95	NA	NA	NA	NA	0.91		
Selective coating										
Material	Black chrome/ nickel		NA		NA	Black chrome	NA			
Absorptance	0.96–0.98		NA		NA	NA	0.87	0.95		
Other characteristics										
Max. Temp. (°C)	288	205	250	NA	220	250	121	270	326	300
Vacuum	No					NA				

NA: no data available.

indicators are then assembled in one piece. Finally, the annulus is evacuated. Figure 7 represents a basic diagram about the manufacturing process. Nonevacuated receivers are easier for assembly. The cover glass, the pipe, and glass-to-metal support are assembled or connected once the pipe and the glass were coated.

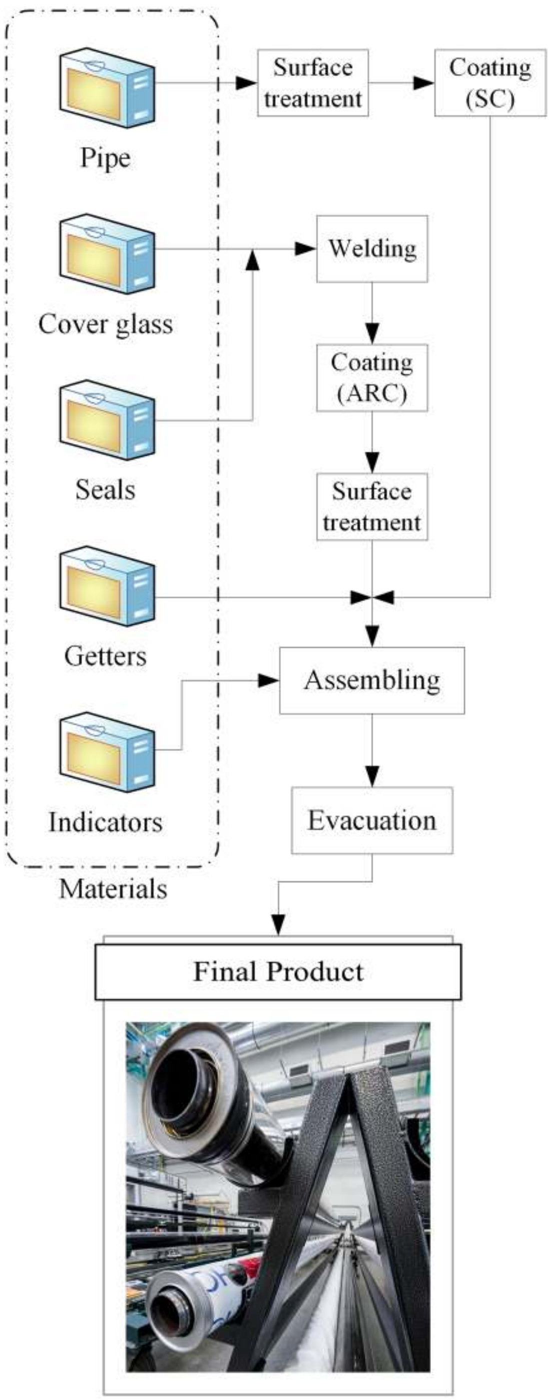

Figure 7: General description of receiver's manufacturing process.

2.4 The HTF

The HTF, also known as working fluid, is a substance that can absorb heat coming from the receiver and uses it as process energy. This fluid should have high thermal capacity and thermal conductivity, low thermal expansion, low viscosity, minimal corrosive activity, low toxicity, and thermal and chemical stability throughout its entire operating temperature range. Liquids are extensively used as HTFs. Table 7 shows the most common HTFs used in industry and their properties, typical operating temperature range, and advantages and disadvantages in operation.

Water is mostly used in low enthalpy and direct steam generation (SG) applications, while thermal oils (such as Syltherm or Therminol) are used in solar power generation along with a heat exchanger to generate steam for use in a Rankine cycle. Both water and thermal oils are the most used HTFs in industrial applications.

Pressurized air is commonly used for drying and heating in buildings using flat-plate collectors, but it has been studied only as an option for using in PTCs [58]. In fact, some studies suggested that pressurized air has a good performance in power plants with solar-assisted gas turbines. Amelio et al. [78] constructed a simulation of a combined cycle in which the PTC solar field preheats the air before entering the combustion chamber, resulting in a yearly global efficiency increment of 15.5% under certain operational conditions when compared with a reference plant without the solar field. Bellos et al. [79] obtained the optimization of a solar-assisted gas turbine using parametric analysis. In addition, they found that the solar field lead to a fuel savings up to 64%, with a small reduction in power due to pressure losses. Ferraro et al. [80] proposed a thermal model to analyze the thermal behavior of a solar-assisted gas turbine with two modes of operation: with constant inlet temperature/variable air flow rate and constant air flow rate/variable inlet temperature, all of them with and without reheating achieved an annual average efficiency of 17.8%. Cipollone et al. [81] analyzed the use of CO_2 and air as HTF for CSP based on PTC with a solar-assisted gas turbine. The energetic and exergetic performances of six different gases as HTF in PTCs were studied and compared by Bellos et al. [82]. They concluded that helium has the higher exergetic performance, and carbon dioxide is the most appropriate gaseous HTF at higher temperatures.

Recent investigation has increased attention in using supercritical carbon dioxide (s-CO_2) as a potential HTF in PTC applications [77]. Its main advantage is thermal enhancement when compared with subcritical CO_2 as it

Table 7: Heat transfer fluids used in PTC fields [64–77]

Fluid	Working temperature (°C)	General properties	Advantages	Disadvantages
Water	Up to 100	Odorless, relative low viscosity, nontoxic	- No environmental risks (pollution or fire) - Low operational pressures. - Simple plant design	- Only for low enthalpy applications - Requires water treatment
Glycols	−50–300	High heat transfer properties (with combined with water), low viscosity, toxic (depending on the preparation)	- Antifreezing properties (with the proper concentration)	- Environmental risks (toxicity) - Used only in low enthalpy applications (when mixed with water) - Degradation with long-term operation
Steam	Up to 500	High pressure and temperature applications	- Higher working temperature - Secondary HTF no needed - No environmental risks (pollution or fire) - Easier plant design	- Evaporation (two-phase flow, heat losses in flashing) - Higher operational pressures - Requires water treatment - More complex solar field control - Lack of suitable TES system
Pressurized air and other gases (CO_2, He, Ne, N_2)	Up to 900	Low cost because of its abundance from atmosphere, low viscosity, low energy density, need to be dehumidified (air)	- Higher steam temperature - Thermal storage enhancement - No environmental risks (pollution or fire) - Nontoxic - Chemically inert - Minimum corrosion	- Poor heat transfer in the receiver - More complex solar field control - Higher operational pressures
Supercritical CO_2	—	A supercritical gas works as a single-phase liquid with the filling property of a gas, higher temperature operation, abundant	- Gas with liquid-like properties - Higher thermal performance when compared with subcritical CO_2	- Challenging operation (leakage, pressure, etc.) - Thermal fatigue of pipes - Corrosion - Under investigation
Synthetic oils	−90–400	High thermal capacity, low flow properties (compared with water), flammable, toxic	- Higher thermal efficiencies are achieved (compared with others) - Relative low operational pressures	- Requires fire protection system - Environmental risk (toxicity) - Heat exchangers required (for power generation)
Mineral oils	−10–300	Stability against thermal degradation and oxidation, relatively inexpensive, noncorrosive and nontoxic, flammable	- Relative lower power consumption (due to its low viscosity and density compared with others)	

Table 7: Continued

Fluid	Working temperature (°C)	General properties	Advantages	Disadvantages
Silicon oils	−40–400	Odorless, low pour point, nontoxic, low viscosity, expensive, flammable		
Molten Salts	200–500	For high temperature applications, stable at high temperatures, low viscosity, high thermal capacity and density, corrosive, nonflammable	- Higher working temperature - Lower operating pressures at high temperatures - No pollution or fire hazards - Higher heat capacity - Smaller TES size	- High melting and freezing point (heat tracing is required) - Highly corrosive at high temperatures - More complex design - Not proven technology
Ionic liquids	−70–400	High thermal properties, wide liquid temperature range, low melting point, high viscosity and density, high chemical stability at high temperature, low volatility and flammability, expensive	- Lower freezing and melting point (compared with molten salts) - Reduced environmental risks (pollution)	- Higher power consumption (pump system) - Not proven technology
Nanofluids	—	Properties depend on type, size, and concentration of the particle; the base fluid and additives. High concentration of particles increases both thermal conductivity and viscosity	- Thermal enhancement - Other advantages depends on base fluid	- Sedimentation, clogging, and erosion - Under investigation

behaves as a hybrid liquid–gas fluid. Unfortunately, there is a lack of experimental research about s-CO_2. But there are many numerical studies about its performance in the literature. A feasibility study about the usage of CO_2 at high temperature and pressure as a potential HTF in PTCs with experimental test was presented by Muñoz-Anton et al. [83]. Aguilar et al. [77] proposed a one-dimensional numerical model for comparing thermal performance of a PTC with thermal oil (Syltherm 800), subcritical CO_2, and s-CO_2 and compared the model and experimental results. Both results are more or less similar and in numerical data results, there was a 2.9% deviation in temperature prediction (for thermal oil and subcritical CO_2), and the prediction of thermal behavior was within 2.7% when compared with [82]. Biencinto et al. [84] proposed a preliminary concept of power plant with s-CO_2 as a working fluid and molten salts as a secondary HTF. The results show that it is possible to reach up to 12.87% annual net efficiency of the plant and up to 6% of saving in cost of energy when compared to conventional thermal oil-based power plants.

Recently, molten salts and ionic liquids with good heat transfer capabilities have been mentioned in the literature. However, these HTFs should overcome some practical challenges. The main challenge for ionic liquids is their cost compared to the cost of conventional thermal oils used [68] and the operational aspects (such as freeze protection, impedance heating, and materials considerations) for molten salts [85].

Nanofluids have been developed for solar energy applications in recent times. A nanofluid is a fluid containing suspended solid nanometer-sized particles called nanoparticles, which enhance the heat capacity and thermal conductivity of the mixture. These particles are commonly metals (in natural form or oxides) and two types of nanofluids are used:

(a) Mono-nanofluids: a base fluid is doped with a single material as nanoparticles

(b) Hybrid nanofluids: a base fluid is doped with two or more materials as nanoparticles.

Thermal enhancement (improvement in properties such as thermal conductivity, heat transfer coefficient, and heat capacity) is the main advantage of nanofluids. The other important characteristic of nanofluids is its stability. The proper mixture of base fluid and nanoparticle will be effectively used in applications with PTCs. Krishna et al. [86] made an analysis about HTFs used in PTC technology. They reported that an enhancement of up to 27.9% in thermal efficiency and up to 234% on convective heat transfer coefficient is achieved with liquid-based nanofluids. They concluded that the addition of particles such as CuO, Ag, SiO_2, carbon nanotubes, or hybrid mixtures will improve thermal conductivity of the based fluid for the applications using PTCs. Ahmadi et al. [87] have given a report about the use of hybrid nanofluids in solar applications, and they concluded that thermal enhancement up to 60% can be reached using hybrid nanofluids. According to Shah and Ali [88], stability studies of hybrid nanofluids in a practical approach are not available, which necessitate further research on the performance of these HTFs for solar energy applications.

Some studies related to its applications in concentrated solar technology are available in the literature on nanofluids. Singh et al. [89] reported an analysis about the use of some common metallic nanoparticles added to organic thermal fluids. Mahian et al. [90], Kasaeian et al. [91], and Verma and Tiwari [92] presented an analysis of the applications of nanofluids in solar energy systems.

2.5 Solar tracking system

Solar tracking systems are needed because PTCs work with direct beam radiation. A solar tracking system aligns the collector with the sun to maximize collector performance in its one-axis rotation, as described before (see Figure 3). Solar trackers can be classified as either passive or active. The thermosiphon effect is used by passive trackers to align the collector, whereas active trackers use electronic signal conversion. But passive trackers are not commonly used in PTCs because misalignment occurs by the forces of wind during operation.

Active trackers are mostly used in concentrating solar systems and are divided into closed-loop and open-loop trackers. The principal difference between these types of active trackers is the use of signal conversion method. Closed-loop trackers use electronic signal conversion with feedback control. Open-loop trackers use algorithms and prerecoded data with a computer and timing controls to track the sun. Figure 8 shows the operation of each type of active solar tracking.

Active closed-loop trackers consist of three parts: a light sensor, a control system, and a drive system (Figure 8a). The sensor is active when the collector is misaligned with the sun (it measures a high light intensity when the collector is aligned), the misalignment triggers it to send a signal to the control system. The control system converts this signal so that movement of the driver occurs for transmitting torque to the structure until the collector is correctly aligned. A pair of light receiving diodes or PV cells is the most used sensors for closed-loop tracking. The main advantage of this tracking method is its high

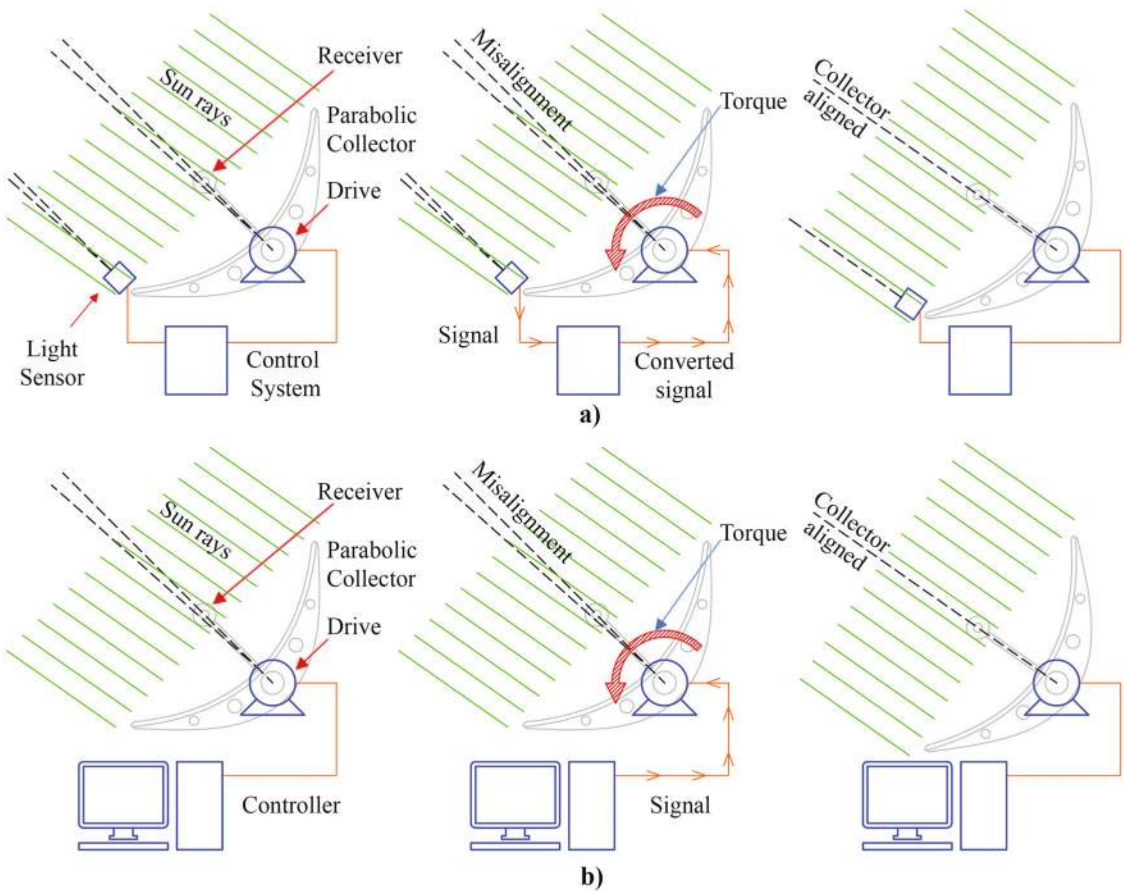

Figure 8: Solar tracker types: (a) active closed-loop, (b) active open-loop.

tracking accuracy but can be affected by shadowing. But the main disadvantage is the inability of the control system to recover or find the direction of the sun under long cloudy periods.

Active open-loop trackers consist of a controller and a drive (Figure 8b). During operation, the algorithm programmed on the controller signals the drive to move the collectors. Open-loop trackers can be classified into timed trackers and altitude/azimuth trackers. Timed trackers use algorithms based on time, so that the collector is controlled by incremental movements. Altitude/azimuth trackers use algorithms based on astronomical data depending on location and time. The disadvantage of these methods is the accuracy of the equations used in the algorithms, which can result in high misalignments.

Hybrid-loop tracking has been developed to overcome the disadvantages of both closed-loop and open-loop trackings. The fundamental strategy of hybrid-loop tracking is the use of algorithm (open loop) to track the sun and to reduce the misalignments by sensors (closed loop). Typical hybrid-loop tracking would be to calculate the position of the sun by the algorithm and activate the drive and later to correct misalignments by the sensor in the case that it is sensed.

Lee et al. [93] and Sumathi et al. [94] presented the report of active closed-loop and open-loop trackers, analyzing some designs published in the literature and showing the general description of the electronic control methodology used in each of them. Further, the strategies employed for light sensing for solar trackers were compiled by Moga et al. [95]. The information on solar tracking algorithms, computer code, and software available on the internet for use in solar trackers was studied and presented by Prinsloo and Dobson [96].

3 Industrial applications

PTCs are used in a variety of industrial applications and it is divided into three main groups, as shown in Figure 9. The heat collected is used directly for a given process in thermal applications. The solar energy is mainly used in heating and cooling applications in the industrial and

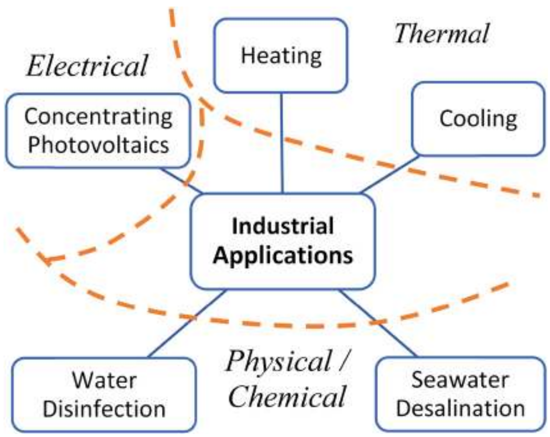

Figure 9: Classification of industrial applications.

commercial sectors, but concentrating PVs are currently under development. It is very important to note that there are small-scale installations and enterprises around the world producing PTC for PV applications. Each of these application groups is described in the following sections.

3.1 Heating

The application of solar energy in the heating application of industries is the extensively studied literature and PTCs are used in various types of industries. The collector transfers heat to the HTF, which is used as a source of energy for a given process (heating a fluid as main purpose of the PTC system). Heating applications can be divided into two groups based upon the temperature achieved by the HTF. Low-temperature applications are for a maximum temperature of 100°C and medium-temperature applications usually reach temperatures up to 400°C. Low-temperature PTC systems are commonly used in preheating and drying processes in commercial, residential, and industrial sectors. SG and CSP are the principal applications for medium-temperature PTC systems. Kalogirou [97] presented a list of potential industrial processes for implementing PTC systems, and Table 8 shows some of the processes. The temperature ranges of the processes are in the operational range of temperature of the PTC systems. The International Energy Agency (IEA), in collaboration with the AEE-Institute for Sustainable Technologies (AE-INTEC), has created a database of solar heating industrial processes (SHIPs) [98] and a guide to integrating solar-assisted systems with industrial heating processes [99]. Figure 10 shows the location of general-purpose nonpower-generation heating plants using PTCs around the world, according to the IEA SHIP database. In addition, Hisan Farjana et al. [100]

Table 8: Temperature range for industrial processes [97,102,104,107]

Industry	Process	Temperature (°C)
Dairy	Pressurization	60–80
	Sterilization	100–120
	Drying	12–180
	Boiler feed water	60–90
Tinned food	Sterilization	110–120
	Pasteurization	60–80
	Cooking	60–90
	Bleaching	60–90
Bricks and blocks	Curing	60–140
Plastics	Preparation	120–140
	Distillation	140–150
	Separation	200–220
	Extension	140–160
	Drying	180–200
	Blending	120–140
Chemical	Soaps	200–260
	Synthetic rubber	150–200
	Processing heat	120–180
	Preheating water	60–90
Paper	Cooking, drying	60–80
	Boiler feed water	60–90
	Bleaching	130–150
Heating of buildings	—	25–75
Desalination	—	100–250
Power cycles (Rankine)	Vapor generation	300–400
	Phase-change materials	300–375
Others	General steam generation	130–210

reviewed the state-of-the-art of SHIPs' focus on identifying the potential of different solar thermal technologies in various industrial processes.

CSP is the most popular PTC application for electricity generation. CSP plants generate electricity using solar-assisted turbines or integrated systems with combined cycles, usually with a thermal storage block. Both direct and indirect SGs are the most commonly used methods in the world for electricity generation with PTCs. These systems generate steam to run a turbine, by direct heating (water as HTF of the PTC system) or by indirect heating (i.e., oil as HTF and heat is transferred to water through a heat exchanger). Figure 11 presents a diagram of a CSP plant with direct SG (a) and indirect SG integrated to a combined cycle (b). The thermal storage block increases the efficiency and the capacity factor, making it possible to generate electricity even when there is no solar resource (nights or cloudy days). Tian and Zhao [101] and Alva et al. [102] presented the analysis of materials used in thermal storage systems for solar

Figure 10: Worldwide locations of thermal plants (nonpower-generation) using PTC systems.

applications. Further, different thermal storage methods and materials used in CSP plants were analyzed and compared by González-Roubaud et al. [103]. Thermal storage systems are not explained in detail as they are not in the scope of this work. Fernandez-García et al. [104] presented an overview of the development of the PTC technology in the last century, describing the collectors used in CSP plants, some prototypes under development, and discussed potential applications (such as heating, cooling, and desalination) for PTCs with examples. Fuqiang et al. [105] presented a review of the current status of CSP technology and its technology advancements. Cogeneration plants are another potential application for heating PTC systems and a preliminary assessment of a solar-assisted cogeneration

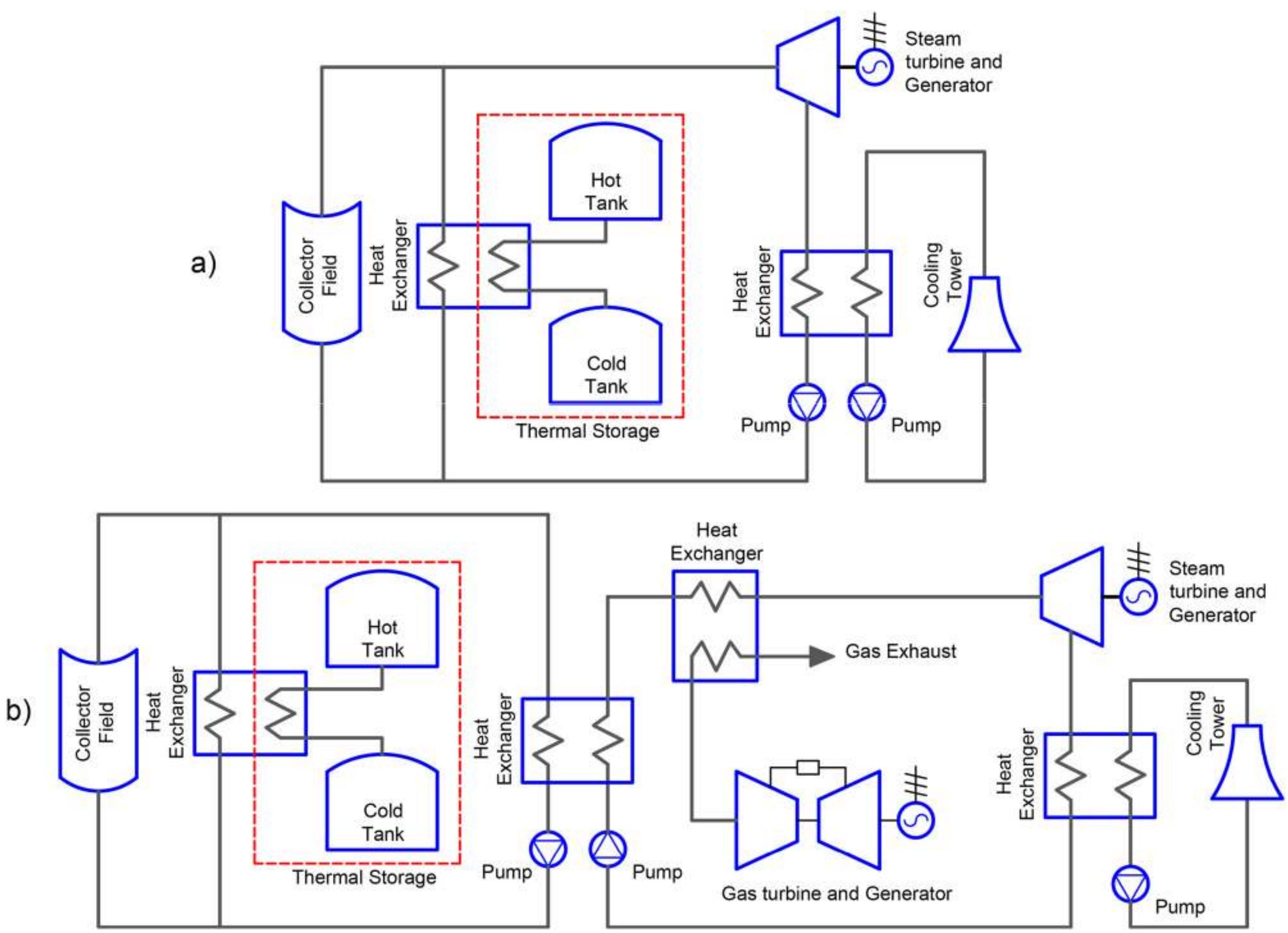

Figure 11: CSP plant diagrams: (a) direct SG, (b) indirect SG integrated with a combined cycle.

plant was presented by Manzolini et al. [106]. They observed and found that the energy costs and CO_2 emissions are lower than conventional cogeneration plants.

3.2 Cooling

Solar cooling refers to the use of solar radiation as a thermal energy source to cool a fluid or a space. Absorption and adsorption are two main solar cooling methods and both the method will replace the mechanical compressor in a conventional cooling process with a thermal compressor.

The absorption process is the most commonly used method for solar cooling with PTCs. Absorption uses a fluid–fluid mixture (also called working pair) as the refrigerant. The fluids of the working pair make a strong solution when mixed at low temperatures and can be separated when the mixture is heated. The solute is converted into a gas and the solvent remains in liquid state when the mixture is heated. The absorption cycle takes place as follows:

1. The mixture is separated in the generator by heating.
2. The solute (gas) is condensed, and it rejects heat to the ambient space. The solute is then expanded and later evaporated by heat collected from the refrigerated space (as in traditional cooling systems).
3. The heated solute is then mixed with the solvent in the absorber.
4. The mixture is pumped to the generator and preheated by a heat exchanger with pure solvent coming from the generator.
5. The mixture is heated again in the generator, closing the cycle.

Single-effect and double-effect cycles are the most common processes in absorption cooling. Figure 12 shows a schematic diagram of single and double-effect absorption cycles. The most commonly used working mixture in solar absorption systems are lithium bromide and water ammonia. Marcriss et al. [107] also reported on other combinations of working mixtures.

Solar adsorption cooling processes are entirely different from the absorption processes. The physical principle behind adsorption cooling is a surface-based phenomenon in which a porous material (adsorbent) captures vapor from a fluid (refrigerant) and the adsorbent is regenerated by heating. Adsorption processes differ from absorption because the working mixture consists of a solid–fluid

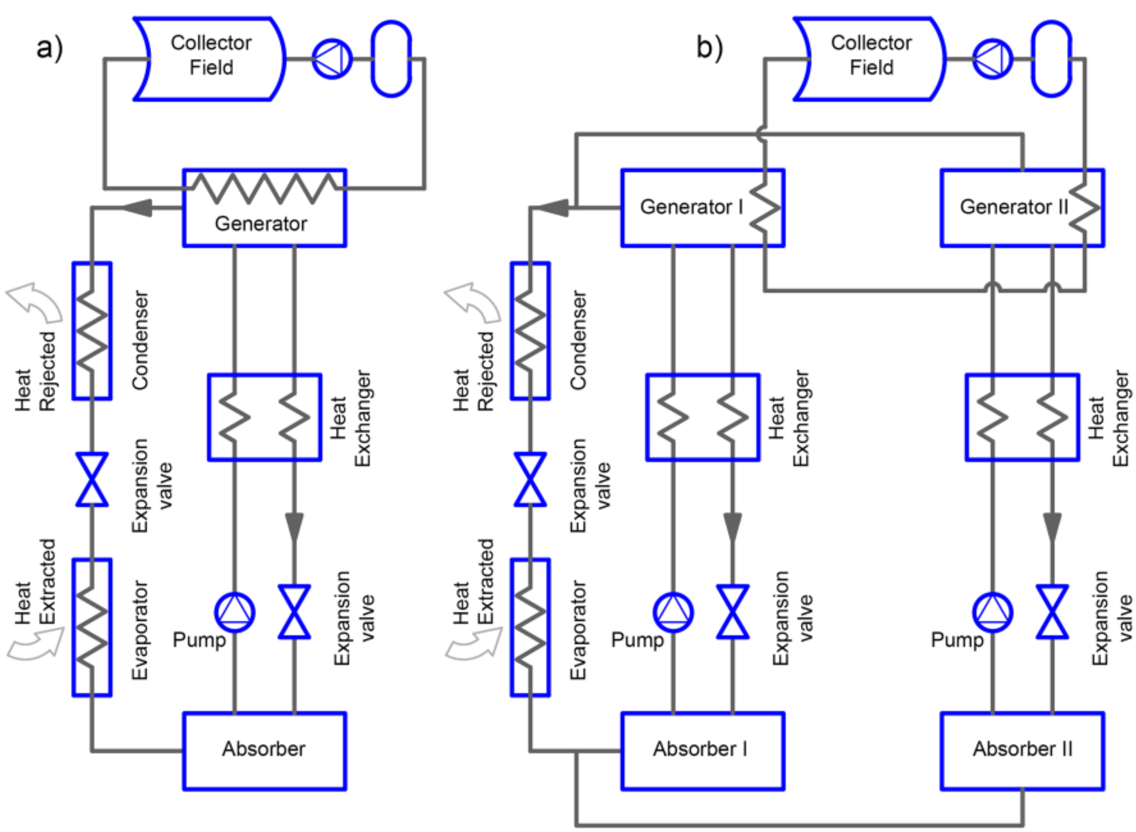

Figure 12: Solar-assisted absorption diagrams: (a) single effect, (b) double effect.

combination and moreover heating is intermittent, not a continuous one (the adsorbent is heated whenever it is saturated) [108]. Adsorption cycles require very low or no mechanical or electrical input but need thermal input (e.g., from the collector field) which is very important, and it works intermittently with the solar resource. A simple adsorption system cycle diagram is shown by Figure 13 and the cycle of working is as follows:

1. The refrigerant is evaporated by heat from the refrigerated space.
2. The vaporized refrigerant is adsorbed in the adsorption chamber.
3. When the adsorption chamber gets heated, the vapor is released and then condensed, resulting in the rejection of heat to the ambient space.
4. The condensates are stored in a tank.
5. Finally, the condensates are evaporated again, closing the cycle.

In solar adsorption cooling, nonconcentrating technologies (such as flat plates or evacuated tubes) are most frequently used. Nevertheless, some literatures suggest good performance for an adsorption cooling pilot plant with PTC technology compared to nonconcentrating technologies. Li et al. [109] conducted an experimental study about an ice maker using a 20-m^2 PTC and 30 kg of $CaCl_2$ + activated carbon, obtaining a coefficient of performance (COP) up to 0.15 and a production of 50 kg under typical summer day in Shanghai. Further, a thermal model of a cooling system using PTCs as generator and activated carbon methanol as working mixture was proposed by Tashtoush et al. [110]. Fadar et al. [111,112] conducted a

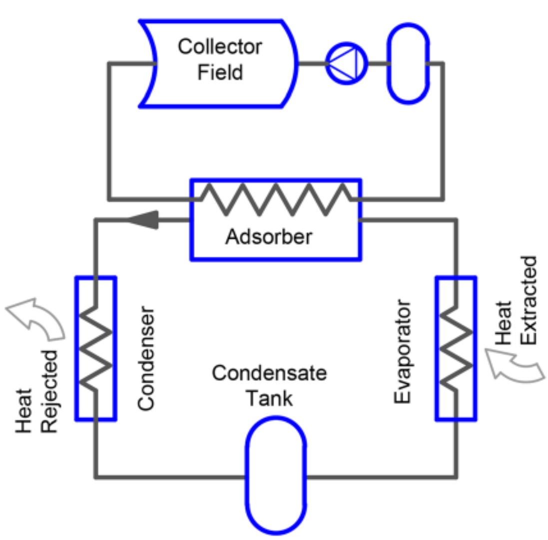

Figure 13: Simple intermittent solar-assisted adsorption diagram.

theoretical and optimization study about an adsorption cooling system using PTCs and activated carbon ammonia, realizing an optimum operational COP of up to 0.18. In addition, a prototype of solar cooling system driven by PTCs for use in remote areas was designed successfully by Abu-Hamdeh et al. [113]. They realized a statistical optimization of the system obtaining a 3.5- to 5-m^2 PTC and an average COP of 0.18–0.2. The most commonly used adsorbent materials are zeolite, activated carbon, and silica gel, and the most commonly used refrigerants are ammonia, methanol, and water. Sumathy et al. [114], Masesh [115], and Fernandes et al. [116] analyzed and reviewed solar adsorption processes as well as the material characteristics of adsorption working mixtures.

Chemical adsorption is another method for cooling. It is based on a reaction between the adsorbent and refrigerant that form a strong chemical bond, increasing heat transfer. The main disadvantage of chemical adsorption is that it cannot be easily reversed as higher amount of energy is needed to break the chemical bond, and the chemical reaction alters the state of both adsorbent and refrigerant in a continuous operation. The most used adsorbent for chemical adsorption is calcium chloride, which can make a working pair with either water or ammonia.

The general advantage of solar cooling technologies is lower energy consumption compare to the conventional vapor-compressor systems. The working pair (in a liquid phase) is pumped in solar absorption cooling rather than using a compressor as in conventional cooling processes, and there is almost no mechanical input in adsorption cooling, as described earlier. So the energy consumption is drastically reduced here. Other advantages are low noise and low vibration because of fewer moving parts. The principal disadvantage is their low COP, with a COP of around 0.7 for single-effect absorption, 1.2 for double-effect absorption, and 0.1–0.2 for adsorption [117], compared with a COP of 3–4 for conventional vapor-compression systems.

Cabrera et al. [118] analyzed the use of solar cooling technologies with PTC systems. They also have given a list of PTC-based solar cooling facilities installed around the world, where most of them used small PTCs. The authors state that the advantages of PTCs over conventional collectors used in solar cooling are their lower thermal losses, higher working temperature, smaller collector area, and no risk of stagnation. The principal disadvantages are the increase in capital cost (due to tracking and other components), geographical limitations, and interruption during windy conditions. Further, they also concluded that the cost of energy of cooling systems using PTCs are the same or lower compared with conventional nonconcentrating technologies used in solar cooling.

3.3 Seawater desalination

Seawater desalination is a process in which minerals are separated from seawater to produce fresh water. Many methods are used for separating salts from seawater in industry, and they are classified into four groups as represented in Figure 14. Thermal processes (phase change) uses thermal energy to separate the brine and the most commonly used methods are multistage flash and multieffect distillation (MED). Single-phase processes use mechanical separation by passing seawater through filter membranes where salts are trapped, and reverse osmosis (RO) and forward osmosis are the most frequently used methods. Electric processes are based on cationic and anionic ion-exchange effects. In this electrolysis process, cathode and anode membranes are arranged alternately and exposed to an electric field, so that salt particles are trapped during the process and separated from seawater. The principal methods of electric processes are electro-dialysis, ion exchange, and capacitive deionization. Hybrid processes usually mix phase change with single-phase processes, such as membrane distillation method.

Solar seawater desalination with PTC technology participates directly only in phase-change processes as PTCs provide thermal energy. However, there are some reports on single-phase processes powered by thermal cycles based on PTCs. Ortega-Delgado et al. [119] performed computational simulations for thermoeconomic comparison analysis of an MED and RO systems coupled to a Direct Steam Generation-CSP plant driven by PTCs that produced 5 MWe.

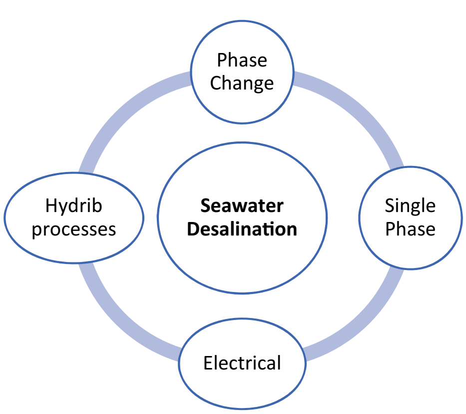

Figure 14: Classification of seawater desalination processes.

Further, a preliminary analysis of an RO plant driven by a solar-heated Rankine power system was performed by García-Rodríguez and Delgado-Torres [120]. They concluded that these types of systems show lower specific solar energy consumption when compared to solar distillation and PV-driven RO systems, resulting in an interesting cost-effective development. Delgado-Torres et al. [121] made a preliminary design of an RO plant which was coupled to a solar thermal-powered Rankine cycle and compared the use of two PTC models (LS-3 and IND300) in the solar system. Nafey and Sharaf [122] simulated a solar-assisted organic Rankine cycle that powers an RO system and then analyzed and compared the parameters using flat-plate, compound parabolic, and parabolic trough solar collectors and different working fluids. They concluded that "according to the current techno-economic framework, the PTC system is the best option." Buenaventura and García-Rodríguez [123] conducted a study about market potential of thermal-powered desalination technology, concluding that a stand-alone RO desalination plant driven by one-axis concentrating collectors (PTCs and LFCs) coupled to a ORC cycle has very good marketing opportunities. Iaquaniello et al. [124] presented a model that the potential of integrating CSP technology into a combined fossil-fueled/solar plant to power an MED/RO desalination plant. They concluded that desalination processes powered by solar (especially CSP) technology have become very attractive in the Middle East and North African countries. According to Ref. [116], with the proposed configuration plant, it is possible to produce fresh water with costs under USD 1.2/m^3. It is important to note the impact of PTC technology on CSP plants and others solar concentrating systems (see Section 3.1).

Brine and fresh water are separated by heating seawater in thermal processes and the process is represented in Figure 15a. Seawater is heated so that water is vaporized, which is physically separated from salt because of its lower boiling point. The water vapor then condenses, leaving fresh water. A Rankine cycle provides the necessary electrical energy to pressurize the seawater and pump it through the membranes in single-phase processes, as shown in Figure 15b. The Rankine cycle operates as a CSP plant (see Section 3.1).

Both thermal processes and membrane processes have advantages and disadvantages over each other. The main ones are described as follows [125]:

- Thermal systems' advantages over membrane systems: proven and established technology, higher quality product, less rigid monitoring required than for membrane processes, less impacted by quality changes in feed water, and no membrane replacement costs.

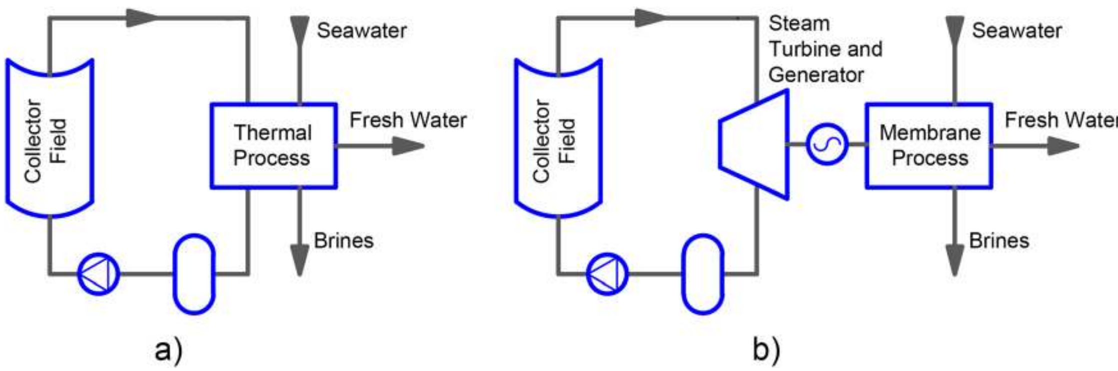

Figure 15: General schematic diagram for desalination: (a) phase change, (b) single phase.

- Membrane systems' advantages over thermal systems: lower capital cost and energy requirements, smaller footprint and higher space/production ratio, higher recovery ratios, modularity allows for upgrades or downgrades and minimal interruption to operation when maintenance or a membrane replacement is required, less vulnerable to corrosion and scaling due to ambient temperature operation, and membranes reject microbial contamination.

RO is the mostly used desalination method worldwide, because of its low energy consumption compared with the phase-change processes. This technology has a market share of around 59% of worldwide desalination capacity [126]. Thermal processes are suitable for medium- and small-scale plants. Sharon and Reddy [127] made a review of solar desalination and they reported information by comparing the performance of desalination methods with factors such as capacity, energy consumption, and efficiency. The data from Sharon and Reddy on the three methods mentioned in this work are exhibited in Table 9. Li et al. [128] reviewed the recent investigation of solar-assisted desalination, and they also discussed modeled and experimental pilot plant installations of desalination using PTCs and other solar technologies. Further Reif and Alhalabi [129] analyzed and presented a review of potential benefits and challenges in cost-effectiveness, energy efficiency, and requirements and other parameters of solar-driven desalination. According to Aboelmaaref et al. [130], hybrid MED/RO desalination systems using PTC technology is a potential option for desalination since it has higher reliability, higher efficiency, and lower cost.

3.4 Water decontamination

Decontamination is the process of removing hazardous compounds such as heavy metals, organic compounds, and chemical substances from water. Advanced oxidation processes (AOPs) offer a feasible and sustainable alternative for disinfection of water. General applications of AOPs include the degradation of resistant material prior to a biological treatment and treatment of refractory organic compounds [131]. The methods for treatment of hazardous organic and inorganic compounds are reviewed by Kabra et al. [132]. They presented a list of previous studies on the removal of heavy metals using photocatalysis process. AOPs generate a high concentration of oxidants (usually hydroxyl radical, OH^-) to oxidize polluting matter that would not be easy to separate by biological degradation. There are some AOPs that use UV radiation as an energy source to produce the oxidants. But heterogeneous photocatalysis (HPC) with TiO_2 and photo-Fenton process (PFP) is the most commonly used

Table 9: Comparison of technology performance for desalination [127]

Technology	Capacity (m^3/d)	Energy consumption (kW h/m^3)	Efficiency (%)	Recovery ratio (%)
MSF	0.009–10	<144	NA	0.6–6
MED	20–3,000	2.5–8.0 (electric) 50–194 (thermal)	NA	6–38
RO	1,000–5,000	2.1–3.0	20–25	20

NA: no data available.

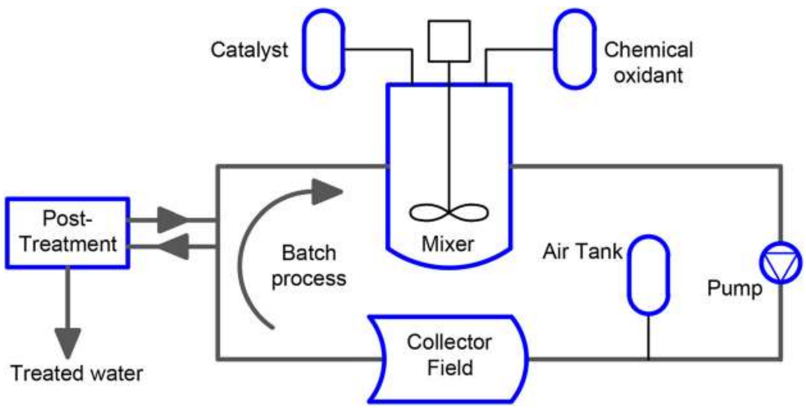

Figure 16: Solar-assisted wastewater treatment plant diagram.

methods in solar applications. These processes generate hydroxyl radicals (*OH) when UV radiation activates the catalyst in an atmosphere with oxygen. A review on decontamination by photocatalysis and comparison of HPC and PFP reactor design requirements were presented by Malato et al. [133].

Solar decontamination is usually realized in batch mode [134,135], as shown in Figure 16. General purposes of water decontamination are performed for drinking water or agricultural applications [136]. Initially the catalyst is mixed in water to suspend particles in the fluid and then the mixture is pumped to the solar field to undergo the chemical processes before returning to the mixer. This process repeats continuously until the pollutants are degraded. The collector has the same characteristics as explained before, but the receiver is replaced with a glass pipe that is transparent to solar UV radiation. Ironically, the first photoreactors developed were based on PTC technology only [133], but nonconcentrating collector (NCC) and compound parabolic collector technologies have improved a lot in the few decades. Table 10 represents the comparison of these technologies. It is not very difficult to compare solar decontamination systems against conventional systems, which is an obstacle to industrial application. But solar photocatalysis is a promising technology when compared to others because of its low impact, according to Malato et al. [133] analysis.

3.5 Concentrating PVs

Concentrating PV (CPV) generation is the direct conversion of solar energy into electrical energy using semiconductor materials. Photoelectric effect is the basic principle behind the operation of the solar cell and that effect generates a potential difference within a semiconductor when it is exposed to sunlight. The information about PV cells appeared in the late nineteenth century but the first performance test records of PV cells under concentrated light occurred in the early 1960s [137]. Research on PV concentrator (PVC) technology has increased since then, and now PTC technology can actively participate in this application due to its advantages and maturity. PVC systems with PTCs have the same equipment as flat-plate PV collectors such as converters, batteries, and voltage regulators because both collectors provide direct current.

PVC operates in the same way as thermal concentrator but works with a modified receiver with PV cells on its surface. Concentrated sunlight strikes the PV cells, and PV cells convert solar radiation into electricity. The cells generate more energy under concentrated sunlight due to the incident energy density, and it is shown in Figure 17a. It is a fact that PV cells do not convert all the incident energy into electricity and most of this rejected energy is converted into heat, which lead to temperature of the cell to increase, affecting its efficiency (Figure 17b). The fluid used in the cells will be flowing inside the receiver. These collectors are known as thermal-PVCs (T-PVCs). PV cells used in concentrating PVs are designed to resist high incident radiation, so the use of Si-based cells fully depends on the concentration factor of the PVCs, as represented in Table 11.

Principal advantages of PVCs over nonconcentrating PV systems is that they have a higher efficiency and require fewer PV cells. Today, a number of PV cells operate under high concentrated sunlight with higher efficiencies compared to the common Si-based cells, as shown in Figure 18. Green et al. [139] presented a list of efficiencies of PV cells and modules for PV technologies. CPVs is still

Table 10: Comparison of collector technologies for decontamination processes

Technology	Advantages	Disadvantages
PTC	- Smaller size of reactors - High volumetric flow (turbulent flow) - Better mass transfer - Low catalyst load - No vaporization of compounds	- It needs direct solar beam radiation - High costs - Mayor optical losses - Low water overheating - Low quantum efficiency
NCC	- High optical efficiency - Use direct and diffuse radiation - Design simple and easy - Low cost - No overheating	- High sizes of reactors - Low mass transfer and volumetric flow (only laminar flow) - Reactant evaporation and contamination (if open) - Weather resistance, chemical inertness and UV transmission
CPC	- Smaller size of reactors - High volumetric flow (turbulent flow) - Better mass transfer - Use direct and diffuse radiation - Low catalyst load	- Difficult to scaled up - Moderate heat generation - Moderate capital cost

under development and it is not yet a commercially proven technology. But it has a good future potential. Karathanassis et al. [140] designed a parabolic trough of 2 m^2 aperture area T-PVC prototype evaluated the thermal and optical performance. They also described the design procedure and technical challenges of the technology. They obtained an overall efficiency of 50% (thermal efficiency of 44% and electrical efficiency of 6%), a temperature rise of 3.5–4 K, and an energy cost of around €1.75/W. The optical performance of a two-stage T-PVC with spectral beam splitting filter using a ray-tracing technique was evaluated by Jiang et al. [141]. They found a reduction in heat loads pf up to 20.7% in the cells. The performance of a prototype using four different solar cells in the array (mono-crystalline Si, poly-crystalline Si, Super cell, and GaAs) was evaluated by Li et al. [142,143]. Further, a technical–economic analysis of combined heat and power solar generators was performed by Quaia et al. [144], concluding that the combined efficiency of this technology is remarkable but not worthy when evaluated separately in terms of the cost of energy. Yazdanifard et al. [145] simulated a parabolic trough T-PVC model focusing on energy and exergy performance with laminar and turbulent flow regimes using nanofluids. It is found that nanofluids can increase the performance (both energetic and exergetic) in T-PVC when compared with NCCs. Mendelsohn et al. [146] made a review of the development of the PV technology in the United States (concentrating and nonconcentrating) and reported a total gain of 471 MW under contract projects.

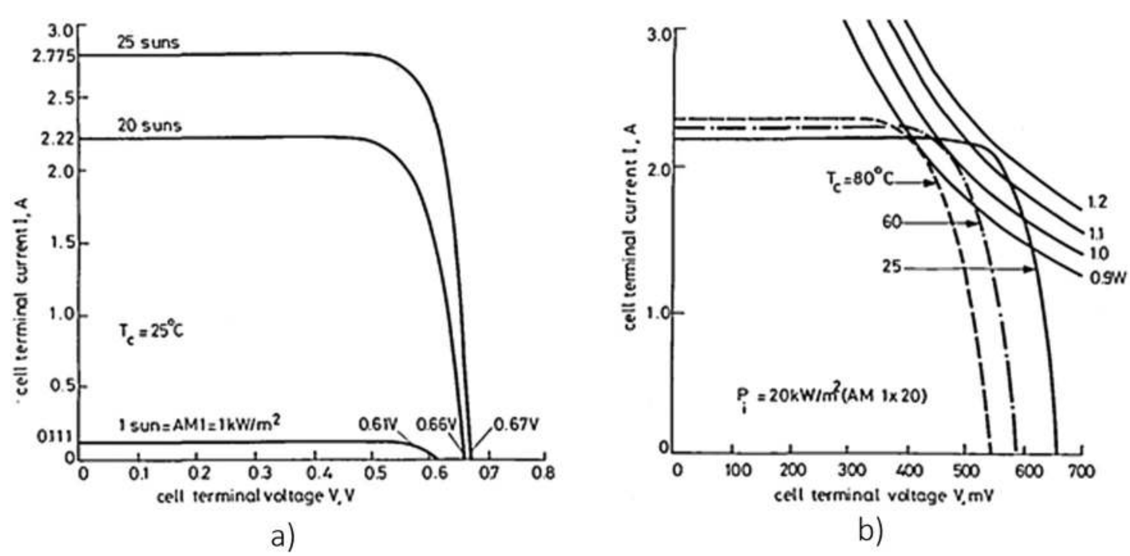

Figure 17: Typical current/voltage characteristics in silicon cells (a) at three different solar direct isolations and constant cell temperature and (b) at three different cell temperatures and constant solar isolation. (Retrieved from: Zakzouk A, Electrochem M, Mujahid A, El-Shobokshy M. Performance evaluation of photovoltaic silicon cells under concentrated sunlight. Solid-St Electron Dev, IEEE Proceedings I. 1984;131(2):66–72 [138].)

Table 11: Characteristics of concentrating photovoltaic applications

Concentration type	Concentration factor	Collector type	Cell type
High	>400	PD	Multijunction
Medium	3–100	PTC, LFC	Silicon and others
Low	3	CPC	Silicon

4 Market overview and economics

This section presents a general status of PTC technology in energy market and economics. There is also a brief description of economic concepts such as cost of energy, estimated prices of components, investment, and O&M of energy systems using PTC. In addition, the future trends of the technology from the economical point of view are also described.

4.1 General status in power-generation market

The utilization of renewable technologies in the international power-generation market has increased steeply in recent years all around the world. The principal reason is the growing interest of governments in implementing renewable energy generation systems to mitigate greenhouse gas (GHG) emissions and provide better energy security. Around 150 countries implemented energy improvement policies, and approximately 128 countries established energy efficiency strategies and targets at the end of 2015 [147]. Figure 19 represents the evolution of countries with renewable energy targets around the world.

One of the most important applications for PTC technology is generation of electricity (CSP plants). The installed capacity of CSP plants has increased in the last decade (as shown in Figure 20), with the United States and Spain being the major contributors in solar thermal power generation. PTC-based solar thermal systems are mostly used in electricity generation systems, accounting for approximately 85% of total current installed capacity worldwide [1]. The US national renewable energy laboratory (NREL), in collaboration with the international program SolarPACES, has compiled data on existing and projected power plants that use solar concentration. A list of those plants is available on the internet and can be classified by technology, country, or status [148]. Figure 21 shows the statuses of installed, under construction, and projected CSP plants.

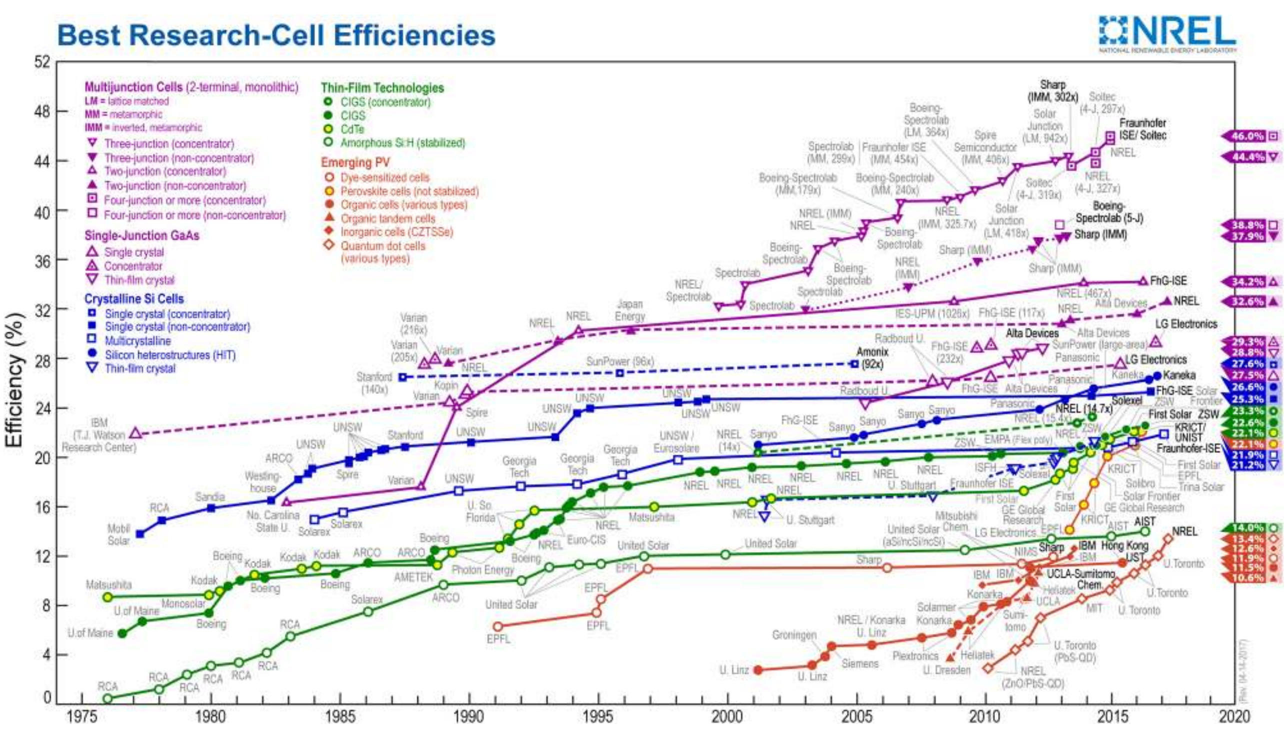

Figure 18: Evolution of solar cell technologies. (Retrieved from the NREL website: www.nrel.gov/pv.)

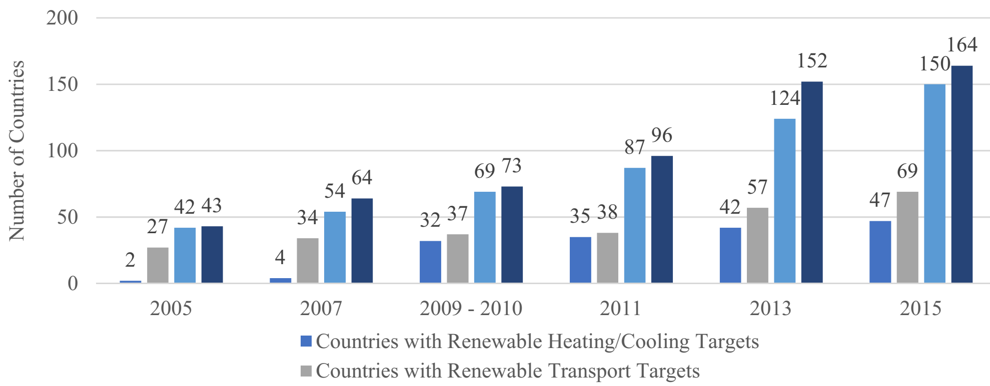

Figure 19: Countries with renewable energy targets. (Retrieved from the Resource IRENA website: resourceirena.irena.org/gateway/.)

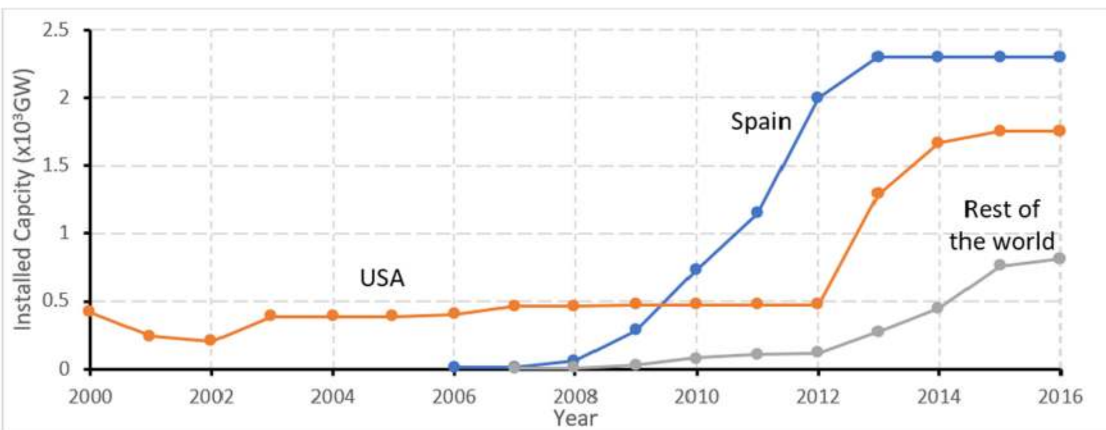

Figure 20: Time series of CSP plants installed capacity. (Data retrieved from the Resource IRENA website: resourceirena.irena.org/gateway/.)

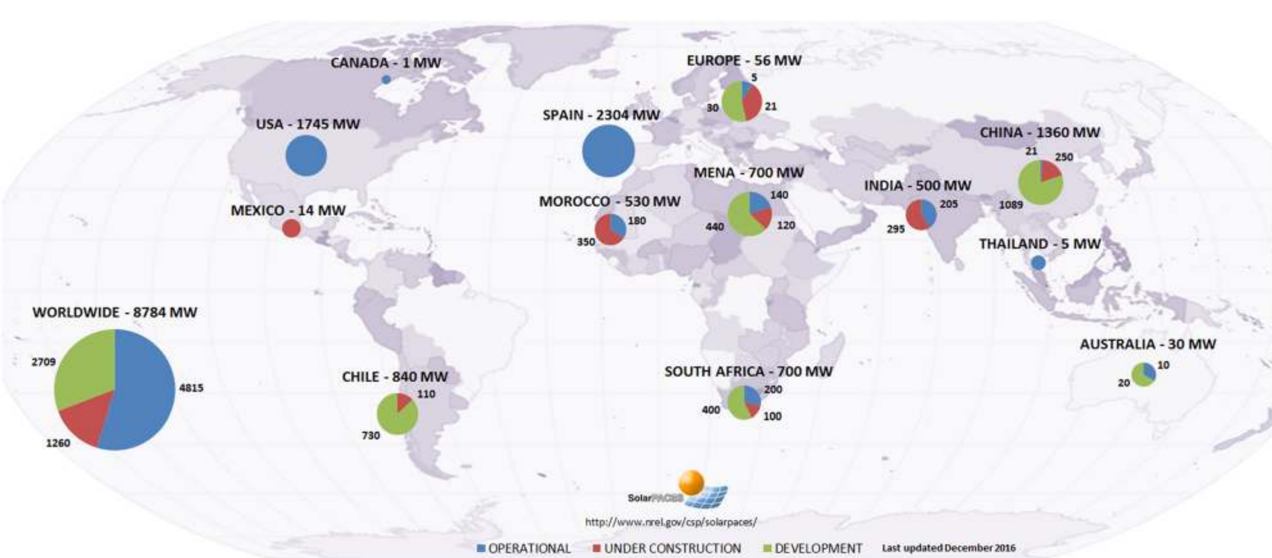

Figure 21: Concentrating solar power plants around the world. (Retrieved from the SolarPACES website: www.solarpaces.org.)

4.2 General status in SHIP market

The demand of thermal energy in industry was around 85.3EJ in 2014, equivalent to 74% of industrial energy needs [149]. Nearly 52% of this demand is involved in low- to medium-temperature heating applications, and this shows that there is a high potential of SHIPs for industrial thermal energy supply. As shown in Ref. [100], there are many industrial processes where PTC technology can be applied.

PTCs are one of the technologies used in SHIPs that have recently been developed and implemented in small- to medium-scale plants around the world. Small-aperture collectors are the mostly used PTCs in these applications, which can reach temperatures up to 250°C [150]. Nowadays, the technology applied to SHIPs is still under development. But a number of installations and collectors with substantial technical improvements have been reported all around the world (see Section 3.1 and Ref. [98]), with good performance and economics during the last years [151]. Figure 22 displays the evolution of every-year installed thermal power, collector area, and number of projects of PTC systems for SHIPs around the world, based on Ref. [90]. But a falling trend occurred between 2008 and 2011, and this trend could be caused by worldwide crisis known as "the great recession" that started on 2008 in the United States and also affected some European states in 2010s. Spain for example (one of the major contributors of developing solar technology) was affected due to this crisis until 2014. In addition, it has been reported that 18 companies produce PTCs, which represent approximately the 25.4% of enterprises that provide solar collectors for SHIPs [140]. IEA SHC Task 49 has made an effort in research to integrate solar heating technology and industrial heat supply systems efficiently.

The principal advantages of this technology are its reduced risk (compared with volatility of fossil fuel prices), zero fuel cost, localized production, and low GHG emission. Nonetheless, it still needs to overcome the barriers of the investment cost and complexity of the systems to have a good penetration into industry. Lack of transfer of technical information, suitable design guidelines, and analysis tools are other barriers [152].

4.3 General status in cooling and desalination applications

Nowadays, the market of cooling systems is generally dominated by nonconcentrating technologies. Up to 3% of the installed capacity is driven by concentrated technologies [153]. Nonetheless, concentrating technologies are suitable to be connected to solar-assisted double-effect absorption systems in locations where there is high solar radiation (e.g., Southern Europe or North America) [154]. IEA SHC Task 53 is making effort to assist in the sustainability of solar-driven cooling systems and heating in buildings [155].

In desalination applications, it is noted that PTC technology is still under development for proven installations. The potential of solar energy application in desalination applications was also reviewed by Buenaventura and García-Rodríguez [156]. They also compared the different methods and technologies used. They concluded that RO/PTC system-driven organic Rankine cycle has great potential in the market.

4.4 Economics

Four key economic factors are used in market analysis. The first (and most important) factor is the levelized cost of energy (LCOE). This cost indicates the equivalent

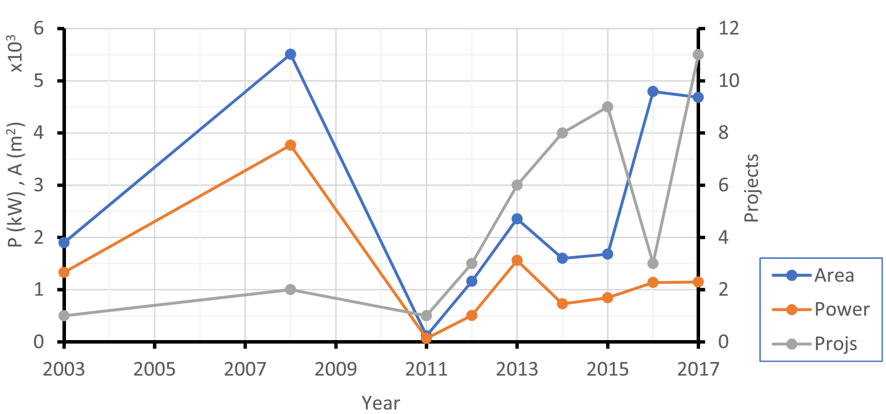

Figure 22: Technical every-year evolution of SHIP plants.

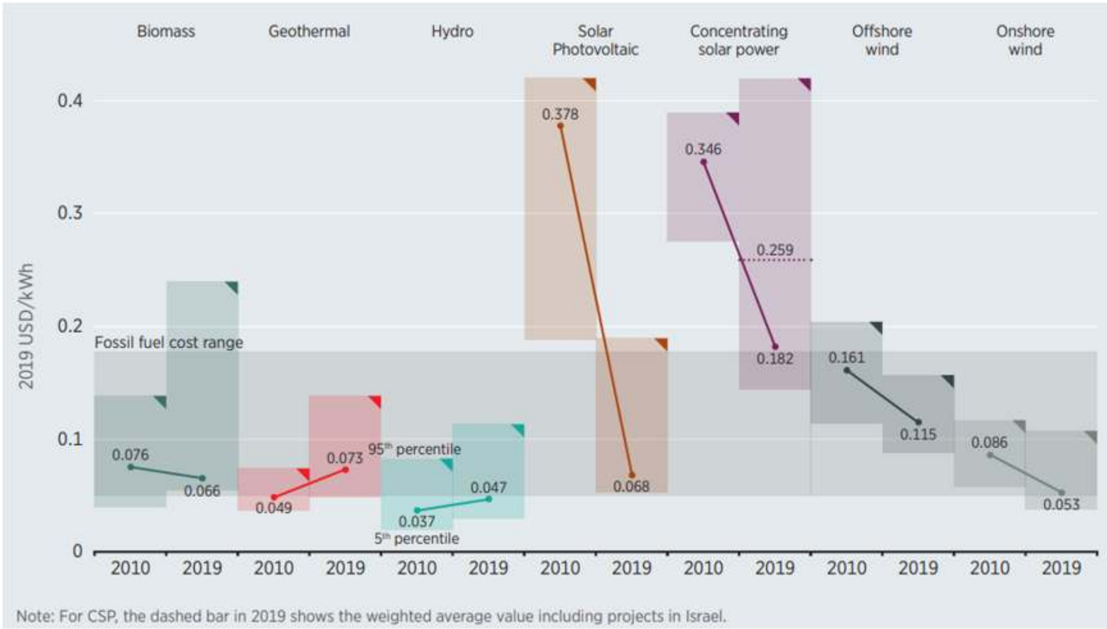

Figure 23: LCOE for electricity generation of some renewable technologies, from 2010 to 2019. (Retrieved from: IRENA (2020), Renewable Power Generation Costs in 2019, International Renewable Energy Agency, Abu Dhabi. [157].)

payback for energy generation during the lifetime of the project. LCOE consists of the investment expenditures, O&M costs, fuel costs, the discount rate, and total energy generated. Figure 23 displays a comparison of the LCOE of different renewable technologies and their behaviors over the past few years. It is found that (thermal and PV) the trend is downward for solar energy. Despite this tendency, solar thermal power generation with PTCs is still not competitive to conventional fossil fuel technologies. But PTC technology has a good potential for development and implementation in power generation due to its advantages over other CSP technologies.

The second factor is the capital cost (also called capital expenditure or CAPEX), which represents around 84% of LCOE [158]. The CAPEX represents the direct costs (materials and equipment), indirect costs (i.e., contingencies), and the owner's costs (land preparation, project development, and others) of the system. Table 12 gives an idea about the estimated breakdown of the capital costs for a 50-MW/7.5 h TES PTC-based CSP plant [2]. The major cost is contributed by the cost of the PTC system (38.5%), where the steel construction, receivers, mirrors, and HTF system represent the other important components of capital cost (29.6% approximately). The investment cost of equipment for PTCs is related to CAPEX. This cost is usually represented as cost of collectors per unit of aperture area. Table 13 gives the breakdown of the average cost of collectors based on two designs with costs between

Table 12: CAPEX distribution for a CSP plants with PTCs [3]

Item	Cost (million 2010 US$)	Share (%)
Site and solar field	62.4	17.1
PTC system	140.3	38.5
Mirrors	23.1	6.4
Receivers	25.9	7.1
Steel construction	39.0	10.7
Pylons	3.9	1.1
Foundations	7.8	2.1
Trackers	1.6	0.4
Swivel joints	2.6	0.7
HTF system	19.5	5.4
HTF	7.8	2.1
Electronics	9.1	2.5
TES block	38.4	10.5
Power block	52	14.3
Others	71	19.5
Total	364	100

Table 13: Breakdown of material costs

Item	Share (%)
Framework	33.232
Mirrors	20.525
Receivers	13.493
Supports	10.231
Drive	7.835
Others	14.683

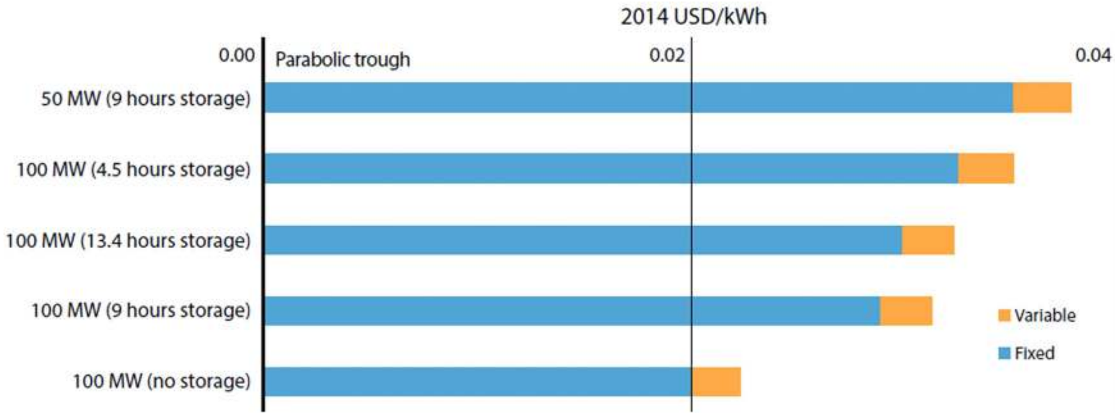

Figure 24: O&M costs for CSP with PTC. (Retrieved from: IRENA (2015), Renewable Power Generation Costs in 2014 [1].)

$170 and $178 per m^2 of aperture (costs based on 2010 USD) [159]. The framework, receivers, and mirrors represent almost 70% of the cost of the collector, according to this information.

The third factor is the O&M cost and it is around 11% of the LCOE [158]. O&M costs are estimated to be between USD $0.02 and USD $0.04/kW h, as shown in Figure 24. But O&M costs depend on the capacity of the plant and the TES system. Fixed costs depend upon the capacity of the plant, and variable costs are related to energy generation costs. Replacement of receivers (e.g., because of a glass breakage) and replacement and cleaning of mirrors are the most significant components of the O&M costs. Finally, the installed cost is another important factor in economics, which is the CAPEX cost per unit power. Table 14 shows a description of these costs.

Table 15 shows some estimated prices of PTCs used in SHIPs in the case of small-aperture PTCs. Most of the PTC systems used in these applications can produce up to 2 MW. Figure 25 shows the evolution of every-year total investment and average costs of PTC systems for SHIPs around the world based on [98]. It shows an increment in investment for installing new systems while the cost tends to slow down.

4.5 Future trends

Installed costs and LCOE are predicted to fall around 30% over the next decade. The total reductions and shares predicted for the total installed cost, LCOE, indirect and owner's costs and investment based on a 160-MW/7.5 h TES CSP plant with PTCs is shown in Table 16 [158]. Technological improvements and installation and operational experiences from long-scale plants are the contributing factors for cost reduction. As an example, the transition of thermal oil to molten salt as HTF could lead to a more efficient operation. Heat exchangers for thermal oil and molten salts are no longer needed under this condition (but require an antifreeze system), and it will also permit operation of the TES block at the same time with fewer requirements [158]. Recent advances in glass materials have reduced the rate of breakage, which further decreased the O&M costs, but advances in mirrors must also be made. Improvements in automatization can also be a significant reducer of O&M costs.

The LCOE of CSP plants is expected to be competitive with other solar technologies in the near future. CPV technology has a good potential for implementation, even with its current uncertainty in market and technology

Table 14: Installed costs for CSP plants with PTCs [158]

TES	Country	Cost (2015 USD $/kW)
No	OECD	4,800–8,000
	Non-OECD	3,500–7,300
Yes (≈8 h)[a]	—	6,100–8,100

[a] Since 2013.

Table 15: Cost of PTCs used in SHIPs [152]

Specific power (kW/m^2)	Location	Cost of collectors ($/m^2)	Installed cost ($/kW)
0.50–0.56	Europe	650	1,160–1,300
0.22–0.28	India	445	1,580–2,040
0.55–0.7	Mexico	400–629	570–1,100

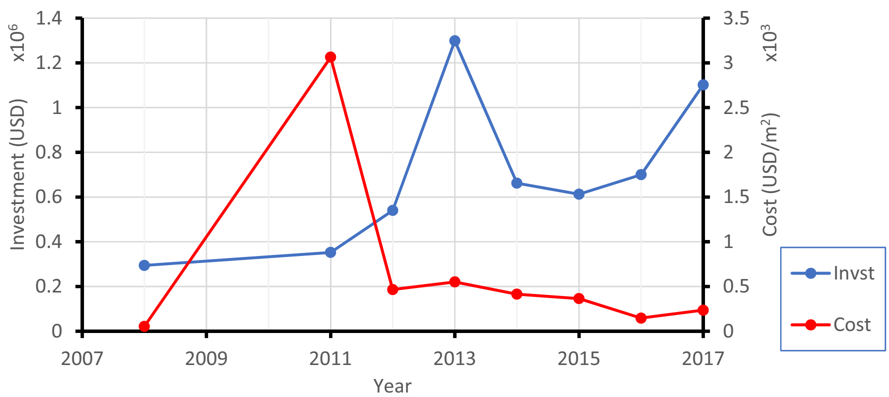

Figure 25: Economic every-year evolution of SHIP plants.

development. The LCOE of concentrating technologies is predicted to be competitive when compared with conventional solar PV electricity generation, as shown in Figure 26. The principal reason of cost reduction is the requirement of lower amount of material for conversion and the decrease in cost of PV cell in recent years.

For small-aperture PTCs, the technology still needs to be upgraded for effective utilization in industry, taking their advantages and using experiences in SHIPs and other small- to medium-scale applications. However, the actual tendency shows an overall increment in interest, investment, and development of this technology [152], principally for industrial thermal energy supply. IEA considers that there is potential market and technological development as there is around 28% of the overall demand for thermal energy in European Union countries in the heat processes with temperatures below 250°C [162]. For efficient use of solar-assisted cooling, the major efforts lie on the integrability of the solar collector system to thermal-driven cooling systems and economic competitiveness when compared with the conventional cooling systems.

5 Thermal performance and modeling

Thermal performance analysis provides the quantity of energy that a collector system can supply to a load, which is important in the design of systems used in industries.

Table 16: Predictions of cost reductions for CSP plants [158,160]

Cost	Component	Share (%)	Actual cost (2,015)	Projected cost (2,025)	Total reduction (%)
Total installed ($/kW)	Solar field	34	5,550	3,700	33
	Indirect costs	24			
	Owner's costs	22			
	Others (power block and TES)	20			
LCOE ($/kW h)	Performance improvement	30	0.165	0.104	37
	O&M costs	2			
	CAPEX (direct)	39			
	CAPEX (indirect)	29			
Indirect and Owner's ($/kW)	Profit margin and contingencies	29	1,338	535	60
	Other indirect costs	18			
	Project development	43			
	Land infrastructure	10			
Investmenta ($)	HTF system (incl. HTF)	34	356	274	23
	Structure and supports	33			
	Receivers	15			
	Others (site preparation, mirrors, drivers, and cabling)	18			

[a] Based on a cost of US$52/$m^2$ for collectors.

There are many studies on thermal analysis and computational tools for measuring PTC system performance used in industry. Thermal performances are evaluated by either mathematical models or experiments. Mathematical models use thermodynamics formulas to compute thermal performance. Experiments are based on field measurements taken to obtain a more realistic performance. The principal advantage of experiments is that they consider complex phenomena (implicit in the measurements) that may be difficult to incorporate into models. The advantages of mathematical models are their simplicity and low cost when compared to experiments. These two models or groups are classified as shown in Figure 27.

Experimental methods may be based on indoor or outdoor analysis, as shown in Figure 27. Indoor analysis is used to testing of receivers for heat losses, whereas outdoor testing is for thermal performance of collectors. Atmospheric factors, such as wind or ambient temperature, are either totally or partially controlled in indoor testing. However, these factors are not at all controlled for outdoor experiments. Many studies in the literature described experiments using indoor and outdoor testing related to PTC technology. Table 17 shows some of these studies found in the literature. Standards are recommended to provide guidelines about instrument quality and how to proceed with the measurements to obtain accurate results. ASHRAE 93, ISO 9806, and SRCC 600 are the most commonly used standards for thermal performance analysis with PTCs. These and other standards are described in the next section. Several studies about the methodologies of mathematical modeling of thermal performanceare available in the literature; some of them include validation with experiments. Table 18 shows a few of these studies with a brief description of the approaches used for thermal modeling of PTC technology. Yilmaz and Mwesigye [205] performed a review about thermal and optical performance studies for thermohydraulic analysis with PTC, which included inserts, nanofluids, and SG. The literatures about thermal performance of PTC system adapted to desalination processes are reported by Aboelmaaref et al. [130]. A summary about thermal and optical modeling implemented in simulation tools of direct SG systems using PTC technology was provided by Sandá et al. [206]. Daneshazarian et al. [207] have given a report about thermal and electrical performance assessments for T-PVCs by comparing some types of collectors. It is found that CPV systems integrated to a PTC can reach up to 70 and 25% as the overall thermal and electrical efficiencies, respectively.

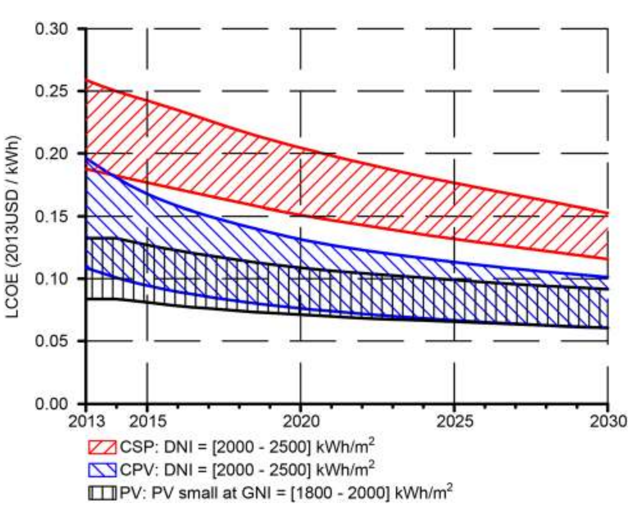

Figure 26: LCOE trend for electricity generation of solar concentrating in places with high solar radiation. (Retrieved from: Philipps S, Bett A, Horowitz K, Kurtz S. Current status of concentrator photovoltaic (CPV) technology. Golden (CO, USA): NREL; 2016. Report No. NREL/TP-6A20-63916 [161].)

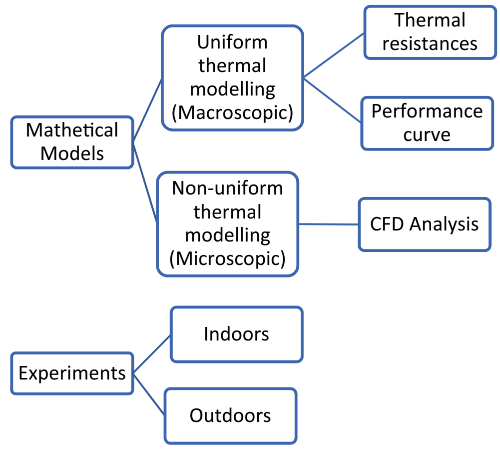

Figure 27: Classification of thermal performance methods.

Thermal performance analysis with thermal resistance modeling and thermal parameter characterization (performance curve) are the most frequently used methods in energy balance for a macroscopic approach. But CFD modeling is the most common methodology used for a microscopic approach. One-dimensional and steady-state heat transfer is the most common assumption made throughout the literature in modeling of the thermal behavior of PTCs. Unfortunately, there are no design criteria in the literature for thermal performance evaluation. However, the methods discussed here will be useful for performance analysis of new design or models of collectors.

Thermal resistance modeling consists of simulating the heat transfer phenomena (convection, conduction, and radiation) using thermal circuits, which are analogous to electric circuits. In this model, surfaces are represented by

Table 17: Experimental studies of collectors

Authors	Ref.	Element (Size)	Model	Test	Procedure	Characteristic equation
Burkholder and Kutscher	[163]	Receiver	UVAC3	Thermal losses	Indoor	$\dot{q}_l = 0.26\Delta T_{ab} + 1.05 \times 10^{-8}\Delta T_{ab}^4$
Pempeintner et al.	[164]	Receiver	PTR70	Thermal losses	Indoor	$\dot{q}_l = 0.176\Delta T_{ab} + 8.14 \times 10^{-9}\Delta T_{ab}^4$ a
Burkholder and Kutscher	[165]	Receiver	PTR70	Thermal losses	Indoor	$\dot{q}_l = 0.141\Delta T_{ab} + 6.48 \times 10^{-9}\Delta T_{ab}^4$
Janotte et al.	[166,167]	Collector (large)	HelioTrough	Themal performance	Outdoor	$\frac{Q}{A} = 0.816 I_b K(\theta) - 0.0622\Delta T_f - 0.00023\Delta T_f^2 - 2653\frac{dT_{1ave}}{dt}$
European Commission	[168]	Collector (large)	EuroTrough	Thermal performance	Outdoor	$\eta = 0.7408 - 4.7851 \times 10^{-5}\Delta T_f - 5.58399 \times 10^{-7}\Delta T_f^2$
Fernández-García et al.	[169]	Collector (small)	CAPSOL 01	Thermal/optical performance	Outdoor	$\eta = 0.63 + 4 \times 10^{-4}\Delta T_f - 1.4 \times 10^{-5}\Delta T_f^2$
Fernández-Reche	[170]	Collector (small)	CAPSOL 01	Photogrammetry	Indoor	NA
Moss and Brosseau	[171]	Collector (large)	LS-2	Thermal performance	Outdoor	$\eta = 0.7859 - 3.57 \times 10^{-4}\Delta T_f - 4.33 \times 10^{-8}\Delta T_f^2$
Dudley et al.	[172]	Collector (large)	LS-2	Thermal performance	Outdoor	$\eta = [0.733 - 7.276 \times 10^{-5}\Delta T_f] K(\theta) - 4.96 \times 10^{-3} T_r - 6.91 \times 10^{-4} T_r^2$ b
Dudley et al.	[173]	Collector (small)	IST	Thermal performance	Outdoor	$\eta = [0.7625 - 6.8366 \times 10^{-5}\Delta T_f] K(\theta) - 0.1468 T_r - 1.672 \times 10^{-3} T_r^2$ c
Brooks	[174]	Collector (small)	—	Thermal performance	Outdoor	$\eta = 0.5381 - 1.0595 T_r$ d
Valenzuela et al.	[175]	Collector (large)	URSSA	Themal/optical performance	Outdoor	$\eta = 0.768 K(\theta) - 6.343 \times 10^{-2} T_r - 2.074 \times 10^{-9} T_r^4$
Sallaberry et al.	[176]	Collector (large)	URSSA	Thermal performance	Outdoor	$\frac{Q}{A} = 0.681 I_b K(\theta) - 2.96 \times 10^{-9}\Delta T_f^4 - 1671\frac{dT_{1ave}}{dt}$ e
McMahan et al.	[177]	Collector (large)/ r eceiver	SkyTrough/ PTR80	Optical efficiency/thermal losses	Outdoor	$\dot{q}_l = 6.41 + 0.308\Delta T_f - 1.95 \times 10^{-3} T_{1ave}^2 + 7.29 \times 10^{-6} T_{1ave}^3 + 1.08 \times 10^{-7} I_b K(\theta)\cos(\theta) T_{1ave}^2 + [0.205\Delta T_f - 2.89]\sqrt{V_w}$
Brost et al.	[178]	Collector (large)	SkyTrough	Optical measurement	NA	NA
Hoste and Schuknecht	[179]	Collector (large)	SkyTrough	Thermal performance	Outdoor	NA
Balghouthi	[180]	Collector (small)	NA	Thermal/optical performance	Outdoor	$\eta = 0.5816 - 1.1777 T_r$
Janotte et al.	[181]	Collector (small)	PTC 1800	Thermal performance	Outdoor	$\frac{Q}{A} = 0.683 I_b K(\theta) + 0.012 I_d - 0.0046\Delta T_f^2 - 2100\frac{dT_{1ave}}{dt}$ f
Alfellag	[182]	Collector (small)	NA	Thermal performance	Outdoor	NA

NA: no data available.
[a] Obtained based on data given in the report. [b] Evacuated receiver with Cermet SC. [c] Nonevacuated receiver, with black-nickel SC and Solgel glass. [d] Glazed receiver. [e] Without soiling factor. [f] Quasi-dynamic model.

Table 18: Studies and models of thermal analysis of PTCs

Authors	Year	Ref.	Analysis		State		Dimensions			Experiments		Description
			Macroscopic	Microscopic	Steady	Transient	1-D	2-D	3-D	Indoor	Outdoor	
Kalogirou et al.	1997	[183]	x			x	x				√	Thermal analysis and parametric optimization model for a PTC system with energy storage for direct SG. Thermal performance parameters of the collector are required
Forristal	2003	[184]	x		x		x	*			√	Thermal resistance model with energy balance around the receiver. The author reported four models, one of them analyzes a series PTC system with pressure drop
Lüpfert et al.	2008	[185]									x	Experimental comparison of three methodologies (steady-state, quasi-dynamic, and surface temperature measurement) to obtain heat losses in a receiver
García-Valladares y Velázquez	2009	[186]	x			x	x				√	Discretized thermal model to compare radial heat transfer in tubular and annular flow in the receiver. Annular flow is analyzed as a counter flow heat exchanger
Schiricke et al.	2009	[187]									x	Experimental study of optical efficiency of a PTC using photogrammetry and heat flux measurement. Ray-tracing simulation is used to compare the results
Montes et al	2010	[188]	x		x		x	*				Numerical study based on energy and exergy balance of a CSP plant to compare thermal performance with 4 HTFs. The thermal model used is a thermal resistance circuit, but the study does not specify the conditions and details of this model
Qu et al.	2010	[189]	x			x	x				NA	Thermal analysis of a heating/absorption cooling system for a building. The thermal model is based on thermal parameters of the collector. Simulations are realized using TRNSYS
Montes et al.	2011	[190]	NA			NA	x					Thermoeconomic analysis of a combined cycle power plant using a PTC system to heat the steam, compared with a nonsolar-assisted power plant
Powell y Edgard	2011	[191]		x		x	x					Thermal analysis model based on energy balance for a receiver and thermal storage of an SG plant. The mathematical model is based on numerical resolution of governing equations using finite-difference method

Table 18: Continued

Authors	Year	Ref.	Analysis		State		Dimensions			Experiments		Description
			Macroscopic	Microscopic	Steady	Transient	1-D	2-D	3-D	Indoor	Outdoor	
Roesle et al.	2011	[192]		x	x			x		NA		Thermal analysis of an evacuated receiver with nonuniform angular radiation flux using CFD simulations
Vázquez-Padilla et al.	2011	[193]	x		x		x				√	Thermal analysis using thermal resistance energy balance model with pressure drop. Comparison with experimental data and Forristal's thermal model
Kalogirou	2012	[194]	x		x		x				√	Thermal resistance model with energy balance around a glass-covered receiver. This model is similar to the Forristal's model, but it does not consider heat losses by brackets
Roldán et al.	2012	[195]		x	x				x		√	CFD simulation of a receiver used in direct SG plant. Superheated steam is the HTF. Surface temperature measurements are used as experimental validation
Zaversky et al.	2012	[196]										Probabilistic thermal model to obtain useful energy of a PTC system using Latin hypercube method
Lobón et al.	2013	[197]		x	x				x		√	Thermal analysis of a PTC system for direct SG. Different conditions of pressure, temperature, incident radiation, and mass flow are analyzed. The method used is CFD simulation using k–ε turbulence model
Silva et al.	2013	[198]	x			x			x		√	Thermohydraulic analysis with 3-D nonlinear heat transfer model in transient state for an SG PTC system. Simulations are realized in SolTrace, TRNSYS, and Modelica (a code developed by the authors) simultaneously. Comparison with experimental data is presented in the study
Valenzuela et al.	2014	[175]									x	Experimental methodology to obtain the thermo-optical performance of a PTC with outdoor tests
Xu et al.	2014	[199]									x	Comparison of three experimental methods (ASHRAE 93, EN 12975-2 and a dynamic method presented by the authors) to determine thermal performance
Biencinto et al.	2015	[200]	x			x	x				x	Thermal performance analysis of a PTC system for direct SG. A quasi-dynamic method is used. It is based on finite-difference method in temporal

Table 18: Continued

Authors	Year	Ref.	Analysis		State		Dimensions			Experiments		Description
			Macroscopic	Microscopic	Steady	Transient	1-D	2-D	3-D	Indoor	Outdoor	
												dimension and thermal performance parameter of the collector
Bellos et al.	2016	[201]		x	NA				NA		x	Comparative study in thermal enhancement of a PTC using nanofluids (oil based) and conventional fluids (oil and pressurized water). Inner surface configurations (smooth and corrugated) in the pipe receiver are also compared
Toghyani et al.	2016	[202]	x		x		x					Thermodynamic analysis of a PTC system integrated to a Rankine cycle power plant. Thermal performance of oil-based nanofluid with four different nanoparticles is compared
Widyolar et al.	2016	[203]		x	x				NA		NA	Design, simulating and test of a two-stage reflective hybrid thermal/photovoltaic PTC. Finite-element analysis is used for thermal analysis, ray tracing for optical performance, and efficiency parameter for electric performance
Srivastara and Reddy	2017	[204]		x	x				x			Numerical study of hybrid thermal/photovoltaic PTC and secondary reflector. Various configurations for solar cells are analyzed. Nanofluid is used for cooling the solar cells. ASAP is used for optical performance, and finite volume method for thermal analysis

√ Validated with experiments. * Hydrodynamics with pressure drop. NA No data available.

thermal nodes, temperature differences correspond to voltage potentials, and heat transfer rates correspond to the currents. Figure 28 displays the thermal model used by Forristal to analyze a glass-covered receiver [184]; in which an energy balance is made at the outer and inner surfaces of the glass and the pipe of the receiver, which is represented by Eq. 1–4. This model used experimental correlations for convection heat transfer and theoretical equations for conduction and radiation. Salgado et al. [208] analyzed thermal performance of PTCs with a description of the mathematical models used in the literature.

$$\text{Node 2 (inner side of pipe)}: \dot{q}_{1\text{ave}2,\text{conv}} = \dot{q}_{23,\text{cond}} \tag{1}$$

$$\text{Node 3 (outer side of pipe)}: \dot{q}_3 = \dot{q}_{23,\text{cond}} + \dot{q}_{34,\text{conv}} + \dot{q}_{34,\text{rad}} + \dot{q}_{3\text{s},\text{cond}} \tag{2}$$

$$\text{Node 4 (inner side of cover glass)}: \dot{q}_{34,\text{conv}} + \dot{q}_{34,\text{rad}} = \dot{q}_{45,\text{cond}} \tag{3}$$

$$\text{Node 5 (outer side of cover glass)}: \dot{q}_{45,\text{cond}} + \dot{q}_5 = \dot{q}_{5\text{a},\text{conv}} + \dot{q}_{5\text{c},\text{rad}} \tag{4}$$

Thermal parameter characterization uses mathematical models of thermal performance as expressed by standards, i.e., Eq. 5, which is the quasi-dynamic thermal model of standard ISO 9806-2017 for concentrating collectors with a glass-covered receiver and a concentrating factor (C_r) higher than 20 (usual for PTCs). The constants η_{peak}, a_1, a_3, and a_5, and the function $K(\theta)$ of the model are obtained by a regression analysis of experimental data. Each collector model has its own constants, so using this method it is not possible to design a system with a noncharacterized PTC. Characterized collector and receiver models (e.g., LS-2 or EuroTrough) are discussed in the literature, which make it possible to obtain the thermal performance constants. Table 17 gives specific thermal performance equations for a variety of PTC models and receivers available in the market. It is noticed that there are some mathematical models developed for thermal performance of PTCs, i.e., URSSA Trough uses a 4th-power polynomial steady-state model for thermal efficiency [175], SkyTrough uses a temperature-based cubic model in which the effect of the wind on thermal losses is included [177], and other collectors (LS-2, IST, CAPSOL, and EuroTrough) use a quadratic steady-state model. Figure 29 shows thermal efficiency curves of some large-sized PTCs based on experimental data reported in references presented in Table 17 (URSSA trough is shown using [175] under normal incidence and $I_b = 1{,}000\ \text{W/m}^2$). Differences in the thermal behavior of these PTCs are noticed.

$$\frac{Q}{A} = \eta_{\text{peak}} K(\theta) I_b - a_1(T_{1\text{ave}} - T_a) - a_3(T_{1\text{ave}} - T_a)^4 - a_5 \frac{dT_{1\text{ave}}}{dt} \tag{5}$$

Discretization, which consists of approximating partial differential equations using a system of algebraic equations, is the important aspect for microscopic analysis. The control volume of analysis (continuous domain) is divided into smaller volumes (discretized domain) and then the differential equations are solved for each small volume. Finite-difference analysis (FDA), finite volume analysis (FVA), and finite-element analysis (FEA) are the common methods used in microscopic analysis of thermal performance. FDA uses truncated series expansions for partial derivatives (usually a Taylor series) and a regular discretization of the domain. This method is very simple and easy to apply in simple geometric shapes. But it is not suitable for cases when many elements are required or a higher order in an expansion series is needed to increase accuracy. FVA and FEA are useful for irregular shapes of

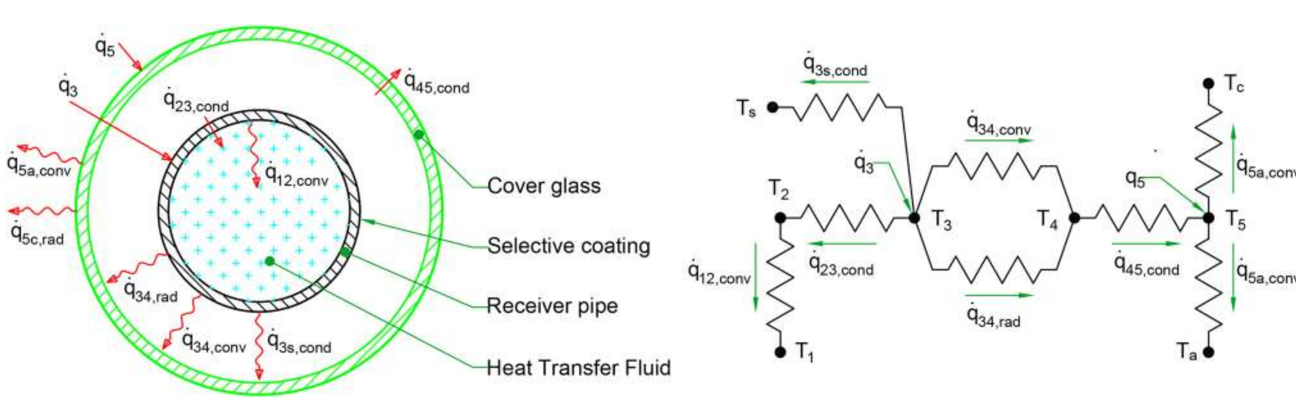

Figure 28: Receiver boundary and thermal resistance model. (Retrieved from: Brooks MJ. Performance of a parabolic trough solar collector [Master's thesis]. Stellenbosch (ZA): University of Stellenbosch; 2005 [174].)

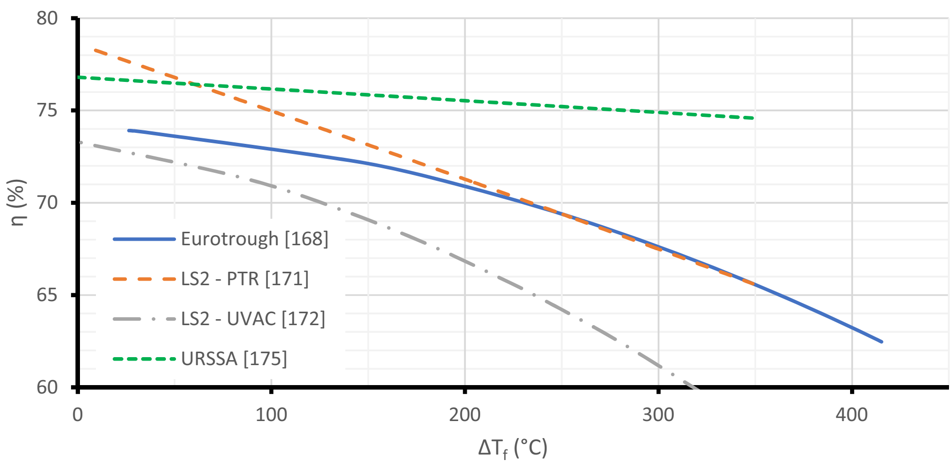

Figure 29: Thermal efficiency curves of large-sized PTCs.

control volume domain or when elements of different sizes or shapes (mesh) need to be used.

As discussed in Section 2.4, nanofluids enhance thermal performance of collectors. Nevertheless, other methods increase heat transfer coefficient, and here the heat transfer coefficient is increased by using turbulators. A turbulator is an element used to create turbulence in the flow inside the receiver. In the literature, many studies are available about thermal enhancement using turbulators, and many of them are reported in Ref. [209–212].

The most common turbulators are listed as follows: Inserts are generally elements fixed to a smooth pipe. The objective of these elements is to enhance thermal performance by swirling the flow of the HTF. Generally twisted tapes are used as the most common inserts.
Vortex generators are protrusions or dimples from the internal surface of the receiver. The flow adopts the shape of the protrusion, so turbulence is generated, enhancing thermal performance.

Baffles are a type of turbulator that deviate the flow of the HTF. The enhancement is made by interrupting both thermal and hydraulic boundary layers and forcing the flowing fluids to hit the internal surface of the pipe. Baffles can also be hollowed to reduce a high drop in pressure in the flow.

Fins are extended surfaces in the internal surface of the receiver. Fins enhance thermal performance by increasing the heat transfer surface area. They can also be twisted to generate a double effect on the swirled flow (i.e., wire coils).

The other important parameter affecting the thermal performance of PTCs is optical efficiency, which measures the quantity of energy in the receiver compared to the energy flux in the collection area. The optical efficiency of a collector (η_{op}) depends on the transmittance of the cover glass (τ_{cg}), the absorptivity of the SC (α_{sc}), the reflectance of the mirrors (ρ_m), and the incident angle modifier ($K(\theta)$), as expressed in Eq. 6. It is known that the shape of mirrors and receiver alignments are not perfect in practical applications, so it also involves a random error. This error is measured by the interception factor (γ), which combines the effects of misalignments and slope random error in mirrors.

$$\eta_{op} = \eta_{op,0} K(\theta) F_c = [\gamma \tau_{cg} \alpha_{sc} \rho_m] K(\theta) F_c \tag{6}$$

Ray-tracing techniques are employed to obtain an estimation of interception factor of a PTC. These methods simulate the propagation of light through media and surfaces with specific optical properties such as reflection, refraction, diffraction, and scattering. The most commonly used method is Monte Carlo ray tracing, which is based on probability distribution functions for predicting light ray paths. Photogrammetry is widely used for experimental measurement of interception factor. This method and other experimental methods were described by Arancibia-Bulnes et al. [17]. Osório et al. [213] compared different ray-tracing software available for linear focusing collectors, where the comparison of simulations was conducted for LFCs and PTCs. Section 2.1 addressed the guidelines and gave some hints about reflectance measurement. The measurement of absorptance and transmittance was addressed in Section 2.3. All the optical properties including the interception factor and the normal-incidence optical efficiency (when the incidence angle is 0°) are estimated.

During normal operation, PTCs are not always at 0° incidence angle and the optical efficiency gets affected.

The incidence angle modifier $K(\theta)$ takes into account the optical losses due to no-normal incidence during operation (such as end-effect losses). This factor is usually measured by experiments. The other important factor is the soiling factor, F_c, which represents the ratio between the real-operation and nominal-clear mirror reflectance. During normal operation, cleaning the mirrors (washing) is a requirement for good performance, and this affects reflectance. For PTCs, the common values of soiling factor are between 0.95 and 1 [58].

Commercial software tools are available in the market to realize thermal, thermoeconomic, or optical analysis in PTCs. Software with PTC systems usually uses the thermal parameters of collectors for thermal analysis. Table 19 exhibits these tools and their characteristics and capabilities. Many software tools are available for CFD analysis (such as STAR-CD, Autodesk CFD, SimFlow, etc.), but Fluent and Comsol are the most popular CFD software tools for FVA and FEA, respectively.

It is important to estimate the losses when focusing on optimizing a specific parameter or strategy in maintenance, which can lead to a better performance of the PTC system. Forristal [184] reported about contribution of thermal and optical losses in a PTC using the mathematical model developed by him. He proved that the heat losses by conduction through the brackets can go up to 3% of the overall heat losses. Convective losses in the receiver by wind can go up to 12 and 105% in conditions of loss vacuum and broken glass, respectively. Incidence angle and reflectivity do have a large impact on performance. The report indicated that thermal performance can reduce around 15% at an incidence angle of 30° and 65% at an incidence angle of 60°. It was also found that a drop of 0.15 in reflectivity can lead to a decrement of 24.5% thermal performance, and an error of 5% in estimating mirror reflectivity is similar to a change of 7% in thermal performance.

Apart from the thermal and optical performance, it is important to analyze the structural performance. The design of supporting structure impacts not only performance but also the costs (see Section 4.2). Structural analysis is important to design a rigid structure, so that it can maintain a parabolic shape of the receivers and ensure that they are located in the focal line of the cylindrical parabola, as fabricated with the EuroTrough PTC [36]. Design criteria for structural analysis of PTCs were also proposed by Giannuzzi et al. [25]. They presented a methodology for estimating structural loads due to wind, snow, or temperature based on European standards for structural analysis.

6 Standards for performance evaluation of PTCs

Experiments are required to validate data from numerical models and provide information on the performance of PTCs under field operation conditions and for ensuring their reliability. Standards prescribe the requirements for good and reliable operation and also the performance measurement data for this method of testing. A number of standards are related to PTC technology, but a brief explanation of the important ones is presented in this study. Standards can be divided into three groups: standards for collectors (as one element), standards for systems (principally related with CSP generation), and standards for components and materials.

6.1 Standards for reliability and performance of collectors

These groups of standards provide guidelines to evaluate the reliability and/or performance by considering the collector as a separated element (unit), and they do not consider the subsystems or other components related to the final application of the collectors. Reliability tests simulate critical conditions that can severely damage a collector under normal operation. The requirements and conditions of the tests are stated in each standard. Performance tests are related specifically with thermal performance (and electrical performance, in the case of T-PVCs). Each standard specifies the procedures of the tests and instruments to be used (including their recommended quality). The principal difference among all the standards is the required tests and conditions used for testing. Fernández-García et al. [221] presented the development of a test loop for thermal performance evaluation of a small-sized PTC model and a comparison under different testing conditions (with experimental results) of standards applicable for thermal performance of PTCs. They report some experimental conditions (i.e., time sampling, or uncertainties of instrumentation) which are recommended for optimal thermal performance testing. Table 20 gives an idea about the recommended tests among the standards related to thermal performance of PTC. Each standard is explained in the following sections.

6.1.1 ASTM E-905

This standard describes a methodology for determining the thermal performance of collectors with tracking systems and concentrating factors greater than or equal to seven, so that

Table 19: Software tools used for analysis with PTCs [214–220]

Name	Developer	Analysis	Method	General capabilities	Strengths/Weaknesses
Advanced system analysis program (ASAP)	Breault Research Organization Inc.	Optical performance	Ray Tracing by Gaussian beam decomposition	- Scattering, diffraction, absorption, refraction and other optical effects - Visible, infrared and ultraviolet light sources - It can also simulate random directional errors (for mirrors)	- Gaussian-beam decomposition treats the light as a wave rather than as a particle (as usual Monte Carlo methods) - Compatible with other CAD programs to simulate complex shapes - Not free software
Fluent	ANSYS Inc.	Thermo-/ hydrodynamics	CFD by FVA	- Fluid mechanics, heat and mass transfer for different volume element forms and boundary conditions - Single-phase or multiphase flow with multidimensional analysis in steady or transient state - Gray, not-gray or reflective surfaces (with specular and/or diffuse properties) - Refraction, absorption, dispersion effects, and even scattering in gases for radiation	- Compatible with other CAD programs - Use an external software to configurated the mesh-grid, materials and boundary conditions - Not free software - It needs a reconfiguration (from the beginning) of all the analysis if the design changes
Comsol	Comsol Inc.	Thermo-/ hydrodynamics	CFD by FEA	- Fluid mechanics, heat and mass transfer for different volume element forms and boundary conditions - Single-phase or multiphase flow with multidimensional analysis in steady or transient state - Radiation heat transfer with absorption, emission, scattering in transparent, opaque or participating media gases	- Compatible with other CAD programs - Meshing component is integrated to the software - Quick convergence with Multiphysics phenomena - Not free software - It needs a re-configuration (from the beginning) of all the analysis if the design changes
Solar advisor model (SAM)	NREL	Thermoeconomics	Energy balance and cash flows	- Thermoeconomic analysis of on-grid power-generation systems for decision making on renewable technologies - Parametric optimization and sensitivity analysis	- For not only renewable energy-based systems, but also conventional fossil-fueled power systems - It can simulate various configurations at the same time - Free software - Limited design with precoded or characterized collector models

Table 19: Continued

Name	Developer	Analysis	Method	General capabilities	Strengths/Weaknesses
SolTrace	NREL	Optical performance	Ray tracing by Monte Carlo method	- Single or multiple planar or curved reflective surfaces - Specific direction and intensity of the rays	- Exclusive for concentrating solar technology - Definition of surfaces by coordinates - Free software
Thermoflex	Thermoflow Inc.	Thermoeconomics	Energy balance and cash flows	- Thermoeconomic analysis of off-grid power-generation systems for decision making on nonrenewable technologies - Power systems with PTC for renewable resource power generation	- Software specialized in conventional power plant design - It can analyze one system at a time - Not free software
Transient system simulation (TRNSYS)	University of Wisconsin	Thermal analysis	Energy balance	- Dynamic system analysis - Industrial, traffic, biological and other processes - The system is simulated by interconnecting the components programed in modules (libraries)	- It simulates transient behavior of systems - Compatible with engineering equation solver - Not free software - Limited design with precoded or characterized collector models

Table 20: Reliability and performance tests included in each standard [222–224,227]

Standard	ASTM E-905	ISO 9806	FSEC 102	SRCC 600
Scope				
SLHC	√	√	√	√
SAHC	NS	√	√	√
T/PV	X	√	X	√
Durability/reliability tests				
Internal pressure	X	√	√	√
Preexposure	X	√	X	√
Leakage/pressure drop[a]	X	√	√	√
Rupture/collapse[a]	X	√	X	X
Max. temp. resistance	X	√	X	X
Stagnation temp.	X	√	X	X
Exposure	X	√	√	√
External thermal shock	X	√	√	√
Internal thermal schock	X	√	√	√
Rain penetration	X	√	X	X
Freeze resistance	X	√	X	X
Mechanical load	X	√	X	X
Impact resistance	X	√	X	√
Protection system	X	X	X	√
Final inspection	X	√	√	√
Thermal performance				
Time constant (τ)	√	√	√	√
Thermal efficiency for SLHC	√	√	√	√
Thermal efficiency for SAHC	NS	√	√	√
Thermal capacity	X	√	X	√
IAM	√	√	√	√
Mathematical model	NS	Polynomial	Depends on the fluid used	Polynomial
State	Steady	Quasi-dynamic		Quasi-dynamic
Test conditions	Clear sky	Clear/partly cloudy sky		Clear/partly cloudy sky
Minimum solar irradiance of tests (W/m^2)	630	800	800	800
Minimum data points	4	4	4	4
Test duration	Max. of 5 min/0.5τ	Max. of 15 min/4τ	*	Max. of 15 min/4τ

SLHC: solar liquid heating collector; √: included; SAHC: solar air heating collector; X: not included; T/PV: thermal/photovoltaic; NS: not specified.
[a] Only for SAHCs.

the effects of diffuse irradiance become insignificant. It can be applied to collectors with one-axis or full-tracking, single-inlet/single-outlet of single-phase fluid and in steady-state conditions. The standard does not include safety or durability. The latest update was made in 2013. This standard provides four tests for one-axis tracking concentrators: response time (to determine the time constant), incidence angle modifier, near-normal incidence angular range for determining heat gain, and heat gain near-normal incidence [222]. Two methods to determine the response time are by abruptly shading the collector and abruptly irradiating the collector. Procedures similar to ASHRAE 93 are presented for heat gain and $K(\theta)$. The standard divides the tests for each type of collector evaluated (single axis or full tracking).

6.1.2 FSEC 102

The Florida solar energy center (FSEC) presented a standard for the evaluation of reliability and thermal performance of solar collectors. It also provides methodologies for reliability tests and thermal performance. It can be applied for both liquid and air heating collectors and also for concentrating and NCCs. Three types of water heating collectors are municipal water (called “street pressure solar collectors”), low-pressure service hot water/swimming pool, and hybrid/alternative fluid solar collectors. The pressure and connection to service water differ in all three types of liquid heating collectors.

This standard presents the minimum requirements for certification of collectors regarding its reliability.

It is similar to SRCC standard 600 and also has the same minimum tests as SRCC 600, except for the impact and protection system test. The standard divides the analysis for thermal performance according to the fluid used. For all parameters (time constant, thermal efficiency, and $K(\theta)$), the procedures established in ASHRAE 93 are used in air heating collectors, and in liquid heating collectors the procedures are used according to ISO 9806 [223]. The last update of the standard was made in 2010.

6.1.3 ISO 9806

ISO 9806 is another important evaluation standard. This standard also provides a methodology for evaluating the reliability and thermal performance of the collector. It is applicable for nonconcentrating and concentrating solar collectors with a single-phase fluid (liquid or air) or hybrid-type (thermal-PV), single-inlet/single-outlet of single-phase HTF, and without storage as part of the collector [224]. This standard replaced EN 12975 to unify methods for evaluating thermal and durability in a single methodology [225]. This standard presents various methods for evaluating thermal performance, but concentrating collectors are evaluated using a quasi-dynamic method. The mathematical model is similar to the model used in EN 12975. In 2017, the last update was made to the standard.

This standard divides the test into two parts, namely, reliability tests and thermal performance tests. The reliability tests evaluate the durability and resistance of each part of the collector. Thirteen tests evaluate the potential failure modes of collectors, such as cracking, corrosion, buckling, and rain penetration. The key difference with other standards is the number of tests and the conditions stated for conducting tests, as shown in Ref. [226].

Further, this standard evaluates the same characteristics for thermal evaluation as ASHRAE 93 (which is withdrawn) but under different conditions and the time constant is optional. The procedures are similar to the standards mentioned earlier; the difference is the state of the conditions and measurements done during the test, as shown in Table 20 and Ref. [226]. This standard also presents a method for estimating the pressure drop across the collector. It also provides a data sheet for recording the test results.

6.1.4 SRCC standard 600

The SRCC standard 600 provides minimum requirements to certify a collector as safe, reliable, and efficient. It is applicable for concentrating collectors with active or passive controls and without thermal storage as part of the collector. Even flat-plate collectors with lenses or reflective panels are considered concentrating collector by this standard. It is also applicable for collectors with hybrid thermal-PV collectors. The last update of the standard was made in 2014.

SRCC standard 600 mainly references to ISO 9806 and EN 12975. It establishes that both durability and thermal performance tests should be performed as described in ISO 9806, but it only presents seven durability tests as the minimum criteria (plus protection system test) [227]. The thermal procedures required by the standards are based on the quasi-dynamic model, but the main differences are the wind speed and type of testing done after the exposure test. For T-PVCs, the performance is divided into electrical and thermal performance. Electrical performance test is based on International Electrotechnical Commission (IEC) 61925 with open circuit.

6.1.5 IEC 62108

This standard establishes the minimum requirements for the qualification of a concentrating PV module with crystalline silicon solar cells for terrestrial use. This standard evaluates the thermal, mechanical, and electrical reliability of a concentrator in long-exposure climates. The methodology of analysis involves the testing sequence for characterization and after that the collector is tested under aging conditions. Finally, it is again characterized by the testing sequence to determine degradation. The sequence of the tests is similar to the procedures described in IEC 61215 (standard for flat-plate PV collectors) but features of CPV receivers such as tracking alignment, high current density, and rapid temperature change are also considered. For example, the thermal cycling test consists of analyzing change in temperature gradient of the receivers and verifying whether it can withstand large temperature gradients due to variable incident radiation flux that occurs during normal operation (cloudy days) [228]. It is not exclusive for PTC but may be generally used for any type of concentrator with a PV or thermal-PV output [229]. The latest update was made in 2007, but now a revised version of this standard is available [230].

6.2 Standards for solar thermal systems with PTCs

Contrary to the above standards, this standard provides guidelines to evaluate the performance of a solar thermal system driven by PTCs as a unit. They are applicable in power generation, so the tests consider not only the solar field but also the TES system or thermal-to-electrical conversion systems. A brief explanation of the principal standards related to the CSP plant performance are presented in the following sections.

6.2.1 AENOR UNE Standards for solar thermal systems

Since 2015 the Spanish association AENOR has presented some standards for testing and qualifying a CSP plant using PTC technology exclusively (STs are not included in this standards). The standards are designed based on the experience of CSP plants in Spain, where 90% of the solar power plants have PTC technology. These standards are applicable for CSP plants of any size, with optional nonsolar backup systems and/or TES system. Three standards applicable for solar thermal systems are as follows.

- UNE 206010: The key features analyzed by the standard are availability of solar energy, power consumption, net power generation, nonsolar energy supply (backup), and net plant efficiency [231]. Other features of the plant are not at all considered in the standard. Further, it also provides general guidelines for instrumentation, estimation of plant performance parameters, and reporting of results. This standard is applicable not only for new CSP plants but also for plants that are online, allowing identifying possible operational problems.
- UNE 206012: This standard presents guidelines to determine the performance and functional characterization of indirect active liquid-state sensible-heat TESs in solar thermal power-generation plants with PTCs [232]. It also gives general loading/unloading procedures for characterization of TES. Furthermore, the standard provides quality requirements for the instruments used for measuring and data processing methods.
- UNE 206014: This standard gives procedures to test the solar system of a PTC-based CSP generation system under quasi-stationary conditions [233]. Information about instrumentation and measurement techniques of available solar irradiant energy and solar field net thermal energy are given in the standard. This standard is applicable for CSP plants with solar fields where the solar energy is its principal energy source. Other equipment of the power plant is not at all considered by this standard.

6.2.2 ASME PTC 52

The American Society of Mechanical Engineers (ASME) is developing a Performance Test Code standard 52 (PTC 52) to evaluate the performance of CSP plants. The standard will provide procedures and methods to evaluate only thermal performance (solar-to-thermal conversion) of the solar field, considering only concentrating technology (it is not exclusive for PTCs, like UNE standard) [24]. The first version of this standard will be available soon, and it is expected to replace NREL Guidelines for evaluating the CSP plants.

The main driver of this standard is the expected improvements in baseline in evaluating and comparing different technologies and projects. “The code should simplify the tendering process for CSP projects by standardizing testing methodologies and acceptance requirements among power companies, financial institutions, developers, and contractors” [234]. The key benefits of this standard to CSP technology will be the improved bankability, expected wider participation, and longer life cycle.

6.2.3 ASME PTC 46

This standard provides test methods and procedures to determine thermal performance and net electrical output of the overall power plant. It is applicable to any power cycle that uses heat as the energy resource and so it can also be applied to CSP plants. In fact, it is used to test the conventional fossil-fueled power plants, including cogeneration systems. The standard does not consider components separately for the analysis, but considers the whole power plant as one element. However, thermoeconomic analysis or comparing with other technologies is not included in this standard. The power plant can be of any size including the parameters, using a specific configuration, operating disposition, fixed power level, and at reference conditions.

The procedures are employed to determine corrected net power, corrected heat rate (efficiency), and corrected heat input [235]. Performance (thermal and electrical) evaluations are based on steady-state models, and tests are conducted for a short-term duration (at least 24 h) due to the thermal stability requirements of TES systems [24]. Performance-related issue tests, such as emission, operational demonstration, and reliability, are out of the scope of this standard.

6.2.4 IEC TC 117

The committee TC 117 from IEC is working to develop standards for solar electric plants driven by solar concentrating technologies [231,236]. These standards will provide specifications for the test collectors to be used in CSP plants. The developing standards related to PTC technology are listed as follows.

- IEC 62862-3-1 provides general requirements for the design of parabolic trough solar thermal electric plants.
- IEC 62862-3-2 provides general requirements and test methods for large-size PTC. This standard is pending for publication [237]. This standard will provide guidelines for evaluating optical performance, thermal performance, and tracking accuracy of large-size PTCs under outdoor conditions with single-phase HTFs.
- IEC TS 62862-3-3 provides general requirements for systems and components and general requirements and test methods for solar receivers.

Every solar concentrating technology is considered in this standard, including tests for TES systems. The standard defines design, safety, power quality issues, and installation requirements and performance test methods [236–238]. It analyzes not only the collector field but also the subsystems and components of a CSP plant.

6.2.5 NREL guidelines

In 2011, NREL published performance acceptance test guidelines as a standard to evaluate the performance of solar plants due to a lack of standards at that time. These guidelines initially focused on PTC technology. In 2013, similar guidelines were presented for ST power plants. The guidelines only evaluate the solar-to-thermal conversion system (solar field and HTF subsystems) excluding TES system, heat exchangers, and the power block. The guideline recommends ASME standards for other subsystems and elements. The main objectives of the test are determining solar thermal power output and thermal efficiency, comparing the measured parameters with projected parameters, monitoring inlet and outlet temperature of the HTF, and measuring parasitic power consumption [239].

Two types of tests mentioned in this standard are the following:

(a) Short-time steady-state test is conducted under clear sky conditions during a short time when the thermal steady-state conditions exist.
(b) Multiday continuous energy test is conducted for a long-term period to gather thermal energy output during continuous operation. Clear sky and partly cloudy days are considered for this test. The functional performance of the solar field should be considered, from the start-up, to normal operation and till shutdown. The minimum recommended period is 10 days in a continuous operation.

6.3 Quality standards for materials and components

To fabricate a collector with high thermal and mechanical quality, qualified materials should be selected by a standard based on their function. The main structural steel grades for mechanical parts of the structural support are ASTM A36 and ASTM A588 for steel beams and plates and ASTM A53 for structural pipe. The most commonly used materials for the receiver are stainless steel (AISI 316L and AISI 304L) and copper (ASTM B42) pipes (used in some prototypes [240]). All these standards provide required properties of materials for their effective function under normal operation.

There is a standard for evaluating the quality of optical properties of materials (e.g., mirrors). The ASTM E-903 standard describes the methodology for determining and measuring the optical properties (transmittance, reflectance, and absorptance) of the materials used, and it is applicable for materials with diffuse and specular optical properties. The main standards applied to concentrating solar technology are the SolarPACES guidelines [19] for reflectance measurement (mirrors) and ASTM standard G-173-03 Section 7.2 for solar-spectral-weighted transmittance and absorptance measurement (cover glass and SC). IEC TS 62727-5 is used for evaluating tracking systems. Important features of these standards are discussed subsequently. Sallaberry et al. [241] made a compilation of other quality standards related to solar concentrating collectors, including standards for qualifying thermal performance and durability and standards related to the quality of HTFs.

6.3.1 AENOR UNE standards for quality of HTFs and reflectors

Two UNE standards characterize the properties of materials of PTC technology used in CSP plants [242]. UNE 206015 determines the physicochemical properties and measurement techniques for characterization of HTFs (mostly organic synthetic) used in in-service plants. Further UNE 206016 determines test methods and minimum requirements for performance of reflectors used in concentrating technologies, and it is applicable for any kind of mirror used in the CSP technology.

6.3.2 ASTM G-173-03

This standard presents a compilation of terrestrial solar spectral irradiance distribution data. It is basically a reference of both direct and diffuse hemispherical solar spectral irradiance in the wavelength range of 280–4,000 nm. It is applied at a reference angle of 37° tilted surface, which is applicable for most part of the United States [243]. The data represent clear sky conditions and applied for determining relative optical performance of materials used in solar energy conversion. Section 7.2 of this standard illustrates how to obtain solar spectral weighted averages of wavelength-dependent properties (such as reflectance, absorptance, or transmittance) based on solar spectral irradiance given in the tables as described previously.

6.3.3 ISO 9845-1

Standard ISO 9845-1 provides modeled direct-normal and hemispherical solar spectral irradiance distribution to determine solar-weighted properties. The data can be applied for 5.8° field-of-view angle (for direct irradiance) at a 37° tilted surface, air mass of 1.5, an albedo of 0.2, and clear sky conditions [244]. The irradiance data are given in a wavelength range between 305 and 4045 nm. Similar to ASTM G173, Section 3 of standard ISO 9845-1 provides methods to evaluate solar-weighted properties for absorptance, reflectance, and transmittance.

6.3.4 ISO 9050

This standard provides guidelines and a methodology for determining light and energy transmittance of glasses used in building and solar applications. It is applicable for near-normal incidence (irradiated beam should not exceed 10° from the normal direction of the surface) [245]. Section 3.5 describes the formulation for solar transmittance, reflectance, and absorptance of glasses. Standard ISO 9050 reference standard ISO 9845-1 for solar spectral irradiance, where spectral data with wavelength between 300 and 2,500 nm are used for obtaining solar properties.

6.3.5 IEC TS 62727-5

This IEC standard provides guidelines and specifications for evaluating a solar tracking system (single tracking or full tracking) and recommendations for measurement techniques to be used in measuring critical tracking-related parameters. It is applicable to PV systems but may be used for other solar applications. It evaluates tracking system's accuracy, functionality, and mechanical performance. Some tests include a pointing error test, data analysis (collection, filtering, and calculation), corrosion test, and durability test [246]. In 2012, the latest update was made.

6.3.6 SolarPACES Guidelines for reflectance measurement

These guidelines provide a methodology for characterizing reflective materials used in solar concentrating technologies [18]. It is also applicable for comparing reflectance characterization of different materials but not used for simulation like ray tracing. The main measurements that are considered in the guidelines are hemispherical reflectance, specular reflectance, solar-weighted reflectance, UV-weighted reflectance, and soiling. The guidelines specify the evaluation of the reflectance of the material in the wavelength range of 280–2,500 nm for solar-weighted reflectance. Solar-weighted reflectance is obtained in accordance with ASTM G173-03 Section 7.2. These guidelines also give recommendations regarding the measuring process to be used for reflectance and the requirements for instrumentation. A draft methodology for measuring reflectance losses of aged/soiled mirrors is included in the latest version [18].

6.4 Standards for terminology of solar technology

Standards for terminology define the terms and concepts used in solar energy standards. They may include terms for both thermal and PV applications. The usual concepts included in these standards are related to solar geometry, components of solar conversion system, instrumentation used to measure solar radiation, solar properties of materials, and definition of different types of solar collectors. The most used standards for solar terminology are listed below.

– ASTM E772 (standard terminology of solar energy conversion) and ISO 9488 (solar energy: vocabulary): These standards provide the definitions of terms used in general solar thermal/PV applications. These standards are referenced in thermal performance testing (ASTM E905 and ISO 9806 respectively) as "vocabulary."
– IEC 62862-1-1 (solar thermal electric plants – Part 1: terminology) and UNE 206009 (solar thermal electric plants. Terminology): The main objective of these standards is defining all terms related to solar thermal electric plants, which means that it is mostly applicable to solar concentrating technology.

7 Discussion

Current status of PTC technology is presented in this review. The materials used, physical properties, relevant information about the reliability of each component, and the design aspects of collectors are discussed in detail. Industrial applications, common processes and methods used in energy conversion, and the details of the application of the collectors are also presented. A general economic and market overviews were described, emphasizing the impact of this technology on the energy market and its economic status and trends. An exposition of methods to evaluate the performance of PTC systems, describing mathematical and experimental methods for testing thermal and optical performance are also presented and analyzed. And finally, the principal standards used to test the performance of collector, with a brief explanation of the approaches and methods used in each standard are described.

Four main ideas stand out in our present analysis. First, it is important to mention the relevance and potential of this technology in the energy market and in industry. The principal highlights are the impact that the PTC systems have in electricity generation using solar resources, their applicability in general-purpose thermal applications, and the potential use in nonthermal industry applications. It is also important to mention the integration of solar systems into conventional power and thermal systems to mitigate GHG emissions. Second, it is important to mention about the influence of materials on cost analysis. Further research should be done to develop cost-effective materials to reduce manufacturing and installation costs, so that this technology is cost competitive with conventional fossil fuel technologies. Third, the impact of PTC system design and evaluation is important. The chronological list of studies presented in this review shows that the implementation and integration of mathematical modeling, experimental validation, and computational tools improve the performance analysis of energy systems. The implementation of software tools benefits the design process, making it possible to quickly and more precisely evaluate a collector than with experiments. Finally, it is important to establish measurement and performance evaluation processes for PTC systems, so that it is possible to compare different collector or system designs and to standardize the processes for energy conversion.

8 Conclusions

From the analysis presented on this review of the PTC, the following conclusions can be drawn:
1. A general overview of the technology was presented. The different aspects of functionality, applicability, and development of PTC technology were discussed from an industrial approach.
2. Even though this technology is mature, still research has to be done to improve its components. Major research efforts must be focused on mirrors and thermal enhancement (with nanofluids or inserts). Other improvements may be changing the design of the receiver, like a rotating receiver proposed by Norouzi et al. [247], or a V-shape receiver proposed by Rafiei et al. [248].
3. The most developed applications of PTC technology are CSP plants (power generation) and SHIPs. Further, the promising areas of applicability of this technology are desalination or concentrating PVs.
4. In recent years, this technology has improved its cost of energy. The general trend of LCOE for a CSP plant is downward, making it more competitive as an alternative to provide thermal energy for power generation instead of using fossil fuels in the following years.
5. The development on modeling and testing has increased in the last decade. Designing tools and standards applicable to industrial systems has played an important role in improving the quality and applicability of this technology in industry.

9 Future work

The authors believe it is relevant to mention three main ideas for future work considering our analysis of PTC technology. The first is a proposal to realize design criteria for

PTC systems due to a lack of information about normalized processes in designing and evaluating the performance of a system. It was shown in this review that standardization of thermal performance for collectors and CSP plants is currently established or will be available soon. But performance and reliability tests for complex systems or solar collector fields integrated with another industrial application is minimum or not existing (e.g., desalination or photocatalytic decontamination systems using PTCs). The second idea is that it is also important to report the impact, benefits, and drawbacks of PTC technology in applications where this technology can be implemented but has a low penetration in market. Some potential applications are described, but most of the reports mentioned are from laboratory-scale or low-scale systems. The theoretical analysis reports mentioned can be a premise to be implemented for testing systems under real conditions. As mentioned in Section 4.2, SHIPs using PTC technology have increased in recent years due to the improvements in technology and gained experience. It may be possible to follow the same way for other industrial applications as shown in this review. The third idea is to develop computational software tools for performance analysis, especially for designing new collectors or systems as most of the software tools available realize performance analysis based on tested large-aperture PTC designs. The implementation of these kinds of computational tools can help to decrease time and resources needed to design collectors, which can lead to a reduction in manufacturing costs. For example, a computational tool that can simulate a solar field using nontested small-aperture PTCs under transient conditions can be applied for estimation of thermal net output or thermo-economic analysis in SHIPs applications or medium-scale DSG plant. R&D centers, like NREL, are working on this simulation tools, but they are focused on heating applications with large-aperture PTC and mostly for CSP plants. IEA SHC Task 49 Subtask B reported about the integrability of solar energy systems to industrial heating processes using software tools, concluding that the introduction of solar systems simulation interfaces into process tools can enhance the integrability of both solar energy and heating processes [249].

Acknowledgments: The authors acknowledge the support of the Energy and Climate Change Research Group at Tecnologico de Monterrey. The authors also thank the Institution of Engineering and Technology (IET) for providing permission to use Figure 17. Finally, they thank NREL and IRENA for permitting the use of public-domain information.

Funding sources: This research did not receive any specific grant from funding agencies in the public, commercial, or not-for-profit sectors.

Conflict of interest: One of the authors (Krishna D.P. Nigam) is a member of the Editorial Board of Green Proccesing and Synthesis.

References

[1] International Renewable Energy Agency. Renewable power generation costs in 2014. Bonn, Germany: IRENA Publications; 2015. [cited 2020 Aug 19]. Available from: https://www.irena.org/-/media/Files/IRENA/Agency/Publication/2015/IRENA_RE_Power_Costs_2014_report.pdf.
[2] International Energy Agency. Technology roadmap: Concentrating solar power. Paris (FR): IEA Publications; 2010. p. 52.
[3] International Renewable Energy Agency. Renewable energy technologies: cost analysis series (concentrating solar power). Bonn, Germany: IRENA Publications; 2012 [cited 2020 Aug 19]. Available from: https://www.irena.org/-/media/Files/IRENA/Agency/Publication/2012/RE_Technologies_Cost_Analysis-CSP.pdf.
[4] Kalogirou S. Solar thermal collectors and applications. Prog Energ Combust. 2004;30(3):231–95.
[5] Burkhardt III J, Heath G, Turchi C. Life cycle assessment of a parabolic trough concentrating solar power plant and the impacts of key design alternatives. Env Sci Technol. 2011;45(6):2457–64.
[6] Klein S, Rubin E. Life cycle assessment of greenhouse gas emissions, water and land use for concentrated solar power plants with different energy backup systems. Energ Policy. 2013;63:935–50.
[7] Kosmadakis G, Karellas S, Kakaras E. Renewable and conventional electricity generation systems: technologies and diversity of energy systems. In: Michalena E, Maxwell Hills J, editors. Renewable Energy Governance: Complexities and challenges. London: Springer; 2013. p. 9–30.
[8] Granqvist CG. Preparation of thin films and nanostructured coatings for clean tech applications: a primer. Sol Energy Mater Sol Cell. 2012;99:166–75.
[9] Kennedy C. Advances in concentrating solar power collectors: Mirrors and solar-selective coatings. Golden (CO, USA): NREL Publications; 2007. p. 10. Report No. NREL/CP-52042260.
[10] Czanderna A, Masterson K, Thomas T. Silver/glass mirrors for solar thermal systems. Springfield (VA, USA): NREL Publications; 1985. p. 72. Report No. SERI/SP-271-2293.
[11] Mescia L, Losito O, Prudenzano F. Innovative materials and systems for energy harvesting applications. Hershey (PA, USA): IGIGlobal; 2015. Chapter 10, Silver coating with protective transparent films for solar concentrators. p. 271–89.
[12] Kennedy C, Terwilliger K, Milbourne M. Development and testing of solar reflectors. Denver (CO, USA): NREL Publications; 2004. p. 5. Report No.: NREL/CP-520-36582.

[13] Silva P. Energia Solare termodinamica [pdf on internet]. Legnano (IT): Politecnico de Milano, Dipartimento d Energia; 2013 [cited 2017 Feb 10]. Available from: www.euroimpresa.it/sites/default/files/131113111951_Concentrating%20Solar%20Power_materiale.pdf.
[14] García-Segura A, Fernández-García A, Ariza MJ, Sutter F, Valenzuela L. Durability studies of solar reflectors: a review. Renew Sust Energ Rev. 2016;62:453–67.
[15] Green Rhino Energy. Solar glass & mirrors [internet]. 2016, [cited 2018 Feb 2]. Available from: http://www.greenrhinoenergy.com/solar/technologies/solar_glass.php.
[16] Atkinson C, Sansom C, Almond H, Shaw C. Coating for concentrating solar systems – A review. Renew Sust Energ Rev. 2015;45:113–22.
[17] Arancibia-Bulnes C, Peña-Cruz M, Mutuberría A, Díaz-Uribe R, Sánchez-González M. A survey of methods for the evaluation of reflective solar concentration optics. Renew Sust Energ Rev. 2017;69:673–84.
[18] Fernández-García A, Sutter F, Martínez-Arcos L, Valenzuela L, Sansom C. Advanced mirror concepts for concentrating solar thermal systems. In: Blanco M, Ramirez SL, editor. Advances in concentrating solar thermal research and technology. Cambridge (MA, USA): Woodhead Publishing Elsevier; 2017. p. 29–43.
[19] Fernández-García A, Sutter F, Montecchi M, Sallaberry F, Heimsath A, Heras C, et al. SolarPaces Guidelines: Parameters and methods to evaluate the solar reflectance properties of reflector materials for concentrating solar power technology (Version 3). Almeria, Spain; 2018. [cited 2020 Aug 19]. Available from: http://www.solarpaces.org/wp-content/uploads/20180320_SolarPACES-Reflectance-Guidelines-V3.pdf.
[20] Zhu G, Kearny D, Mehos M. On characterization and measurement of average solar field mirror reflectance in utility-scale concentrating solar power plants. Sol Energy. 2014;99:185–202.
[21] Sutter F, Meyen S, Fernández-García A, Heller P. Spectral characterization of specular reflectance of solar mirrors. Sol Energ Mat Sol Cell. 2016;145:248–54.
[22] Fernández-García A, Sutter F, Martínez-Arcos L, Sansom C, Wolfertstetter F, Delord C. Equipment and methods for measuring reflectance of concentrating solar reflector materials. Sol Energ Mat Sol Cell. 2017;167:28–52.
[23] Sansom C, Fernández-García A, King P, Sutter F, García A. Reflectometer comparison for assessment of back-silvered glass solar mirrors. Sol Energ. 2017;155:496–505.
[24] Fernández-García A, Sutter F, Fernández-Reche J, Lüpfert E. Mirrors. In: Heller P, editor. The performance of concentrated solar power (CSP) systems: Analysis, measurement and assessment. Cambrigde (MA, USA): Elsevier; 2017. p. 67–98.
[25] Giannuzzi G, Majorana C, Miliozzi A, Salomoni V, Nicolini D. Structural design criteria for steel components of parabolic-trough concentrator. J Sol Energ-T ASME. 2007;129: 382–90.
[26] Hosoya N, Peterka J, Gee R, Kearny D. Wind tunnel tests of parabolic trough solar collectors. Golden (CO): NREL; 2008. p. 243. Report No. NREL/SR-550-32282.
[27] Randall D, McBride D, Tate R. Steady-state wind loading on parabolic-trough solar collectors. Albuquerque (NM): SANDIA; 1980. p. 21. Report No. SAND79-2134.
[28] Torres-García E, Ogueta-Gutiérrez M, Ávila S, Franchini S, Herrera E, Meseguer J. On the effects of windbreaks on the aerodynamic loads over parabolic solar troughs. Appl Energy. 2014;115:293–300.
[29] Mier-Torrecilla M, Herrera E, Doblaré M. Numerical calculation of wind loads over solar collectors. Energ Procedia. 2014;49:163–73.
[30] Paetzold J, Cochard S, Fletcher D, Vassallo A. Wind engineering analysis of parabolic trough collectors to optimize wind loads and heat loss. Energ Procedia. 2015; 69:168–77.
[31] Naeeni N, Yaghoubi M. Analysis of wind flow around a parabolic collector (1) fluid flow. Renew Energ. 2007;32(11):1898–916.
[32] Zemler M, Bohl G, Ríos O, Boetcher S. Numerical study of wind forces on parabolic solar collectors. Renew Energ. 2013;60:498–505.
[33] Hachicha A, Rodríguez I, Castro J, Oliva A. Numerical simulation of wind flow around a parabolic trough solar collector. App Energ. 2013;107:426–37.
[34] Dinçer I, Zamfirescu C. Sustainable energy systems and applications. New York (NY, USA): Springer; 2012. Chapter 9, Renewable energies; p. 283–388.
[35] Lüpfert E, Zarza E, Geyer M, Nava P, Langenkamp J, Schiel W, et al. EuroTrough collector qualification complete – Performance test results from PSA. Goteborg, Sweden: ISES Solar World Congress; 2003.
[36] CIEMAT. CRES, DLR, FICHTNER Solar, FLABEG Solar, INABENSA, SBP. Development of a low cost european parabolic trough collector EUROTrough; 2001. p. 20. Report No. JOR3-CT98-0231.
[37] Lüpfert E, Geyer M, Schiel W, Esteban A, Osuna R, Zarza E, et al. EuroTrough design issues and prototype testing at PSA. Proceedings of Solar Forum. Washington, DC, USA: ASME; 2001.
[38] Günther M, Joemann M, Csambor S. Advanced CSP teaching materials. Kassel (GER): Deutsches Zentrums für Luft- und Raumfahrt; 2011. Chapter 5, Parabolic trough technology. p. 106.
[39] Fernández-García A, Zarza E, Valenzuela L, Pérez M. Parabolic-trough solar collectors and their applications. Renew Sust Energ Rev. 2010;14(7):1695–721.
[40] Kearney D. Parabolic Trough Collector Overview [pdf on internet]. Golden (CO, USA): NREL; 2007 [cited 2017 Feb 10]. Available from: http://edge.rit.edu/edge/P15484/public/Detailed%20Design%20Documents/Solar%20Trough%20Preliminary%20analysis%20references/Parabolic%20Trough%20Collector%20Overview.pdf.
[41] Valenzuela L, López-Martín R, Zarza E. Optical and thermal performance of large-size parabolic-trough solar collectors from outdoor experiments: a test method and a case study. Energ. 2014;70:456–64.
[42] SkyFuel Inc. SkyTrough Brochure [pdf on internet]. Lakewood (CO, USA); 2010 [cited 2018 Feb 26]. Available from: http://www.skyfuel.com/wp-content/uploads/Brochure-SF-SkyTrough_EN.pdf.
[43] SkyFuel Inc. SkyTrough Thermal Performance [pdf on internet]. Arvada (CO, USA); 2010 [cited 2018 Feb 26]. Available from: http://www.skyfuel.com/wp-content/uploads/WP-SF-SkyTroughThermalPerformance.pdf.

[44] Solarlite. SolarLite – 4600 [internet]. [cited 2018 Feb 26]. Available from: http://www.solarlite.de/en/products.cfm.
[45] Channiwala SA, Ekbote A. A generalized model to estimate field size for solar-only parabolic trough plants. Proceedings of the 3rd Southern African Solar Energy Conference (SASEC); 2015.
[46] Abengoa Solar. A new generation of parabolic trough technology [pdf on internet]. Phoenix (AZ, USA); 2013 [cited 2018 Feb 26]. Available from: https://energy.gov/sites/prod/files/2014/01/f7/csp_review_meeting_042513_price.pdf.
[47] von Reeken F, Arbes S, Weinrebe G, Wöhrbach M, Finkbeiner J. CSP Parabolic trough technology for Brazil: A comprenhensive documentation on the current state of the arte of parabolic trough collector technology. GIZ GmbH; 2014 [cited 2020 Aug 19]. Available from: http://edge.rit.edu/edge/P15484/public/Detailed%20Design%20Documents/Solar%20Trough%20Preliminary%20analysis%20references/CSP%20Parabolic%20Trough%20Technology%20for%20Brazil.pdf.
[48] Abengoa Solar. Parabolic trough structures [pdf on internet]. Sevilla (Spain); [cited 2018 Feb 26]. Available from: http://www.abengoasolar.com/export/sites/abengoasolar/resources/pdf/20151217_Abengoa_Solar_es_Products__Power_Structures.pdf.
[49] Rifflemann K, Richert T, Nava P, Schweitzer A. Ultimate trough: a significant step towards cost-competitive CSP. Energ Proc. 2014;49:1831–39.
[50] Gossamer Space Frames, 3M. Large Aperture Trough (LAT) 73 [pdf on internet]. (USA); 2012 [cited 2018 Feb 26]. Available from: http://multimedia.3m.com/mws/media/813507O/large-aperture-trough-lat-73.pdf?fn=GossamerLargeApertureTrough_LAT7.
[51] Archimede Solar Energy. Receiver tube – Download [internet]. Italy [cited 2017 Mar 02]. Available from: www.archimedesolarenergy.it/download.htm.
[52] Siemens. The unrivaled benchmark in solar receiver efficiency [pdf on internet]. Erlangen (GER): Siemens Press; 2010 [cited 2017 Mar 02]. Available from: www.energy.siemens.com/nl/pool/hq/power-generation/renewables/solar-power-solutions/concentrated-solar-power/downloads/Siemens-UVAC-2010.pdf.
[53] Steitz C, Sheahan M. Rioglass Solar buys some solar assets from Siemens [internet]. Reuters. Thomson Reuters; 2013 [cited 2018 Feb 17]. Available from: www.reuters.com/article/rioglass-siemens/rioglass-solar-buys-some-solar-assets-from-siemens-idUSL5N0HE0JY20130918.
[54] Rioglass. Rioglass UVAC 70 7G. [internet]. Spain [cited 2017 Mar 02]. Available from: www.rioglass.com/?page_id=1925.
[55] Rioglass. Rioglass UVAC 90 7G. [internet]. Spain [cited 2017 Mar 02]. Available from: www.rioglass.com/?page_id=1899.
[56] Rioglass. Rioglass PTR 70 4G. [internet]. Spain [cited 2017 Mar 02]. Available from: www.rioglass.com/?page_id=2296.
[57] Sunda Solar. Products [internet]. China [cited 2017 Mar 02]. Available from: www.sundasolar.com/product_index.html.
[58] Zarza Moya E. Parabolic trough concentrating solar power (CSP) systems. In: Lovegrove K, Stein W, editors. Concentrating solar power technology: principles, developments and applications. Cambridge, UK: Woodhead Publishing; 2012. p. 197–239.
[59] Fernández-García A. Tool optimization to design and evaluate parabolic-trough solar collectors for thermal energy supply at temperaturas below 250°C: Practical approach to CAPSOL prototype [Optimización de herramientas para el diseño y evaluación de captadores solares cilindroparabólicos para el suministro de energía térmica a temperaturas inferiores a 250°C: Aplicación práctica al prototipo CAPSOL]. PhD thesis. Almería (ESP): Universidad de Almería; 2013.
[60] Integration of renewable energy systems in Mediterranean countries [pdf on internet]. [cited 2018 Mar 05]. Available from: http://www.ahk.es/fileadmin/ahk_spanien/Jornadas/III_Jornada_Hispano-Alemana/Presentaciones/6._SOLITEM_Ahmed_Lokurlu.pdf.
[61] Technical data for Polytrhoug. 1800 [pdf on internet]. [cited 5 Mar 2018]. Available from: http://www.nep-solar.com/wp-content/uploads/2013/11/NEP-Solar-Polytrough1800_Datasheet.pdf.
[62] Deubener J, Helsch G, Moiseev A, Bornhoft H. Glasses for solar energy conversion systems. J Eur Ceram Soc. 2009;29(7):1203–10.
[63] Wijewardane S, Goswami D. A review on surface control of thermal radiation by paints and coatings for new energy applications. Renw Sust Energ Rev. 2012;16(4):1863–73.
[64] Price H, Lupfert E, Kearney D, Zara E, Cohen G, Gee R, et al. Advances in parabolic trough solar power technology. J Sol Energ Eng. 2002;124(2):109–25.
[65] Vivar M, Everett V. A review of optical and thermal transfer fluids used for optical adaptation or beam-splitting in concentrating solar systems. Prog Photovolt. 2014;22(6):612–33.
[66] Vignarooban K, Xu X, Arvay A, Hsu K, Kannan A. Heat transfer fluids for concentrating solar power systems – a review. Appl Energ. 2015;146:383–96.
[67] Bellos E, Tzivanidis C, Antonopoulus K, Daniil I. The use of gas working fluid in parabolic trough collectors – an energetic and exergetic analysis. App Therm Eng. 2016;109:1–14.
[68] He G, Fang X, Xu T, Zhang Z, Gao X. Forced convective heat transfer and flow characteristics of ionic liquid as a new heat transfer fluid inside smooth and microfin tubes. Int J Heat Mass Tran. 2015;91:170–7.
[69] Wadekar V. Ionic liquids as heat transfer fluids – an assessment using industrial exchanger geometries. App Therm Eng. 2017;111:1581–7.
[70] Van Valkenburg M, Vaughn R, Williams M, Wilkes J. Thermochemistry of ionic liquid heat-transfer fluids. Thermochim Acta. 2005;425(1–2):181–8.
[71] Chen H, He Y, Zhu J, Alias H, Ding Y, Nancarrow P, et al. Rheological and heat transfer behavior of the ionic liquid, [C4min][NTf2]. Int J Heat Fluid Flow. 2008;29:149–55.
[72] Hussein A. Applications of nanotechnology to improve the performance of solar collectors – recent advances and overview. Renew Sust Ener Rev. 2016;62:767–92.
[73] Weinrebe G, von Reeken F, Arbes S, Schweitzer A, Wöhrbach M, Finkbeiner J. Solar thermal heat & power-parabolic trough technology for Chile: Current state of the art of parabolic trough collector technology. GIZ GmbH; 2014. p. 116.
[74] Enteria N, Akbarzadeh A. Solar energy sciences and engineering applications. London (UK): CRC Press; 2014. Chapter 14, Solar energy conversion with thermal cycles. p. 413–84.

[75] Andrej L, Nam Y, Wang E. Heat transfer fluids. Annu Rev Heat Transf. 2012;15:93–129.
[76] Benoit H, Spreafico L, Gauthier D, Flamant G. Review of heat transfer fluids in tube-receivers used in concentrating solar thermal systems: properties and heat transfer coefficients. Renew Sust Energ Rev. 2016;55:298–315.
[77] Aguilar R, Valenzuela L, Avila-Marin A, Garcia-Ybarra P. Simplified heat transfer model for parabolic trough solar collectors using supercritical CO_2. Energ Conv Manag. 2019;196:807–20.
[78] Amelio M, Ferraro V, Marinelli V, Summaria A. An evaluation of the performance of an integrated solar combined cycle plant provided with air-linear parabolic collectors. Energy. 2014;69:742–8.
[79] Bellos E, Tzivanidis C, Antonopoulos KA. Parametric analysis and optimization of a solar assisted gas turbine. Energy Conver Manag. 2017;139:151–65.
[80] Ferraro V, Imineo F, Marinelli V. An improved model to evaluate thermodynamic solar plants with cylindrical parabolic collectors and air turbine engines in open Joule–Brayton cycle. Energy. 2013;53:323–31.
[81] Cipollone R, Cinocca A, Gualtieri A. Gases as working fluid in parabolic trough CSP plants. Proced Comp Scien. 2013;19:702–11.
[82] Bellos E, Tzivanidis C, Antonopuolos K, Daniil I. The use of gas working fluids in parabolic trough collectors – an energetic and exergetic analysis. Appl Therm Eng. 2016;109:1–14.
[83] Muñoz-Anton J, Bienciento M, Zarza E, Díez L. Theoretical basis and experimental facility for parabolic trough collectors at high temperature using gas as heat transfer fluid. App Energ. 2014;135:373–81.
[84] Biencinto M, González L, Valenzuela L, Zarza E. A new concept of solar termal power plants with large-aperture parabolic-trough collectors and sCO_2 as working fluid. Energ Conv Manag. 2019;199:112030.
[85] Kearny D, Kelly B, Herrmann U, Cable R, Pacheco J, Mahoney R, et al. Enginerring aspects of a molten salt heat transfer fluid in a trough solar field. Energ. 2004;29:861–70.
[86] Krishna Y, Faizal M, Saidur R, Ng K, Aslfattahi N. State-of-the-art heat transfer fluids for parabolic trough collector. Int J Heat Mass Tansf. 2020;152:119541.
[87] Ahmadi M, Ghazvini M, Sadeghzadeh M, Nazari M, Ghalandari M. Utilization of hybrid nanofluids in solar energy applications: A review. Nano-struct nano-obj. 2019;20:100386.
[88] Shah T, Ali H. Applications of hybrid nanofluids in solar energy, practical limitations and challenges: A critical review. Sol Energ. 2019;183:173–203.
[89] Singh D, Timofeeba E, Moravek M, Cingarapu S, Yu W, Fischer T, et al. Use of metallic nanoparticles to improve the thermophysical properties of organic heat transfer fluids used in concentrates solar power. Sol Energ. 2014;105:468–78.
[90] Mahian O, Kiannifar A, Kalogirou S, Pop I, Wongwises S. A review of the applications of nanofluids in solar energy. Int J Heat Mass Tran. 2013;57(2):582–94.
[91] Kasaeian A, Toghi A, Sameti M. A review on the applications of nanofluids in solar energy systems. Renew Sust Energ Rev. 2015;43:584–98.
[92] Verma S, Tiwari A. Progress of nanofluid application in solar collectors: a review. Energ Conver Manag. 2015;100: 324–46.
[93] Lee C-Y, Chou P-C, Chiang C-M, Lin C-F. Sun tracking systems: a review. Sensors. 2009;9(5):3875–90.
[94] Sumathi V, Jayapragash R, Bakshi A, Akella P. Solar tracking methods to maximize PV system output – a review of the methods adopted in recent decade. Renew Sust Energ Rev. 2017;74:130–8.
[95] Moga D, Sita I, Stroia P, Droba P, Moga R, Petreus D. Sensing and control strategies in tracking solar systems. 20th International Conference on Control Systems and Computer Science; 2015; Bucharest. 2015. p. 989–95.
[96] Prinsloo G, Dobson R. Solar tracking. Stellenbosch (South Africa): SolarBooks. Chapter 3, Solar position algorithms and programs; 2015. p. 65–92.
[97] Kalogirou S. The potential of solar industrial process heat applications. Appl Energ. 2003;76(4):337–61.
[98] Database for applications of solar heat integration in industrial processes [internet]. [cited 2017 July 20]. Available from: http://ship-plants.info/?collector_type=5.
[99] IEA. Solar process heat for production and advanced applications: Integration guideline [pdf on internet]. 2014 [cited 2017 July 20]. Available from: http://task49.iea-shc.org/Data/Sites/7/150218_iea-task-49_d_b2_integration_guideline-final.pdf.
[100] Hisan Farjana S, Huda N, Parvez Mahmud MA, Saidur R. Solar process heat in industrial systems: a global review. Renew Sust Energ Rev. 2018;82:2270–86.
[101] Tian Y, Zhao C. A review of solar collectors and thermal energy storage in solar thermal applications. Appl Energy. 2013;104:538–53.
[102] Alva G, Liu L, Huang X, Fang G. Thermal energy storage materials and systems for solar energy applications. Renew Sust Energy Rev. 2017;68:693–706.
[103] González-Roubaud E, Pérez-Osorio D, Prieto C. Review of commercial thermal energy storage in concentrated solar power plants: steam vs. molten salts. Renew Sust Energy Rev. 2017;80:133–48.
[104] Fernández-García A, Zarza E, Valenzuela L, Pérez M. Parabolic-trough solar collectors and their applications. Renew Sust Energy Rev. 2010;14(7):1695–721.
[105] Fuqiang W, Ziming C, Jianyu T, Yuan Y, Yong S, Linhua L. Progress in concentrated solar power technology with parabolic trough collector system: a comprehensive review. Renew Sust Energy Rev. 2017;79:1314–28.
[106] Manzolini G, Bellarmino M, Macchi E, Silva P. Solar thermodynamic plants for cogenerative industrial applications in southern Europe. Renew Energy. 2011;36(1):235–43.
[107] Marcriss R, Gutraj J, Zawacki T. Absorption fluid data survey: final report on worldwide data, ORLN/sub/8447989/3. Inst. Gas Tech; 1988, p. 286. Report No.: ORLN/sub/8447989/3.
[108] Kim D, Infante C. Solar refrigeration options – a state-of-the-art review. Int J Refrig. 2008;31(1):3–15.
[109] Li C, Wang R, Wang L, Li T, Chen Y. Experimental study on an adsorption icemaker driven by parabolic trough solar collector. Renew Energy. 2013;57:223–33.

[110] Tashtoush GM, Jaradat M, Al-Bader S. Thermal design of parabolic solar concentrator adsorption refrigeration system. Appl Sol Energy. 2010;46(3):212–23.
[111] Fadar AE, Mimet A, Pérez-García M. Study of an adsorption refrigeration system powered by parabolic trough collector and coupled with a heat pipe. Renew Energy. 2009;34(10):2271–9.
[112] Fadar AE, Mimet A, Pérez-García M. Modelling and performance study of a continuous adsorption refrigeration system driven by parabolic trough solar collector. Sol Energy. 2009;83(6):850–61.
[113] Abu-Hamdeh NH, Alnefaie KA, Almitani KH. Design and performance characteristics of solar adsorption refrigeration system using parabolic trough collector: experimental and statistical optimization technique. Energy Conver Manag. 2013;74:162–70.
[114] Sumathy K, Yeung K, Yong L. Technology development in the solar adsorption refrigeration systems. Prog Energy Combust Sci. 2003;29(4):301–27.
[115] Mahesh A. Solar collectors and adsorption materials aspects of cooling system. Renew Sust Energy Rev. 2017;73:1300–12.
[116] Fernandes M, Brites G, Costa J, Gaspar A, Costa V. Review and future trends of solar adsorption refrigeration systems. Renew Sust Energy Rev. 2014;39:102–23.
[117] Sarbu I, Sebarchievici C. Review of solar refrigeration and cooling systems. Energy Build. 2013;67:286–97.
[118] Cabrera F, Fernández-García A, Silva R, Pérez-García M. Use of parabolic trough solar collectors for solar refrigeration and air-conditioning applications. Renew Sust Energy Rev. 2013;20:103–18.
[119] Ortega-Delgado BCA, García-Rodríguez L, Alarcón-Padilla D-C. Thermoeconomic comparison of integrating seawater desalination processes in a concentrating solar power plant of 5 MWe. Desalin. 2016;392:102–17.
[120] García-Rodríguez L, Delgado-Torres A. Solar-powered Rankine cycles for fresh water production. Desalin. 2007;212(1):319–27.
[121] Delgado-Torres A, García-Rodríguez L, Romero-Ternero V. Preliminary design of a solar thermal-powered seawater reverse osmosis system. Desalin. 2007;216(1):292–305.
[122] Nafey A, Sharaf M. Combined solar organic Rankine cycle with reverse osmosis desalination process: energy, exergy, and cost evaluations. Renew Energy. 2010;35(11):2571–80.
[123] Buenaventura A, García-Rodríguez L. Solar thermal-powered desalination: a viable solution for a potential market. Desalin. 2018;435:60–9.
[124] Iaquaniello G, Salladini A, Mari A, Mabrouk AA, Fath HES. Concentrating solar power (CSP) system integrated with MED/RO hybrid desalination. Desalin. 2014;336:121–8.
[125] Eltawil M, Zhengming Z, Yuan L. A review of renewable energy technologies integrated with desalination systems. Renew Sust Energ Rev. 2009;13(9):2245–62.
[126] Reif JH, Alhalabi W. Solar-thermal powered desalination: its significant challenges and potential. Renew Sust Energy Rev. 2015;48:152–65.
[127] Sharon H, Reddy K. A review of solar energy driven desalination technologies. Renew Sust Energy Rev. 2015;41:1080–118.
[128] Li C, Goswami Y, Stefanakos E. Solar assisted sea water desalination: a review. Renew Sust Energy Rev. 2013;19:136–63.
[129] Reif J, Alhalabi W. Solar-thermal powered desalination: its significant challenges and potential. Renew Sust Energy Rev. 2015;48:152–65.
[130] Aboelmaaref M, Zayed M, Zhao J, Li W, Askalany A, Ahmed M, et al. Hybrid solar desalination systems driven by parabolic trough and parabolic dish CSP technologies: technology categorization, thermodynamic performance and economical assessment. Energ Conv Manag. 2020;220:113103.
[131] Tchobanoglous G, Burton F, Stensel H. Wastewater engineering: treatment and reuse. 4th ed. Boston: McGraw-Hill; 2003. p. 1197.
[132] Kabra K, Chaudhary R, Sawhney R. Treatment of hazardous organic and inorganic compounds through aqueous-phase photocatalysis: a review. Ind Eng Chem Res. 2004;43(24):7683–96.
[133] Malato S, Fernández-Ibáñez P, Maldonado M, Blanco J, Gernjak W. Decontamination and disinfection of water by solar photocatalysis: recent overview and trends. Catal Today. 2009;147(1):1–59.
[134] Blanco J, Malato S, Fernández-Ibañez P, Alarcón D, Gernjak W, Maldonado M. Review of feasible solar energy applications to water processes. Renew Sust Energy Rev. 2009;13(6–7):1437–45.
[135] Malato S, Blanco J, Maldonado M, Fernández-Ibañez P, Alarcón D, Collares M, et al. Engineering of solar photocatalysis collectors. Sol Energ. 2004;77(5):513–24.
[136] Zhang Y, Sivakumar M, Yang S, Enever K, Ramezanianpour M. Application of solar energy in water treatment process: a review. Desalination. 2018;428:116–45.
[137] Tallent RJ, Oman H. Solar-cell performance with concentrated sunlight. Trans AIEE Part II. 1962;81(1):30–3.
[138] Zakzouk A, Electrochem M, Mujahid A, El-Shobokshy M. Performance evaluation of photovoltaic silicon cells under concentrated sunlight. Solid-St Electron Dev, IEEE Proc I. 1984;131(2):66–72.
[139] Green M, Emery K, Hishikawa Y, Warta W, Dunlop E. Solar cell efficiency tables (version 45). Prog Photovolt. 2015;23(1):1–9.
[140] Karathanassis I, Papanicolaou E, Belessiotis V, Bergeles G. Design and experimental evaluation of a parabolic-trough concentrating photovoltaic/thermal (CPVT) system with high-efficiency cooling. Renew Energy. 2017;101:467–83.
[141] Jiang S, Hu P, Mo S, Chen Z. Optical modeling for a two-stage parabolic trough concentrating photovoltaic/thermal system using spectral beam splitting technology. Sol Energy Mater Sol Cell. 2010;94(10):1686–96.
[142] Li M, Ji X, Li G, Wei S, Li Y, Shi F. Performance study of solar cell arrays based on a trough concentrating photovoltaic/thermal system. Appl Energy. 2011;88(9):3218–27.
[143] Li M, Li G, Ji X, Yin F, Xu L. The performance analysis of the trough concentrating solar photovoltaic/thermal system. Energy Convers Manag. 2011;52(6):2378–83.
[144] Quaia S, Lughi V, Giacalone M, Vinzi G. Technical-economic evaluation of a combined heat and power solar (CHAPS) generator based on concentrated photovoltaics. International Symposium on Power Electronics Power Electronics, Electrical Drives, Automation and Motion; 2012.

[145] Yazdanifard F, Ebrahimnia-Bajestan E, Ameri M. Performance of a parabolic trough concentrating photovoltaic/thermal system: effects of flow regime, design parameters, and using nanofluids. Energy Conver Manag. 2017;148:1265–77.
[146] Mendelsohn M, Lowder T, Canavan B. Utility-scale concentrating solar power and photovoltaics projects: A technology and market overview. Golden (CO): NREL; 2012. p. 65. Report No.: NREL/TP-6A20-51137.
[147] REN21. Renewables 2016: Global status report. Paris: REN21 Secretariat; 2016. p. 272.
[148] NREL. Concentrating Solar Power Projects [internet]. USA: NREL. [cited 2017 Ene 19]. Available from: https://www.nrel.gov/csp/solarpaces/index.cfm.
[149] SANEDI. Solar heat for industry [pdf on internet]. [cited 2018 Mar 06]. Available from: https://www.sanedi.org.za/img/Brochure%20Solar%20PayBack_4.pdf.
[150] IEA. Process Heat Collectors: State of the Art and available medium temperature collectors [pdf on internet]. 2015 [cited 2018 Mar 07]. Available from: http://task49.iea-shc.org/data/sites/1/publications/Task%2049%20Deliverable%20A1.3_20160504.pdf.
[151] Hess S. Solar thermal process heat (SPH) generation. In: Stryi-Hipp G, editor. Renewable heating and cooling: Technologies and applications. Cambridge, UK: Woodhead Publishing; 2016. p. 41–66.
[152] IRENA. ETSAP. Solar heat for industrial processes: Technology brief. Bonn, Germany; 2015. [cited 2020 Aug 19]. Available from: https://www.irena.org/-/media/Files/IRENA/Agency/Publication/2015/IRENA_ETSAP_Tech_Brief_E21_Solar_Heat_Industrial_2015.pdf.
[153] Allouhi A, Kousksou T, Jamil A, Bruel P, Mourad Y, Zeraouli Y. Solar driven cooling systems: an updated review. Renew Sust Energ Rev. 2015;44:159–81.
[154] Ghafoor A, Munir A. Worldwide overview of solar thermal cooling technologies. Renew Sust Energ Rev. 2015;43:763–74.
[155] IEA SHC. New generation solar cooling and heating systems: PV or solar thermally driven systems [pdf on internet]. 2013 [cited 2018 Mar 07]. Available from: http://task53.iea-shc.org/Data/Sites/53/media/documents/work-plan-task-53-solar-cooling_2016_05_15.pdf.
[156] Buenaventura A, García-Rodríguez L. Solar thermal-power desalination: A viable solution for a potential market. Desalination. 2018;435:60–9.
[157] International Renewable Energy Agency. Renewable power generation costs in 2019. IRENA Publications; 2020. p. 144.
[158] International Renewable Energy Agency. The power to change: Solar and wind cost reduction potential to 2025. IRENA Publications; 2016. p. 112.
[159] Kurup P, Turchi C. Parabolic trough collector cost update for the System Advisor Model (SAM). Golden (CO, USA): NREL; 2015. p. 40. Report No.: NREL/TP-6A20-65228.
[160] Dieckmann S, Dersch J, Giuliano S, Puppe M, Lüpfert E, Hennecke K, et al. LCOE reduction potential of parabolic trough and solar tower CSP technology until 2025. AIP Conference Proceedings. 2017.
[161] Philipps S, Bett A, Horowitz K, Kurtz S. Current status of concentrator photovoltaic (CPV) technology. Golden (CO, USA): NREL; 2016. p. 26. Report No.: NREL/TP-6A20-63916.
[162] International Energy Agency. 2015 Highlights SHC Task 49: Solar heat integration in industrial processes [pdf on internet]. 2016 [cited 2018 Sep 10]. Available from: http://task49.iea-shc.org/Data/Sites/1/publications/IEA-SHC-Task49-Highlights-2015.pdf.
[163] Burkholder F, Kutscher C. Heat-loss testing of Solel's UVAC3 parabolic trough receiver. Golden (CO, USA): NREL; 2008. p. 19 Report No.: NREL/TP-550-42394.
[164] Pempeintner J, Anger M, Lichtenthäler N, Ant P, Happich C, Thoss J. Measurement of parabolic trough receiver thermal loss power and relative optical efficiency under solar simulator light: Test report. Köln (GER): DLR Quarz; 2012. p. 30.
[165] Burkholder F, Kutscher C. Heat loss testing of Schott's 2008 PTR70 parabolic trough receiver. Golden (CO, USA): NREL; 2009. p. 58. Report No.: NREL/TP-550-45633.
[166] Janotte N, Lüpfert E, Pottler K, Schmitz M. Full parabolic trough qualification from prototype to demonstration loop. AIP Conference Proceedings. 2017.
[167] Janotte N, Feckler G, Kötter J, Decker S, Herrmann U, Schmitz M, et al. Dynamic performance evaluation of the HelioTrough® collector demonstration loop towards a new benchmark in parabolic trough qualification. Energ Proc. 2014;49:109–17.
[168] European Commission. EuroTrough II: Extension, test and qualification of EUROTRPUGH from 4 to 6 segments at Plataforma Solar de Almería [pdf on internet]. 2004 [cited 2018 Mar 08]. Available from: https://cordis.europa.eu/docs/publications/6668/66682891-6_en.pdf.
[169] Fernández-García A, Zarza E, Pérez M, Valenzuela L, Rojas E, Valcárcel E. Experimental assessment of a small-sized parabolic trough collector. CAPSOL Project. Proceedings of EuroSun 2010, 2010.
[170] Fernández-Reche J, Valenzuela L. Geometrical assessment of solar concentrators using close-range photogrammetry. Energ Proc. 2012;30:84–90.
[171] Moss T, Brosseau D. Final test results for the Schott HCE on a LS-2 collector. Albuquerque (NM, USA): SANDIA; 2005. p. 22. Report No.: SAND2005-4034.
[172] Dudley V, Kolb G, Sloan M, Kearney D. SEGS LS2 solar collector: Test results. Springfield (VA, USA): SANDIA; 1994. p. 140. Report No.: SAND94-1884.
[173] Dudley V, Evans L, Matthews C. Test results: Industrial solar technology parabolic trough solar collector. Albuquerque (NM, USA): SANDIA; 1995. p. 140.
[174] Brooks MJ. Performance of a parabolic trough solar collector [Master's thesis]. Stellenbosch (ZA): University of Stellenbosch; 2005. p. 174.
[175] Valenzuela L, López-Martín R, Zarza E. Optical and thermal performance of large-size parabolic-trough solar collectors from outdoor experiments: a test method and a case study. Energ. 2014;70:456–64.
[176] Sallaberry F, Valenzuela L, Luis P. On-site parabolic-trough collector testing in solar thermal power plants: experimental validation of a new approach developed for the IEC 62862-3-2 standard. Sol Energ. 2017;155:398–409.
[177] McMahan A, White D, Gee R, Vijoen N. Field performance validation of an advanced utility-scale parabolic trough concentrator. Proceeding of SolarPACES Conference 2010; 2010.
[178] Brost R, Gray A, Burkholder F, Wendelin T, White D. SkyTrough optical evaluations using VSHOT measurement. Proceedings of SolarPACES 2009; 2009.

[179] Hoste G, Schuknecht N. Thermal efficiency analysis of SkyFuel's advanced, large-aperture parabolic trough collector. Energ Proc. 2015;69:96–105.
[180] Balghouthi M, Bel Hadj Ali A, Eddine Trabelsi S, Guizani A. Optical and thermal evaluations of a medium temperature parabolic trough solar collector used in a cooling installation. Energ Conv Manag. 2014;86:1134–46.
[181] Janotte N, Meiser S, Krüger D, Lüpfert E, Pitz-Paal R, Fischer S, et al. Quasy-dynamic analysis of thermal performance of parabolic trough collectors. Proceedings of SolarPACES 2009; 2009.
[182] Alfellag M. Modeling and experimental investigation of parabolic trough solar collector [master's thesis]. Daytona Beach (FL, USA): Embry-Riddle Aeronautical University; 2014. p. 112.
[183] Kalogirou S, Lloyd S, Ward J. Modelling, optimisation and performance evaluation of a parabolic trough solar collector steam generation system. Sol Energy. 1997;60(1):49–59.
[184] Forristall R. Heat transfer analysis and modelling of a parabolic trough solar receiver implemented in Engineering Equation Solver. Golden (CO): NREL; 2003. p. 164. Report No. NREL/TP-550-34269.
[185] Lüpfert E, Riffelmann K-J, Price H, Burkholder F, Moss T. Experimental analysis of overall thermal properties of parabolic trough receivers. J Sol Energy Eng. 2008;130(2):021007.
[186] García-Valladares O, Velázquez N. Numerical simulation of parabolic trough solar collector: improvement using counter flow concentric circular heat exchangers. Int J Heat Mass Transf. 2009;52(3–4):597–609.
[187] Schiricke B, Pitz-Paal R, Lüpfert E, Pottler K, Pfänder M, Riffelmann K, et al. Experimental verification of optical modeling of parabolic trough collectors by flux measurement. J Sol Energy Eng. 2009;131(1): 011004–011004-6.
[188] Montes M, Abánade SA, Martínez-Val J. Thermofluidynamic model and comparative analysis of parabolic trough collectors using oil, water/steam, or molten salt as heat transfer fluids. J Sol Energy E. 2010;132(2):021001.
[189] Qu M, Yin H, Archer D. A solar thermal cooling and heating system for a building: experimental and model based performance analysis and design. Sol Energy. 2010;84(2):166–82.
[190] Montes M, Rovira A, Muñoz M, Martínez-Val J. Performance analysis of an integrated solar combined cycle using direct steam generation in parabolic trough collectors. Appl Energy. 2011;88(9):3228–38.
[191] Powell KM, Edgar TF. Modeling and control of a solar thermal power plant with thermal energy storage. Chem Eng Sci. 2012;71:138–45.
[192] Roesle M, Coskun V, Steinfeld A. Numerical analysis of heat loss from a parabolic trough absorber tube with active vacuum system. ASME 2011 5th International Conference on Energy Sustainability, Parts A, B, and C; 2011.
[193] Vasquez-Padilla R, Demirkaya G, Goswami D, Stefanakos E, Rahman M. Heat transfer analysis of parabolic trough solar receiver. Appl Energy. 2011;88(12):5097–110.
[194] Kalogirou SA. A detailed thermal model of a parabolic trough collector receiver. Energy. 2012;48(1):298–306.
[195] Roldán M, Valenzuela L, Zarza E. Thermal analysis of solar receiver pipes with superheated steam. Appl Energy. 2013;103:73–84.
[196] Zaversky F, García-Barberena J, Sánchez M, Astrain D. Probabilistic modeling of a parabolic trough collector power plant – an uncertainty and sensitivity analysis. Sol Energy. 2012;86(7):2128–39.
[197] Lobón DH, Baglietto E, Valenzuela L, Zarza E. Modeling direct steam generation in solar collectors with multiphase CFD. Appl Energy. 2014;113:1338–48.
[198] Silva R, Pérez M, Fernández-García A. Modeling and co-simulation of a parabolic trough solar plant for industrial process heat. Appl Energy. 2013;106:287–300.
[199] Xu L, Wang Z, Li X, Yuan G, Sun F, Lei D, et al. A comparison of three test methods for determining the thermal performance of parabolic trough solar collectors. Sol Energy. 2014;99:11–27.
[200] Biencinto M, González L, Valenzuela L. A quasi-dynamic simulation model for direct steam generation in parabolic troughs using TRNSYS. Appl Energy. 2016;161:133–42.
[201] Bellos E, Tzivanidis C, Antonopoulos K, Gkinis G. Thermal enhancement of solar parabolic trough collectors by using nanofluids and converging-diverging absorber tube. Renew Energy. 2016;94:213–22.
[202] Toghyani S, Baniasadi E, Afshari E. Thermodynamic analysis and optimization of an integrated Rankine power cycle and nano-fluid based parabolic trough solar collector. Energy Convers Manag. 2016;121:93–104.
[203] Widyolar BK, Abdelhamid M, Jiang L, Winston R, Yablonovitch E, Scranton G, et al. Design, simulation and experimental characterization of a novel parabolic trough hybrid solar photovoltaic/thermal (PV/T) collector. Renew Energy. 2017;101:1379–89.
[204] Srivastava S, Reddy K. Simulation studies of thermal and electrical performance of solar linear parabolic trough concentrating photovoltaic system. Sol Energy. 2017;149:195–213.
[205] Yilmaz I, Mwesigye A. Modeling, simulation, and performance analysis of parabolic trough solar collectors: a comprehensive review. App Energ. 2018;225:135–74.
[206] Sandá A, Moya S, Valenzuela L. Moelling and simulation tools for direct steam generation in parabolic trough solar collectors: a review. Renew Sust Energ Rev. 2019;113:109226.
[207] Daneshazarian R, Cuce E, Cuce P, Sher F. Concentrating photovoltaic thermal (CPVT) collectors and systems: theory, performance assessment and applications. Renew Sust Energ Rev. 2018;81:473–92.
[208] Salgado L, Rodriguez-Pulido A, Calderón G. Thermal performance of parabolic trough solar collectors. Renew Sust Energy Rev. 2017;67:1345–59.
[209] Manikandan G, Iniyan S, Goic R. Enhancing the optical and thermal efficiency of a parabolic trough collector – A review. App Energ. 2019;235:1524–40.
[210] Akbarzadeh S, Valipour M. Heat transfer enhancement in parabolic trough collectors: a comprehensive review. Renew Sust Energ Rev. 2018;92:198–218.
[211] Rashidi S, Kashefi M, Hormozi F. Potential applications of inserts in solar thermal energy systems – A review to identify the gaps and frontier challenges. Sol Energ. 2018;171:929–52.

[212] Bellos E, Tzivanidis C, Tsimpoukis D. Enhancing the performance of parabolic trough collectors using nanofluids and turbulators. Renew Sust Energ Rev. 2018;91:358–75.
[213] Osório T, Horta P, Larcher M, Pujol-Nadal R, Hertel J, van Rooyen DW, et al. Ray-tracing software comparison for linear focusing solar collectors. AIP Conference Proceedings. 2016. p. 1734.
[214] Ho C. Software and codes for analysis of concentrating solar power technologies. Albuquerque (NM, USA): SANDIA; 2008. p. 35. Report No.: SAND2008-8053.
[215] Breault Reserach Organization Inc. ASAP Capabilities [internet]. Tucson, AZ (USA): BRO; [cited 2017 Jun 27]. Available from: http://www.breault.com/software/asap-capabilities.
[216] ANSYS. Fluent [internet]. ANSYS [cited 2017 Jun 27]. Available from: http://www.ansys.com/Products/Fluids/ANSYS-Fluent.
[217] COMSOL Inc. CFD Module [internet]. Burlington, MA (USA): COMSOL Inc; [cited 2017 Jun 27]. Available from: https://www.comsol.com/cfd-module.
[218] National Renewable Energy Laboratory. System Advisor Model (SAM) [internet]. Golden, CO (USA): NREL; [cited 2017 Jun 27]. Available from: https://sam.nrel.gov/.
[219] Thermoflow Inc. Thermoflex & Peace: Solar thermal modelling [internet]. Southborough, MA (USA): Thermoflow Inc; [cited 2017 Jun 27]. Avaiable from: https://www.thermoflow.com/solarthermal_overview.html.
[220] Thermal Energy System Specialist LLC. TRNSYS [internet]. Madison, WI (USA): TESS; [cited 2017 Jun 27]. Available from: http://www.trnsys.com/#1.
[221] Fernández-García A, Valenzuela L, Zarza E, Rojas E, Pérez M, et al. SMALL-SIZED parabolic-trough solar collectors: development of a test loop and evaluation of testing conditions. Energy. 2018;152:401–15.
[222] ASTM. Standard E-905. Standard test method for determining thermal performance of tracking concentrating solar collectors; 2013.
[223] FSEC. Standard 102: Test methods and minimum standards for certifying solar thermal collectors; 2010.
[224] ISO. Standard 9806: Solar energy - Solar thermal collector – Test methods; 2013.
[225] Epp B. EN ISO 9806: Upcoming global collector standard [internet]. 2012 May 26 [cited 2014 Sep 18]. Available from: http://solarthermalworld.org/content/en-iso-9806-upcoming-global-collector-standard.
[226] QAIST. A guide to the standard EN 12975 [pdf on internet]. 2012 [cited 2018 Mar 11]. Available from: http://www.estif.org/fileadmin/estif/content/projects/QAiST/QAiST_results/QAiST%20D2.3%20Guide%20to%20EN%2012975.pdf.
[227] SRCC. Standard 600: Minimum standard for solar thermal concentrating collectors; 2013.
[228] Petrina I, Cueli AB, Díaz J, Moracho J, Laguna AR. CENER experience testing CPV modeles. Energética Internacional. 2012; 123:68–71.
[229] IEC. Standard 62108: Concentrator photovoltaic (CPV) modules and assemblies – Design qualification and type approval. 2007.
[230] IEC. IEC 62108:2016 [internet]. 2016 [cited 2018 Mar 11]. Avaiable from: https://webstore.iec.ch/publication/25938.
[231] AENOR. UNE 206010: Test for the verification of the performance of solar thermal power plants with parabolic trough collector technology [Ensayos para la verificación de las prestaciones de las centrales termosolares con tecnología de captadores cilindroparabólicos]. 2015
[232] AENOR UNE 206012:2017. General characterization of the thermal energy storage system for solar thermal power plants with parabolic trough collector technology [Caracterización del Sistema de almacenamiento térmico para aplicaciones de concentración solar con captadores cilindroparabólicos] [pdf on internet]. 2017 [cited 2018 Oct 15]. Available from: https://portal.aenormas.aenor.com/revista/pdf/jun17/(EX)UNE_206012=2017.pdf.
[233] AENOR UNE 602014:2017. Tests for the determination of the solar field efficiency of solar thermal power plants with parabolic trough collector technology [Ensayos para la determinación del rendimiento del campo solar de las centrales termosolares con tecnología de captadores cilindroparabólicos] [pdf on internet]. 2017 [cited 2018 Oct 15]. Available from: https://portal.aenormas.aenor.com/revista/pdf/sep17/(EX)UNE_206014=2017.pdf
[234] Performance Test Code [PTC] 52. New CSP standards set to broaden supply chain and prolong plant life [internet]. New Energy Update. 2017 [cited 2018 Mar 12]. 12 p. Available from: http://1.newenergyupdate.com/LP=18185?extsource=linked_energy.
[235] ASME. PTC 46: overall Plant Performance (Review draft). 2013.
[236] Sallaberry F, Valenzuela L, Palacín G, León J, Fischer S, Bohren A. Harmonization of Standards for Parabolic Trough Collector Testing in Solar Thermal Power Plants. AIP Conference Proceedings; 2017.
[237] Sallaberry F Standardization of thermo-solar sector [Normalización del sector termosolar] [pdf on internet]. 2018 [cited 2018 Oct 15]. Available from: http://www.solarconcentra.org/wp-content/uploads/2018/06/Actividaes-Estandarizaci%C3%B3n.pdf.
[238] International Electrotechnical Commission. TC 117 Scope [internet]. Geneva (Switzerland): IEC; [cited 2017 Jul 23]. Available from: http://www.iec.ch/dyn/www/f?p=103:7:0:FSP_ORG_ID,FSP_LANG_ID:7851,25.
[239] Kearny D. Utility-Scale Parabolic Trough Solar Systems: Performance Acceptance Test Guidelines. Golden (CO): NREL; 2011. p. 67. Report No.: NREL/SR-5500-48895.
[240] Coccia G, Di Nicola G, Hidalgo A. Parabolic Trough Collector Prototypes for Low-Temperature Process Heat. Madrid (ES): Springer; 2016. p. 80.
[241] Sallaberry F, Bello A, Burgaleta J, Fernández-García A, Fernández-Reche J, Gómez J, et al. Standards for components in concentrating solar termal power plants – Status of the spanish working group. . SolarPACES 2015: International conference on concentrating solar power and chemical energy systems; 2015. Cape Town, SUD: AIP Conference Proceedings; 2016. p. 110003-1–8.
[242] UNE. Standarization programm 2018: Second semester [Programa de trabajo Normalización 2018: Segundo semestre] [pdf on internet]. 2018 [cited 2018 Oct 16]. Available from: https://www.une.org/normalizacion_documentos/programa%20de%20trabajo%202018%20normalizaci%C3%B3n.pdf.
[243] ASTM. G-173-03: standard tables for reference solar spectral irradiance: direct normal and hemispherical on 37° tilted surface.

[244] ISO 9845-1: Reference solar spectral irradiance at the ground at different receiving conditions – Part 1: direct normal and hemispherical solar irradiance for air mass 1.5. 1992.
[245] ISO 9050. Glass in building – Determination of light transmittance, solar direct transmittance, total solar energy transmittance, ultraviolet transmittance and related glazing factors. 2003.
[246] IEC. Standard TS 62727: photovoltaic systems – Specifications for solar trackers. 2012.
[247] Norouzi A, Siavashi M, Oskouei M. Efficiency enhancement of the parabolic trough solar collector using the rotating absorber tube and nanoparticles. Renew Energ. 2020;145:569–84.
[248] Rafiei A, Loni R, Ahmadi M, Najafi G, Bellos E, Rajaee F, et al. Sensitivity analysis of a parabolic trough concentrator with linear V-shape cavity. Energ Sci Eng. [internet] 2020 [cited 2020 Oct 21]. Available from: https://onlinelibrary.wiley.com/doi/pdf/10.1002/ese3.763.
[249] Krummenacher P, Muster B Methodologies and software tools for integrating solar heat into industrial processes [pdf on internet]. 2015 [cited 11 Mar 2018]. Available from: http://task49.iea-shc.org/Data/Sites/7/iea-task-49_deliverable-b1_20150218.pdf.